

R-02-37

Sedimentary dykes in the Oskarshamn-Västervik area

A study of the mechanism of formation

Kennert Röshoff, BBK AB
John Cosgrove, Imperial College

July 2002

Svensk Kärnbränslehantering AB

Swedish Nuclear Fuel
and Waste Management Co
Box 5864
SE-102 40 Stockholm Sweden
Tel 08-459 84 00
+46 8 459 84 00
Fax 08-661 57 19
+46 8 661 57 19



Sedimentary dykes in the Oskarshamn-Västervik area

A study of the mechanism of formation

Kennert Röshoff, BBK AB
John Cosgrove, Imperial College

July 2002

Keywords: sedimentary dykes, sediments, overpressure, hydraulic injection, hydraulic fracturing.

This report concerns a study which was conducted for SKB. The conclusions and viewpoints presented in the report are those of the authors and do not necessarily coincide with those of the client.

Abstract

This study of the sedimentary dykes from the Oskarshamn-Västervik area, near Äspö and surrounding region, is aimed at understanding the mechanism of their formation. In particular it is important to establish whether or not they formed by the injection of high pressure fluidized sediments and if so what the likely effect of any future overpressured sediments will be on the stability of the fracture network in the basement rocks at Äspö.

This report is made up of a review of the literature on sedimentary dykes, a discussion of the various mechanical models for hydraulic fracturing and a description of the field and laboratory study carried out on the sedimentary dykes.

The field work in the study area shows that, with the exception of the sedimentary dyke at Granhultå whose internal fabric clearly indicated gravitational infill from above, all the dykes examined by the present authors have fabrics and textures characteristic of forcefully injected sediments, i.e. clasts fining from the centre of the dykes to the edges and as a result layering forming parallel to the dyke walls.

Cross cutting tectonic fractures combined with mineralization of the sedimentary dykes, possibly linked to the break-up of Pangea in the Permian, indicate that the dykes are relatively ancient features.

It is suggested that the most likely cause of an increase in the fluid pressure of the sediments overlying the basement rocks in the area (and the associated formation of sedimentary dykes by the process of fluid induced fracturing) is the advance of a glaciation.

Summary

This study of the sedimentary dykes from the Oskarshamn-Västervik area, near Äspö and surrounding region, is aimed at understanding the mechanism of their formation. In particular it is important to establish whether or not they formed by the injection of high pressure fluidized sediments and if so what the likely effect of any future overpressured sediments will be on the stability of the fracture network in the basement rocks at Äspö.

This report is made up of a review of the literature on sedimentary dykes, a discussion of the various mechanical models for hydraulic fracturing and a description of the field and laboratory study carried out on the sedimentary dykes.

The literature review indicates a remarkable consensus on the mode of formation of these structures based on their fabric (particularly layering generated in part by variation in clast size) and the composition of the infilling material. Two modes of origin have been recognised. These are the passive infilling of dykes where the dyke material has entered an open fracture under the influence of gravity, and active, i.e. forceful injection of a fluidized sediment under high pressure into a pre-existing fracture or into a fracture generated by the high pressure fluid.

The discussion of the theory of fluid induced fracturing leads to the recognition of three systems which are the two end members and an intermediate form of a complete spectrum of materials ranging from unconsolidated and incohesive sediments, through cemented but porous rocks to crystalline rocks with no intrinsic porosity and whose only porosity relates to that imparted by the fracture network that the rock contains.

The theory best suited to analyses this latter system is one based on fracture mechanics and is known as the theory of external hydraulic fracturing. From the point of view of the sedimentary dykes in the study area around the Äspö Hard Rock Laboratory, where the dykes occur in the fractured granitic basement, this is clearly the most appropriate model.

The field work in the study area shows that, with the exception of the sedimentary dyke at Granhultea whose internal fabric clearly indicated gravitational infill from above, all the dykes examined by the present authors have fabrics and textures characteristic of forcefully injected sediments, i.e. clasts fining from the centre of the dykes to the edges and as a result layering forming parallel to the dyke walls.

Cross cutting tectonic fractures combined with mineralization of the sedimentary dykes, possibly linked to the break-up of Pangea in the Permian, indicate that the dykes are relatively ancient features.

It is suggested that the most likely cause of an increase in the fluid pressure of the sediments overlying the basement rocks in the area (and the associated formation of sedimentary dykes by the process of fluid induced fracturing) is the advance of a glaciation.

Sammanfattning

Denna undersökning av sedimentära gångar inom Oskarshamn-Västervikområdet, i närheten av Äspö och kringliggande trakter, har som mål att förstå mekanismen för hur de bildades. Det är särskilt viktigt att fastställa om de bildats genom injektering av en sedimentslurry under högt tryck eller annan mekanism. Om bildningsättet var enligt förra fallet, vilka blir de sannolika effekterna på stabiliteten i sprickmönstret i bergmassan vid Äspö för framtida sediment om de utsätts för ett liknande övertryck.

Den här rapporten inkluderar en litteraturstudie om sedimentära gångar, en diskussion om olika mekaniska modeller för hydraulisk spräckning, och en beskrivning och analys av fält- och laboratorieundersökningar utförda på sedimentära gångar i undersökningsområdet. Litteraturstudien visar en märklig samstämmighet av bildningsätten för dessa strukturer baserad på deras mikromönster (särskilt lagringen som delvis bildas av variationer i fragmentstorlek) och sammansättningen av fyllnadsmaterialet. Två olika mekanismen har föreslagits. Den första mekanismen är passiv utfyllning av gångar varvid gångmaterialet har fallit ner i en öppen spricka på grund av gravitationen. Den andra mekanismen är ett aktivt sätt; kraftfull injektering av en sedimentslurry under högt tryck s k hydraulisk spräckning, antingen in i en existerande spricka, eller in i en ny spricka, som utvecklas på grund av det höga vätsketrycket.

Diskussionen om teorien om sprickor som utvecklas genom hydraulisk spräckning har lett till tre accepterade system. Dessa består av två ytterlighetsformer och en mellanliggande form med ett komplett spektrum av material som varierar från okonsoliderade och icke kohesiva sediment, igenom cementerade men poröst bergmaterial, till kristalliniska bergarter som inte har någon porositet. De kristalliniska bergarterna har i huvudsak enbart den porositet som härrör från bergets sprickor.

Den teori som är lämpligast för att analysera det sistnämnda systemet är baserat på brottmekanisk teori och är känd som teorien om hydraulisk spräckning. Med kunskap från de sedimentära gångarna omkring Äspölaboratoriet, där gångarna befinner sig i kristallint berg, är den teorin klart den lämpligaste modellen.

De arbeten som företogs i Oskarshamn-Västervikområdet och redovisas i denna rapport visar att, med undantag av de sedimentära gångarna vid Granhultå, som har en textur som tydligt visar gravitativ utfyllning, har alla övriga gångar som studerats mikrotexturer och strukturer som karakteriserar hydraulisk spräckning av en sedimentslurry under högt tryck. Det som författarna observerat är bland annat att bergartsfragmenten blir finare från gångens mitt ut mot kanterna och laminering som bildats parallellt med gångens kontakt mot sidoberget.

Två observationer ger antydning om gångarnas ålder. Den första är att det finns tektoniska sprickor i det kristallina berget som skär över gångarna. Dessutom finns det mineraliseringar i de sedimentära gångarna som möjligen kan knytas till delningen av Pangea under Permisk tid.

Det föreslås att den mest sannolika orsaken till det ökande hydrauliska trycket i de sediment som överlagrade det kristallina urberget var en framskridande glaciation.

Contents

1	Background	9
2	Objectives	13
3	Sedimentary dykes a global feature	15
3.1	Literature review.	15
3.1.1	Introduction	15
3.1.2	Fractures occupied by sedimentary dykes	16
3.1.3	The material infilling	17
3.2	Mechanical implications of sedimentary dykes	23
3.2.1	Stress environment	23
3.2.2	Mobilization and emplacement of the infilling material	24
3.2.3	Dyke emplacement	24
3.2.4	Timing of dyke emplacement	25
3.2.5	Dyke orientation	25
3.2.6	Source beds and the direction of dyke injection	29
3.3	Conclusions	30
4	Fluid induced fractures	31
4.1	Introduction	31
4.2	Basic concept of fluid induced fracturing	31
4.2.1	The law of effective stress	31
4.2.2	Poroelastic Behaviour	39
4.3	The stress-pore pressure relationship at fracture initiation	40
4.4	The expression of hydraulic fractures in rocks and sediments	45
4.4.1	The orientation of fluid induced tensile fractures	46
4.4.2	The type of fluid induced fractures	48
4.4.3	Fluidisation	48
4.5	Conclusions	50
5	The sedimentary dykes in the Småland granite	51
5.1	Introduction	51
5.2	Händelöp	51
5.3	Tindered	54
5.4	Granhulteå	55
5.5	Emån	60
5.5.1	Fluid induced fracturing in simple fracture network	62
5.5.2	Fluid induced fracturing in complex fracture networks	63
5.6	The quarries at Kråkemåla and Götemar	66
5.7	Road section north of Västervik	83

6	Discussion	85
6.1	General	85
6.2	The implication of the field observations regarding the mechanism of emplacement of the sedimentary dykes	87
6.3	The implication of the field observations regarding timing of dyke emplacement	87
6.4	Cause of intrusion	88
7	Conclusion	91
	References	93

1 Background

A series of sedimentary dykes occur in the Precambrian shield in the Oskarshamn-Västervik area in the vicinity of the SKB underground laboratory at Äspö, Figure 1-1. These dykes are filled with clastic sediments and sometimes contain angular clast of the granitic wall rock. Two important and fundamentally different processes of dyke formation have been proposed in the literature. The first is passive infill driven by gravity and the second is forceful injection driven by high fluid pressures. This latter process relates directly to the problem of fluid induced fracturing of crystalline rock masses with effectively zero intrinsic permeability such as the rock that hosts the Äspö laboratory.

An understanding of the mechanics by which these dykes formed is of wider interest and impacts directly on establishing the role of fluid pressure on fracture initiation and propagation in a massive, non-porous crystalline rock.

A considerable literature exists concerning the theory of hydraulic fracturing in porous media such as granular, porous sediment. This work assumes that the internal fluid pressure in the pores opposes the rock stresses (lithostatic stress) and leads to the concept of effective stress. This concept has been applied extensively in both geology and rock engineering to account for the formation and pattern (orientation) of hydraulic fractures in rocks.

A key question relates to whether or not we can apply the theory of hydraulic fracturing developed for porous media to crystalline non-porous rocks containing

- i) isolated fractures,
- ii) both isolated and interconnected fracture.

It is argued that this theory is not appropriate and that the theory of 'external fluid fracturing' should be used in order to understand the behaviour of such a rock mass.

The study of the sedimentary dykes for this project has been concentrated in an area from south of Oskarshamn to north of Västervik. A number of sedimentary dykes in the Pre-Cambrian basement are reported from the East Sea but are most frequent along the Småland coast and the islands of Åland. The dykes in the Oskarshamn-Västervik area were reported by Gavelin 1904 on the Loftahammar geological map and were described to consist of sandstone material probably of Cambrian age. /Nordenskjöld, 1944; Mattsson, 1962; Bergman, 1982/ have documented and presented valuable field observations. About 150 dykes are reported from that area. /Nordenskjöld, 1944/ reports that the dykes are mainly oriented in N-S to NNE and ENE and follow the orientation of the fracture sets in the basement. Those orientations are confirmed by /Sundblad and Alm, 2000/. The dykes normally have a width of a few cm to some tens of cms, are vertical and occur as fillings in fractures. The quartz and feldspar grains are rounded to angular and some with typical sandstone texture. The colour varies within the same dyke from greyish, brownish, yellowish to greenish.

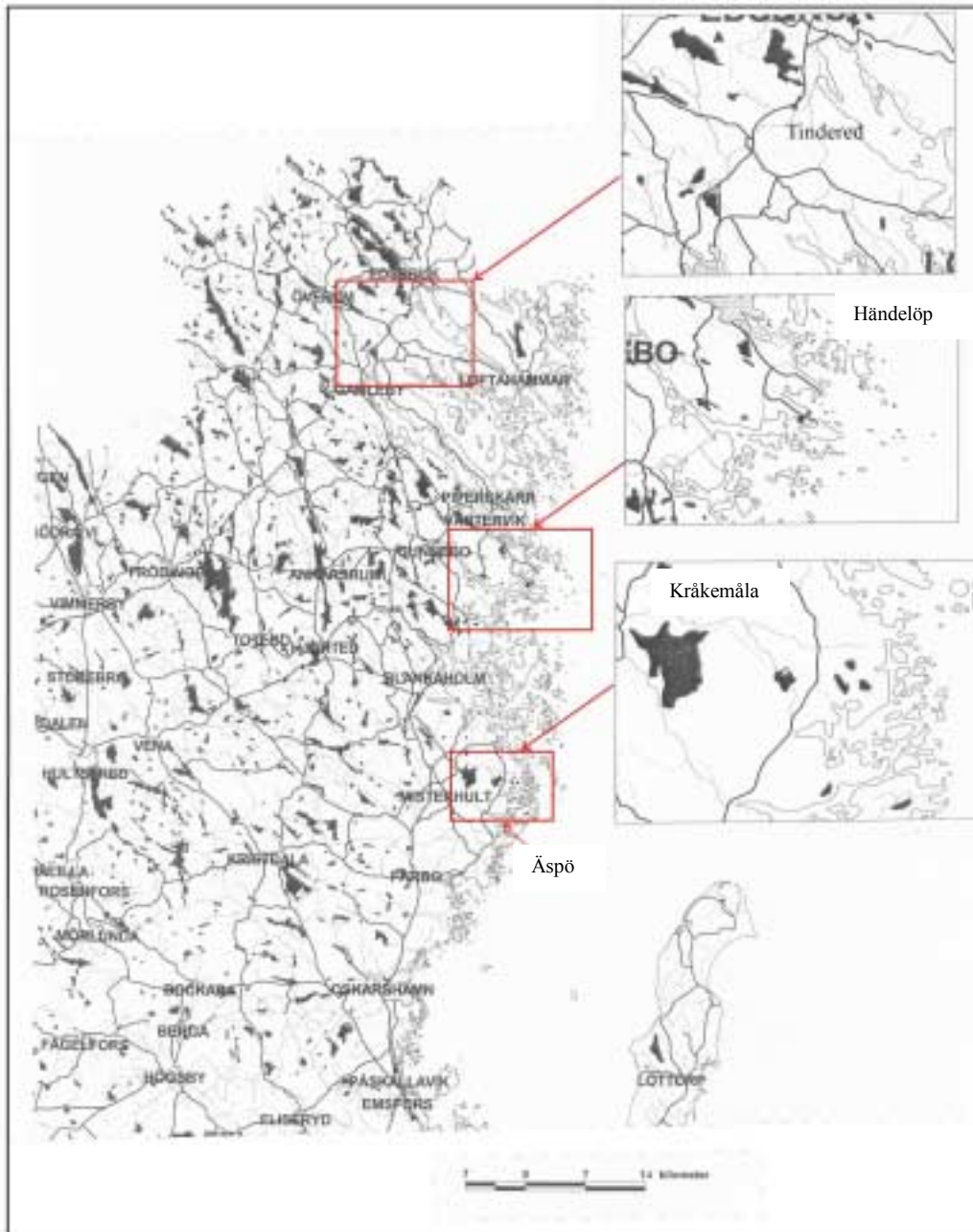


Figure 1-1. Map showing the location of the main study sites.

A “Precambrian” peneplane was developed from about 900 to 600 my by exogenic processes and covered large areas of Scandinavia. Part of that peneplane is still observed and has been mapped and described by /Lidmar-Bergström, 1996/. Cambrian sandstones were sedimented on the peneplane in the studied area followed by younger Cambro-Ordovicium sediments.

Some dykes are related with fluoride, calcite and galena mineralisation indicating that the depth of formation for the mineralisation probably was less than 100 m and for the sedimentary dykes the formation a few tens of meter below the peneplane /Sundblad and Alm, 2000/. /Sundblad and Alm, 2000/ have observed the relation between fluorite mineralisation and sedimentary dykes. The fluorite crystals have grown at the contact between the dyke and host rock towards the host rock, that the calcite-fluorite mineralisation postdate the sedimentary dyke and that fluorite minerals have penetrated the dykes.

/Kresten and Chyssler, 1976/ have reported close relation between the fluorite filled fractures, the sedimentary dykes and faults oriented in N-S.

/Sundblad and Alm, 2000/ conclude the following age relations of fluorite fillings and sedimentary dykes:

Cambrium age:

- a) Calcite filled fractures with sporadic fluorite.
- b) Calcite filled fractures with frequent infilling of fluorite.
- c) Fluorite dominating filling in rare cases with galena.

Late Palaeozoic age:

Fluorite dominating fillings with vast amount of galena.

Age of sedimentary dykes:

The fluorite fillings are syn-diagenetic or post dates the sedimentary dykes and that the dykes are early Palaeozoic in age.

2 Objectives

The objective with the field study is to make a detailed analysis of the mechanisms of the formation of the sedimentary dykes in the Precambrian basement rock especially in the area around Äspö. The work should also give some information of age relations both to the formation and if possible to other structures as joints.

If the formation is by hydraulic fluids the condition of stress regimes are analysed and discussed and under what geological conditions and environment were at the time of formation. The analyses should also consider the role of fluid pressure in controlling fracture initiation and propagation in non-porous fractured rock mass.

Of interest is that if the dykes were formed by fluid pressure the direction of the pressure must have been from above down wards. There is no other such mechanism for formation of sedimentary dykes found or reported elsewhere in the world. Such a scenario is interesting as it has direct implication of link to a glaciation mechanism.

This project involves three main parts namely:

- i) A literature survey of sedimentary dyke and the mechanisms of their formation.
- ii) A consideration of hydraulic fracturing in non-porous but fractured rocks.
- iii) Field work in the Oskarshamn-Västervik area.

The aim of the study is to improve our understanding of:

- The mechanism of formation of the sedimentary dykes in the ‘granite’ at Äspö in particular whether this process involved high fluid pressures or are infilling in open fractures.
- The role of fluid pressures in controlling fracture initiation and propagation in non-porous fractured rock masses of the type containing the underground laboratory at Äspö.
- If formed by high fluid pressure the mechanism of formation and possibility to simulate the development.
- The effect of any future glacial advance on the fracture network at Äspö.

This report will cover the two first objectives. The effect of future glaciation is only briefly discussed, as the impact must be separately investigated with help of numerical analyses based on field data. In Chapter 3 is given a state of the art review of sedimentary dykes phenomena regarding observations, formation, stress environment and dyke orientation. Chapter 4 then take up the theory of fluid induced fracturing. In Chapter 5 the field observations and the analyses in the studied area are presented and discussed.

3 Sedimentary dykes a global feature

3.1 Literature review

3.1.1 Introduction

Sedimentary or clastic dykes have been known since the 19th century. /Darwin, 1840/ described such structures in Patagonia: /Murchison, 1827; Peach et al, 1907/ in Scotland and /Cross, 1894; Crosby, 1897; Diller, 1889/ in Colorado. These dykes have a worldwide distribution, appear in every rock type – sedimentary, igneous and metamorphic – and cut through the whole span of geological time from the Archean to the Quaternary. They are usually made up of arenaceous material although dykes of breccia, gravel, clay, till and bitumen are known. They vary considerably in dimensions: thicknesses range from fractions of cms. to tens of meters, lengths from a few cms. to several kilometres and the exposed vertical height can be in excess of 300m.

Several modes of emplacement have been recognised. They range from the passive gravitational infilling of holes and cracks through infilling associated with the slumping of unstable sediments or thawing of ice to forceful injection of clastic material triggered by a variety of phenomena ranging from glacial advance, diagenetic compaction and faulting sometimes related to earthquakes.

The term sedimentary dyke has no mechanical implications and refers simply to intrusive, sheet-like, discordant (usually vertical) clastic bodies contrasting with their host rock.

Reviews are abundant in the literature and these are often stimulated by specific interests. For example /Jenkins, 1925/ focussed on the economic aspects of sedimentary dykes, /Williams, 1927/ on lithology, /Hayashi, 1966/ on timing of intrusions, /Winslow, 1983/ on morphology. Other workers give more general reviews e.g. /Dionne and Shilts, 1974/ who discuss dykes in both consolidated and unconsolidated sediments and /Allen, 1982/ who discusses the formation of both syn-depositional and post-depositional dykes.

A classification based on genesis would be ideal but this is complicated by the fact – repeatedly mentioned in the literature – that fissuring and filling do not necessarily occur in one single episode. Although both phases generally require some sort of tectonic stress, the stress field responsible for each may be quite unrelated. These two phases of dyke formation are now considered in turn.

3.1.2 Fractures occupied by sedimentary dykes

The type of fracture and fissure hosting sedimentary dykes can be divided into five categories.

1. Cracks, holes and depressions caused by weathering.

This phenomena mainly occurs particularly in limestones /Schrock, 1948; Samuelson, 1975/.

2. Contractional joint.

- (i) opened in cooling lava flows /Fackler, 1941; Walton and O'Sullivan, 1950; Van Biljon and Smitter, 1956/,

- (ii) desiccation cracks associated with the drying out of exposed sediments.

3. Cracks, channels and fissures produced by slumping.

These are developed during the penecontemporaneous reworking of soft sediments. This process is especially noticeable in turbidites on steep marine slopes /Dzulynski and Walton, 1965; Truswell 1972/. Similar effects result from the reworking of glacial sediments by partial thawing, thawing of ice veins or wedges and the movement of ice sheets /Goldthwait and Kruger, 1938; Kruger, 1938; Lupper 1944; Birman, 1952; Spencer, 1971; Dionne and Shilts, 1974; von Brun and Talbot, 1986; Talbot and von Brun, 1989/, Figure 3-1.

4. Burial and exhumation joints.

Joints formed as a result of either an increase in overburden stress during burial and diagenesis or the reduction of the overburden stress linked to exhumation.

5. Tectonically induced fractures.

These are the fractures (Faults and joints) that are linked to tectonism that may affect a region. It is important to note that tectonic events are likely to reactivate old planes of weakness so that earlier formed fractures, unrelated to the current phase of tectonism, may be reopened.

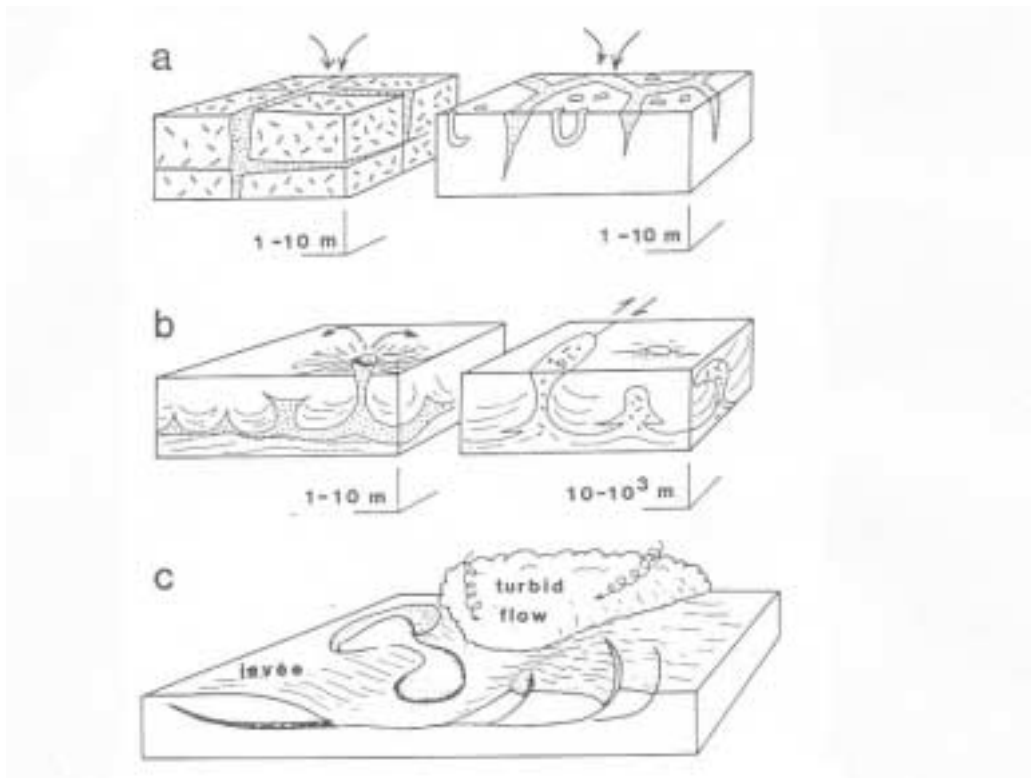


Figure 3-1. Apparent intrusions development when sediments infill pre-existing fractures in the substrate. a) Neptunian (or clastic) dykes in sediments or crystalline rocks, frost wedges, desiccation cracks, animal burrows, root infillings, etc. True sedimentary intrusions move along decreasing pressure gradients whatever their direction. b) Upward intrusion (with or without extrusion and down-slope sliding and slumping) by dewatering, load casting and diapers that can range in scale from centimetres to tens of kilometres. c) Sideways intrusion beneath banks of aerial or underwater channels temporarily overtopped by floods or flows. Note the possible hydraulic-jacking component in the construction of levees. From /Talbot and von Brun, 1989/.

3.1.3 The material infilling

The infilling of the fractures listed in the previous section, to form sedimentary dykes is often triggered by the same process that generated the fractures. This is particularly evident in the example of the reworking of soft sediments. However, it is sometimes related to a completely unrelated event. The different mechanisms of infilling produce characteristic features that form a convenient basis for classification and in the following section four types of infilling are described. These are:

- Passive infilling.
- Filling from unconsolidated sediments.
- Filling during burial and minor tectonism.
- Filling by tectonic dewatering.

Passive infilling

The infilling of fractures may occur passively in response to gravity, either dry or more often washed down with water, as sediments are deposited over an open set of fractures. In these examples, the dyke material is invariably younger than the host rock and is always sourced from above. The dyke may include occasional fragments of wall rock and sometimes shows a horizontal layering.

These true Neptunian dykes usually have a tapered cross section and die out rather quickly with depth. The sides of the infilled fractures are often irregular and the country rock at the dyke contact may show evidence of weathering. Neptunian dykes have been observed in Dolerite sheets /Fackler, 1941; Van Biljon and Smitter, 1956/; in glacial deposits /Lupher, 1944; Birman, 1952/ and in recent deposits e.g. the infilling of desiccation cracks /Dionne and Shilts, 1974/.

The morphology of true Neptunian dykes and of actively filled dykes has been thoroughly described and compared by /Matsson, 1962; Samuelson, 1975/. It also appears that passively infilled dykes are much less common than those that are actively filled.

Filling from unconsolidated sediments

In unstable, freshly deposited sediments (and in periglacial environments), layers, or pockets of plastic muds, quicksand etc with a high water content, may be compressed, dewatered and injected into adjacent layer, usually upward, (sometimes reaching the surface as mud or sand volcanoes), less frequently downwards and indeed, although rarely, in all directions.

Sedimentary dykes formed in this way are reviewed by /Allen, 1982/ and termed 'penecontemporaneous clastic intrusions'. They are usually of modest dimensions (thicknesses from less than 1cm to a maximum of 20–30cm.). They often have an irregular sinuous shape, sometimes vermicular; showing branching and small, lateral apophyses. They can normally be traced back to their feeder beds. Their walls are smooth with occasional structures such as grooves or flutes. Although usually structurless, the filling sometimes shows a preferential orientation of elongate minerals, mud clasts etc, parallel to the walls. This is usually taken as a proof of their somewhat forceful injection.

Injections of the type described in the previous paragraph can also be initiated tectonically and one of the most spectacular examples is described by /Reimnitz and Marshall, 1965/ who observed the effects of the 1964 earthquake in Alaska on modern deltaic sediments. The structures developed in the upper part of the sedimentary pile and include sand sheets, Sand dykes, pipes and sand spouts. These structures are of considerable dimensions; the sand dykes for example may be 10s or even 100s of metres long.

Filling during burial and minor tectonism

These dykes are formed during burial and diagenesis and are usually found in shales or slates or in interbedded sequences of arenites and pelites that are now lithified. Their occurrence has been reported in:

- **Precambrian terrains** in SW Australia and Tasmania /Boulter, 1974, 1983; Powell 1974/, in Idaho /Clark, 1970/ and Michigan /Powell, 1969, 1972/, in Norway /Williams, 1976/.

- **Cambrian and Lower Palaeozoic rocks** in Vermont /Moench, 1966; Powell, 1973/, in Scotland /Smith and Rast, 1958/.
- **Ordovician slates** of New Jersey, Pennsylvania and Maryland /Maxwell, 1962; Carson, 1968; Alterman, 1973; Groshong, 1976; Beutner et al, 1977; Gregg, 1979/.
- **Upper Silurian** of the Lake district U.K. /Powell, 1972/.
- **Mid Devonian** slates of Germany /Borradaile, 1977/.

These dykes closely resemble those described in the previous section in which filling was from unconsolidated sediments. Their shapes can be irregular with branching and apophyses, Figure 3-2. They result from the upward or downward injection of sands into shales, or less commonly of clays into sandstones from a feeder that can usually be recognised.

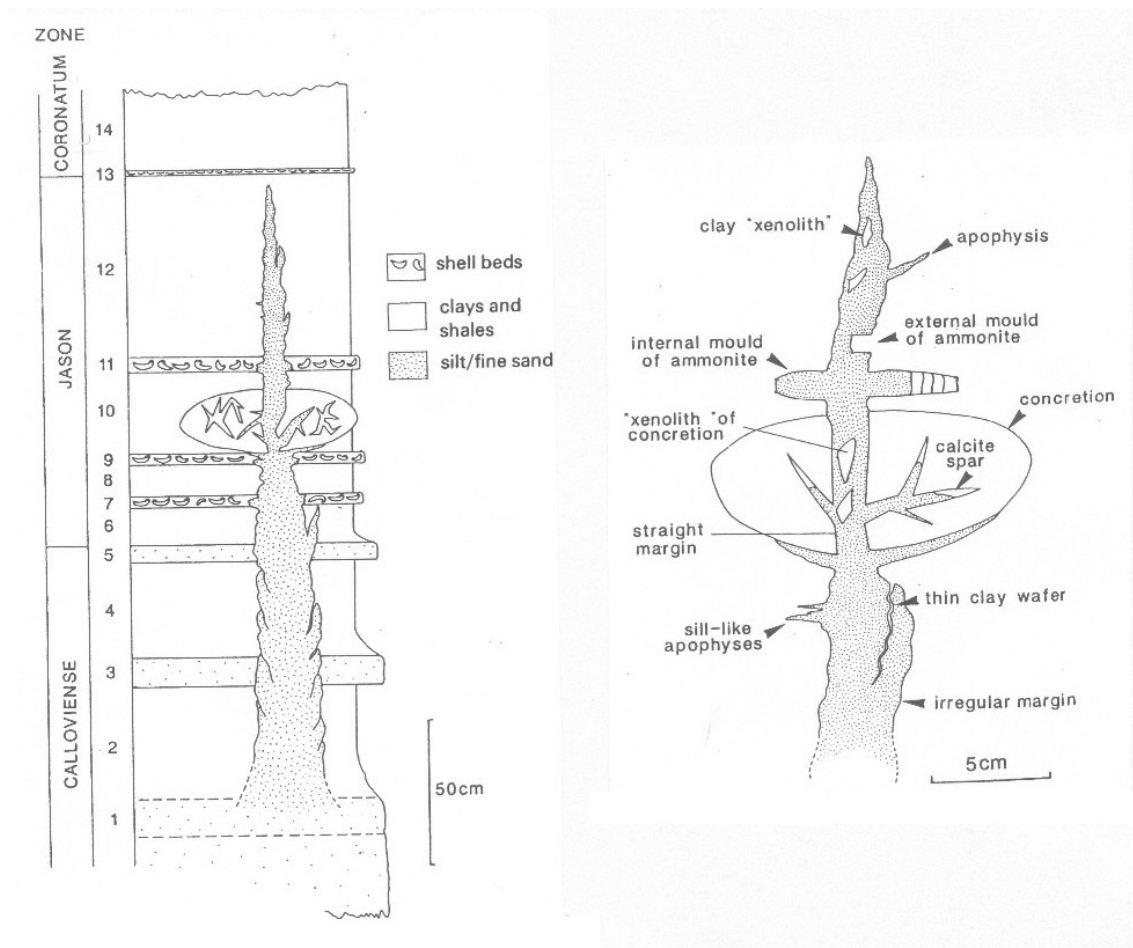


Figure 3-2. a) Simplified stratigraphic log for the basal Lower Oxford clay in the Peterborough area showing the limit of intrusion by a sandstone dyke. Dotted lines at the base of the dyke indicate the inferred source of the dyke. From /Martill and Hudson, 1989/.

More recent work on the formation of sand dykes in thick, hydrocarbon charged sequences such as those that occur in the North Sea show that dykes of considerable magnitude (tens of metres wide and up to a half kilometre long /Cosgrove and Hillier, 2000/ can form during burial and diagenesis, Figure 3-3.

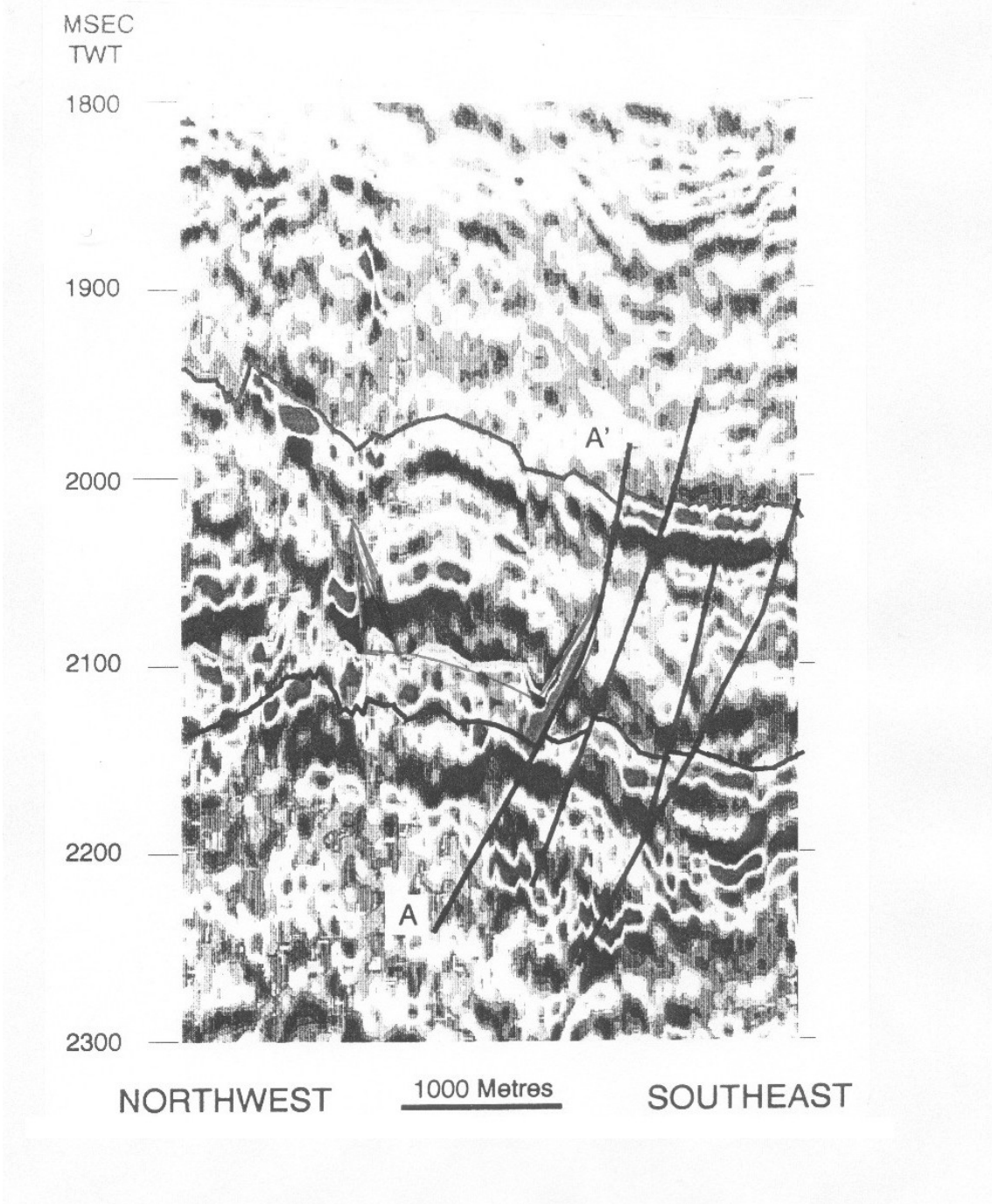


Figure 3-3. Reconstruction seismic line along the axis of the Alba sandstone channel. Sedimentary dykes have been intruded from the edge of the channel along faults. They extend for approximately 500m. From /Cosgrove and Hillier, 2000/.

Filling by tectonic dewatering

This group is similar to the previous group but occurs on a larger scale and are thought to be associated with major tectonic events. They are placed in a separate category because of their relatively large size and the amount of energy involved in their emplacement. Their occurrence has been reported in the:

- **Precambrian** terrains of Colorado /Roy, 1946; Vitanage, 1954; Harms, 1965/ and Sweden /Lindstrom, 1967; Samuelson, 1975/.
- **Cambrian** (Dalradians) of Scotland /Spencer, 1971/.
- **Carboniferous** of Ireland /Brandon, 1972/.
- **Jurassic** of Scotland /Waterson, 1950; Bailey and Weir, 1932/.
- **Cretaceous** of Canada /Williams, 1927/, of California /Peterson, 1966/ and in the Southern Andes /Winslow, 1977, 1983/.
- **Oligocene** of Dakota /Smith, 1952/, and in the recent sediments of Alaska /Reimnitz and Marshall, 1965/.

They usually occur in Swarms of parallel or sub-parallel vertical sheets, with occasional branches linking adjacent sheets, Figure 3-4. Their thickness varies between 1cm and 100m and they can sometimes be traced for as much as 5km. Their exposed vertical dimensions may be as high as 50–100m and their walls are straight and clean cut.

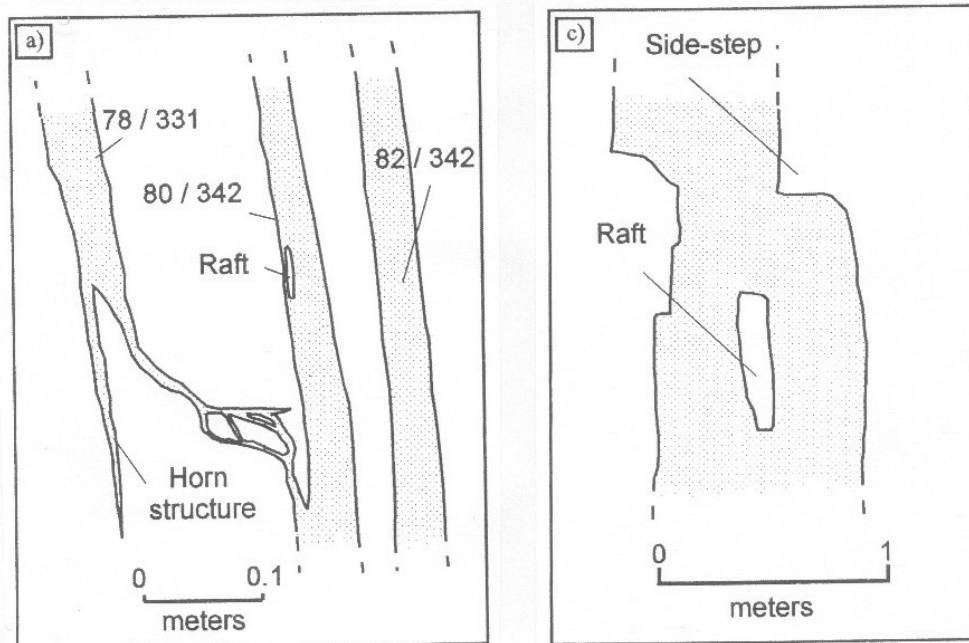


Figure 3-4. Map of dykes from the Sacramento Valley California. a) A thin, anastomosing dyke, showing irregular geometries, and linkages between two dykes. c) Thicker dyke with a raft of host shale suspended within the intrusion. The rafts are associated with dyke wall irregularities. From /Jolly, Cosgrove and Dewhurst, 1998/.

Their internal structure is very variable /Peterson, 1968/, Figure 3-5. Although they can appear structures or displaying a graded horizontal layering, they most commonly show a vertical layering parallel to their walls with a preferred orientation of elongate grains.

These dykes can seldom be traced back to their feeder so that the source bed is usually identified by matching lithologies only.

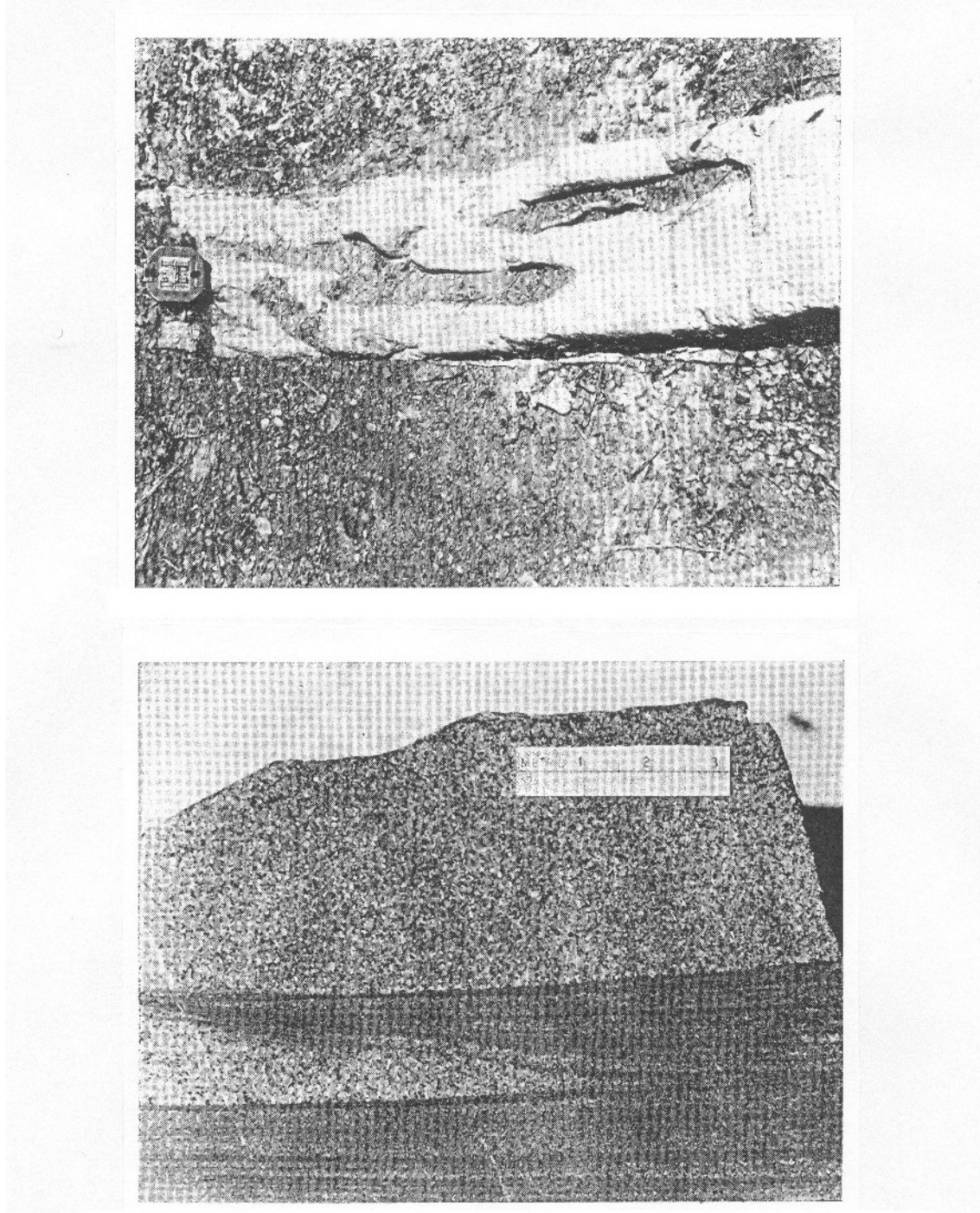


Figure 3-5. Oriented large tabular slabs of mudstone within a sandstone dyke. Except for the deviation of the smaller slab, the orientation of the three larger slabs with the tabular direction parallel with the dyke walls is typical of the dykes of the area (Sacramento Valley, California). Lower photograph shows lateral termination of coarse-grained sandstone layer within a clastic dyke. The layers are parallel to the dyke walls. From /Peterson, 1966/.

3.2 Mechanical implications of sedimentary dykes

In this section various implications regarding the broad boundary conditions under which this last category of dykes form are considered. In particular the stress environment, the mobilization and emplacement of the infilling material, the orientation of the dykes and the upward injection from the source bed.

3.2.1 Stress environment

Although it has long been suggested that these dykes are tectonically controlled, it was not until the 1980s that a rigorous analysis was carried out on a specific field area. /Winslow, 1983/ presents a detailed description of the Southern Andes in Patagonia and Tierra del Fuego. In the central part of the belt, numerous thrusts and high angle reverse faults run parallel to the general NW-SE orogenic trend. The sub-vertical axial planes of associated disharmonic folds strike in the same direction and a regional cleavage has developed parallel to the axial planes. Sets of joints run parallel (longitudinal or b-c joints) and perpendicular (extension a-c joints) to the fold axes. The tectonic stress field is therefore well defined; the maximum principal compression σ_1 is sub-horizontal and oriented NE-SW.

The numerous sedimentary dykes intruded in this area are overwhelmingly oriented parallel to the a-c extension joints. They are mostly concentrated near thrust planes and specifically located within the hanging wall of the overriding nappes. They are accompanied by sedimentary sills.

(It is interesting to note that fluid induced fractures formed in a stress regime where thrusts are forming would be horizontal (i.e. they will be mode I fractures opening against a vertical minimum principal compression. If vertical intrusions also occur in these settings then it implies that the values of the intermediate and minimum principal stress are very close or that some local structure such as a fold generates a local stress field in which the minimum principal stress is horizontal).

Winslow's observations clearly establish two important facts:

- The sedimentary intrusions are especially abundant near thrust planes.
- They fill extensional fractures directly related to the stress fields responsible for the folding and thrusting.

It is interesting to establish whether this association of dykes, thrusting and folding has been reported from elsewhere.

As discussed above in the section 3.1.3, dykes have been related, often rather loosely, to faulting and earthquakes. In Scotland they have been linked to wrench faulting and earthquakes, in Sweden and Ireland to earthquakes and faults, to thrust and reverse faults in Colorado where they occur in the upthrust block, and to wrench faults in California.

The relationship between earthquakes and reactivation of faults is well established. In brittle rocks movement occurs when the tectonically induced shear stress on the fault is high enough to overcome the frictional resistance to sliding. The regular build up and release of the shear stress along a fault is linked to the 'stick-slip' mechanism of fault movement, each slip event being associated with an earthquake.

It has been established that, all other things being equal, the value of the differential stress ($\sigma_1 - \sigma_3$) required to induce re-shear on a fault is highest for thrust faults and least for a normal fault /Sibson, 1974/. The ratio of the magnitudes of differential stresses needed to reactivate thrust, wrench and normal faults is 1:16:4. The amount of stored strain energy stored in the rock (and thus available to be released as seismic energy capable of stimulating sedimentary dyke formation) is determined by the square of the differential stress. Thus the energy available for dyke injection for the three faults is in the ratio of 1:2.56:16. The association of sedimentary dykes with faults, particularly thrust and wrench faults are therefore not surprising.

3.2.2 Mobilization and emplacement of the infilling material

The study by /Reimnitz and Marshall, 1965/ demonstrates clearly that earthquakes can produce sedimentary dykes of large dimensions in unconsolidated sediments. The question remains however whether or not they could have a similar effect on lithified rocks. Although abundant references are made in the literature /e.g. Harms, 1965/ to examples where it is considered that tectonic shocks caused fluidisation of already lithified rocks, this idea is still contentious and is discussed fully in the section of the report dealing with hydraulic fracturing and fluidisation.

3.2.3 Dyke emplacement

The build up of tectonic (and overburden) stress and the accompanying increase in fluid pressure can have a considerable influence on the migration and redistribution of fluids (including fluidised sediments) in the rock.

/Sibson et al, 1975/ describe a process whereby high fluid pressures are generated by the release of stored elastic strain energy associated with a pulse of reshear on a fault linked to an earthquake. It is argued that after the shock, the partial release of stress decreases the tension in the rocks adjacent to the fault and the resulting closure of the dilatant fractures results in an increase in fluid pressure. The fluids are expelled and either partially redistributed into adjacent rocks or sometimes expelled as springs of hot brine at the surface /Tsuneiki and Nakamura, 1970/.

It seems reasonable to assume that fluidised sediments in nearby layers behave in a similar way to brines and are injected into adjacent layers as sedimentary dykes. In this process the mobilization of the sediments is the result of relief of external stress rather than by the build up of stress. It is interesting to note that as early as 1950, Walton et al suspected a mechanism of this kind and suggested that ...“the primary force responsible for injection is an elastic potential possessed by the material itself and due to its internal pressure, so that it responds to any local fall in internal pressure. It is not external pressure that forces the material into place in a plastic or fluid manner”.

In summary it can be concluded that when the level of energy along an active faults sufficiently high, movement on the fault could liquefy an already consolidated sediment and inject it into the surrounding rock.

3.2.4 Timing of dyke emplacement

The existence of sedimentary dykes in old formations is of course no proof that their emplacement was achieved in or from consolidated sediments. It might have taken place during or soon after deposition.

When host and dyke material differ widely in age, as for example in Colorado and Sweden where dykes are intruded into Precambrian granites, the age of emplacement is generally tacitly accepted as being the age of the feeder beds, and little attention has been paid to precise time relationships with tectonic movements associated with injection, so the question remains open. When the host and dykes both belong to relatively small successive units within the same formation, it is generally considered that they were in a comparable state of lithification. The fact, commonly emphasised, that the dykes cut a number of units, sometimes considerable, at right angles to the bedding, and follow planar fractures, is usually considered as proof that the succession was rigid and therefore somewhat lithified during dyke emplacement. However, as discussed by /Cosgrove, 2001/ the state of lithification, specifically the cohesive strength of a sediment in a succession undergoing burial and diagenesis, can vary dramatically from sediment to sediment. It is quite likely that during burial and the build up of high fluid pressures in low permeability sediments, some sediments will behave cohesively and others as cohesionless aggregates of clastic grains. The later will fluidise in response to an increase in fluid pressure acting as the source material for the sedimentary dykes that penetrate pre-existing fractures or generate new fractures in the adjacent sediments.

3.2.5 Dyke orientation

The injection of incoherent material into a homogeneous isotropic host rock will occur along new extension fractures that form at 90° to the least compressive stress, σ_3 . See for example /Winslow, 1983/. In such examples fracturing and filling are both the result of the same stress field and can be assumed to be contemporaneous. However, if the host rock contains fractures then there is a possibility of injection exploiting these, even if they are not ideally oriented (i.e. at 90° to σ_3), rather than generate new fractures. The easiest pre-existing fractures to open are those normal to σ_3 . Fractures, which do not have this orientation, may open as discussed in the following paragraph, but their opening direction will be at right angles to the stress field operating during the time of injection. This will be oblique to the fracture sides.

The general case of the effect of fluid pressure on the opening of fractures in a rock mass with a range of fracture orientations has been considered by /Delany et al, 1986/. They were interested in the exploitation of pre-existing vertical joints by ascending magmas and in their model the maximum and minimum principal stresses are horizontal and represented by S_H and S_h respectively. They derive a relationship between these regional stresses, the magma pressure P_m and the range of orientations of fractures that can be dilated by the fluid.

$$\frac{(P_m - S_H) + (P_m - S_h)}{S_H - S_h} > -\cos 2\alpha \quad 3-1$$

α is the angle between the normal to the fracture and the least principal stress. Inset Figure 3-6a. Delaney et al, 1986, term the left hand expression the stress ratio R and point out that this equation defines four fields on a graph of stress ratio R versus the angle α , Figure 3-6. They note that in the lowest field, $R < -1$, the magma pressure is less than the least regional compressive principal stress and is therefore insufficient to dilate a joint of any orientation. In the highest field, $R > 1$, the magma pressure is greater than the most compressive regional horizontal stress and is therefore sufficient to dilate any vertical joint. Two fields are contained within the middle region, $-1 < R < 1$. Above the curve defined by Equation 3-1 the fluid pressure is sufficient to dilate suitably oriented joints (assuming that there is negligible tensile strength across the fracture); below the line suitably oriented joints are absent but the magma pressure may be sufficient to propagate new fractures.

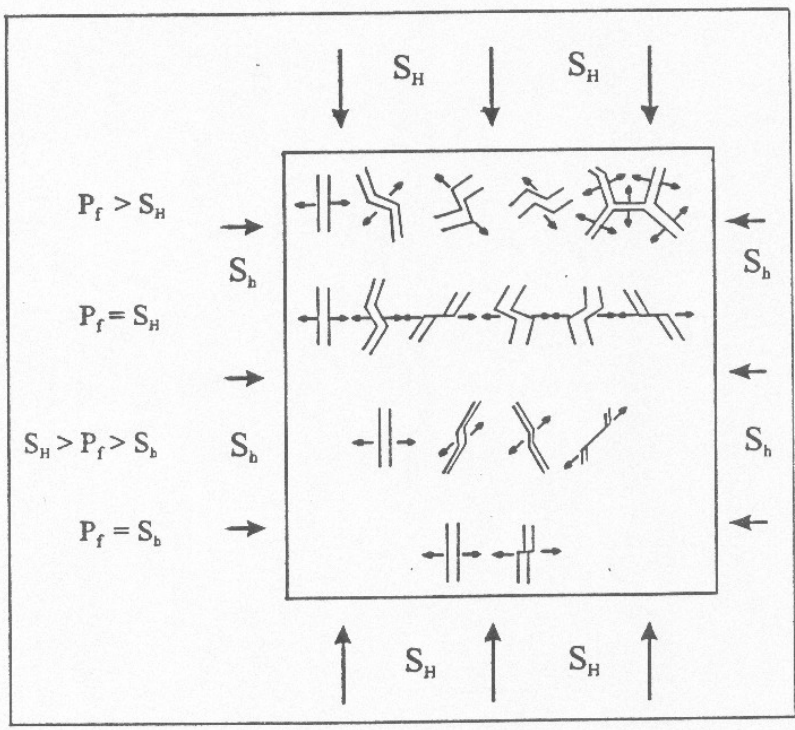
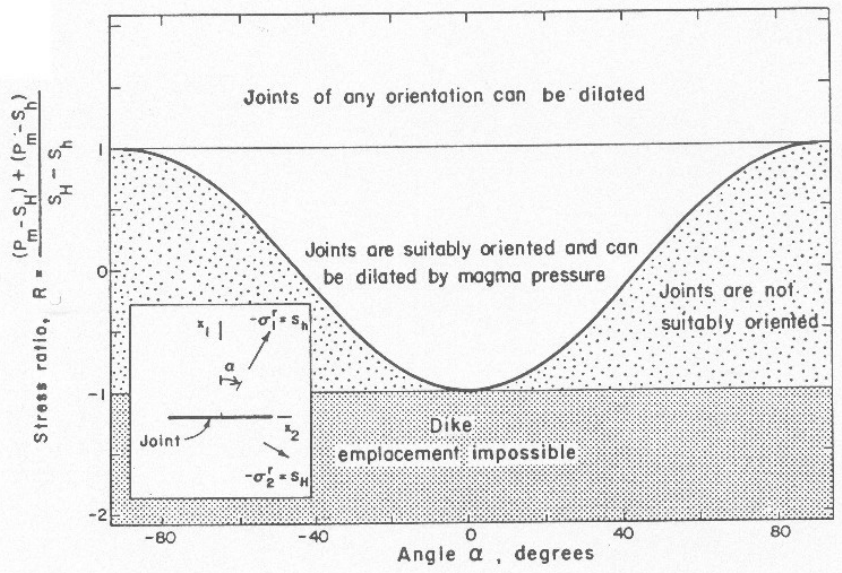


Figure 3-6. The top diagram is the graphical expression of Equation 3-1. The area beneath the curve shows the range of orientations of joints that are not suitably oriented to open response to the fluid pressure. The area above the curve shows the range of fracture orientations which will open in response to the fluid pressure. See text for discussion. After /Delaney et al, 1986/. The lower diagram shows the increasing range of orientations of fractures that will open as the fluid pressure increase.

Examples from the literature on sedimentary dykes in which the relationship between the strike and opening direction have been noted are discussed below.

a) /Winslow's, 1983/ work in the Patagonian Andes clearly establish two important facts:

- The sedimentary intrusions are especially abundant near thrust planes.
- They fill extensional fractures directly related to the stress fields responsible for the folding and thrusting and are contemporaneous with the fracturing.

The majority of fractures formed by the Alaska earthquake described by /Reimnitz and Marshall, 1965/, experienced a contemporaneous injection of sediments and opened normal to the fracture walls (and to σ_3).

b) In contrast, in the Göteborg region of Sweden, the vertical dykes measured by /Samuelson, 1975/ fall into three categories. E-W, E.NE-W.SW and ESE-WNW, Figure 3-7a. The angle between the two latter being approximately 50° . Other tectonic structures in the area show that the prevailing direction of extension is N-S. Further south in Sweden and on Bornholm Island, /Lindstrom, 1967/ observed sedimentary dykes and funnel shaped intrusive structures showing a very similar distribution, Figure 3-7b. Fractures and sedimentary dykes on Bornholm Island are oriented mainly N $60\text{--}65^\circ\text{W}$, with a few others striking E-W. Here again the prevailing extension direction is N-S. Quoting the author, “the funnel graben of South Sweden are commonly arrayed along lines with NW and SW strikes.”

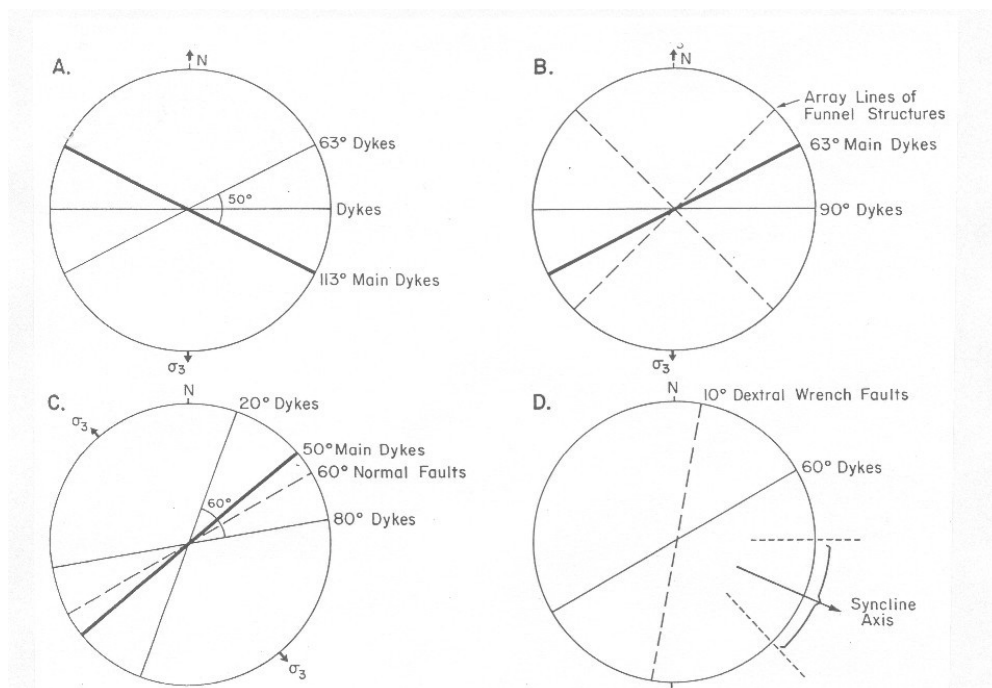


Figure 3-7. Orientation of dykes and their relationship to other structures and to the stress field thought to be operating during the injection. From various sources, see text for discussion.

The vertical dykes of the White River Badlands in South Dakota show a comparable pattern of distribution /Smith, 1952/, Figure 3-7c, with an average acute angle of 60°.

The pattern of dykes from these last three examples have been interpreted by their respective authors as representing two conjugate shear fractures (indeed, horizontal slickensides and lateral displacements have been observed) together with pure extensional fractures parallel to their bisector.

In each of these three examples, the orientation of the dykes fits into the regional tectonic stress field so that their emplacement is likely to have occurred during the same tectonic event. However, this does not mean that fracturing and infilling were exactly contemporaneous. If they were the pure extension dykes parallel to the opening direction would be dominant. It seems likely that the wrench fractures pre-date the infilling and were obliquely opened during a later stage of extension.

- c) In the Sacramento Valley of California, all the dykes measured by /Peterson, 1966/ show a constant trend, Figure 3-7d. The author relates them to dextral wrench faults, which appear further north (trend N10°W). However, the dykes occur in a major syncline trending east to southeast. If the syncline axial plane is taken as being parallel to σ_3 , the dykes appear to follow the direction of the sinistral wrench faults, Figure 3-7d, and in this example do not form parallel to the deduced east to southeast extension direction. It is argued therefore that the fracturing pre-dates the infilling. During a later extension phase, the wrench fractures (in fact only one of the two conjugate sets) were obliquely opened and filled with clastic material, their openings having apparently required less energy than the formation of new, ideally oriented extension fractures.

3.2.6 Source beds and the direction of dyke injection

There is usually no direct field connections linking tectonically generated sedimentary dykes to their feeder beds; the origin of the feeder material has to be established by comparing its lithology with that of other members of the succession. In most examples the dyke material is older than the host rock. The injection results from an upward movement of mobilised sediments.

With dykes emplaced from thrusts or reverse faults however, the filling is sometimes found to be younger than the host rock, Figure 3-8. These dykes, mostly located in the hanging walls, have also been injected upwards from younger beds overridden by the thrust blocks. This is the case for example in the Pikes Peak region of Colorado, where dykes of Cambrian sandstone are found in Archean Granites. This spatial relationship is very similar to the upward injection of fault gouge from a thrust surface described by /Brock and Engelder, 1977/. This age relationship between host and younger feeder has sometimes been misleading and taken as proof of downwards injection.

Nevertheless, there is at least one occurrence where a downward injection of younger sediments appears to be the only possible mechanism of injection. This is the sedimentary dykes of South Sweden, which are made of Cambrian sandstone, have been intruded into Archean gneiss in a region where no thrust movements are known to have taken place. These dykes are the main focus of the present study and their mode and timing of injection are considered in Chapter 5.

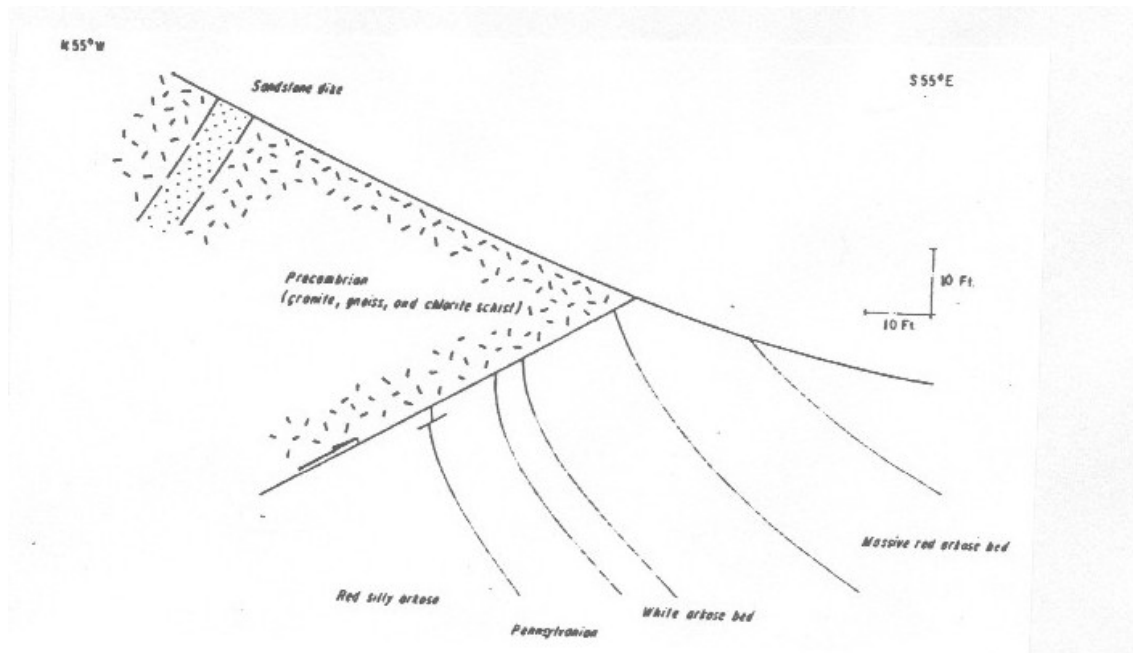


Figure 3-8. Localised drag beneath a reverse fault that places Precambrian granite over a younger Arkose. Sedimentary dykes have been injected from the younger sediments into the overthrust block. From /Harms, 1965/.

3.3 Conclusions

- Sedimentary dykes can be classified on the basis of their mode of infilling.
- Vertical sedimentary dykes of tectonic origin, occasionally accompanied by sills, tend to be large, intrusive bodies, up to 100m thick and several kilometres long.
- They are formed in a high-energy stress environment during movement along active faults, often accompanied by earthquakes.
- The build up of pore pressures accounts for the fluidisation of their filling material, and the release of stored elastic strain energy after an episode of slip on a fault for their emplacement.
- In the simplest examples the orientation of the dykes is directly related to the opening direction (perpendicular to σ_3) of the stress field operating during their emplacement.
- Sometimes the strike distribution of the dykes shows a more complex pattern. It seems likely in these examples that the fractures formed in response to a stress field that pre-dated the stress field operating during dyke injection and that the dykes exploited these pre-existing fractures.

4 Fluid induced fractures

4.1 Introduction

There is a vast and detailed literature on the link between fluid pressure and brittle failure and it is therefore necessary when discussing this problem to be selective. In draughting the following brief review, the present authors have borne in mind that the principal aim of the present report is to consider the effect of high fluid pressures on the propagation of existing and the generation of new fractures in the basement rocks at Äspö. This would enable the likely response of the site to another episode of high-pressure fluids caused, for example, by the next glacial advance to be determined.

Numerous references are drawn upon but three main references have been used. These are /Fyfe et al, 1978; Engelder, 1992; Mandl, 1999/. These authors address the problem of hydraulic fracturing in slightly different ways and a consideration of the three approaches helps clarify the role of effective stress, fracture mechanics, failure of poro-elastic media, and the theory of internal and external hydraulic fracturing in *understanding* Fluid Induced Failure.

4.2 Basic concept of fluid induced fracturing

4.2.1 The law of effective stress

The influence of pore fluid pressure on the Stress State in a porous, impermeable rock is summarised by the Law of Effective Stress:

$$\sigma_e = \sigma - p \quad 4-1a$$

where σ

is the lithostatic stress,

p the pore fluid pressure and

σ_e the effective stress.

/Fyfe et al, 1978/ argue that if the pore fluids are filled with a static fluid (i.e. the system is closed and undrained with the fluids unable to move out of the pore spaces), the tendency for the pore spaces to decrease in volume in response to an external compression will result in an increase in pressure in the almost incompressible fluid. The pressure in the pore fluids will everywhere act perpendicular to the surface of the individual grains, Figure 4-1a.

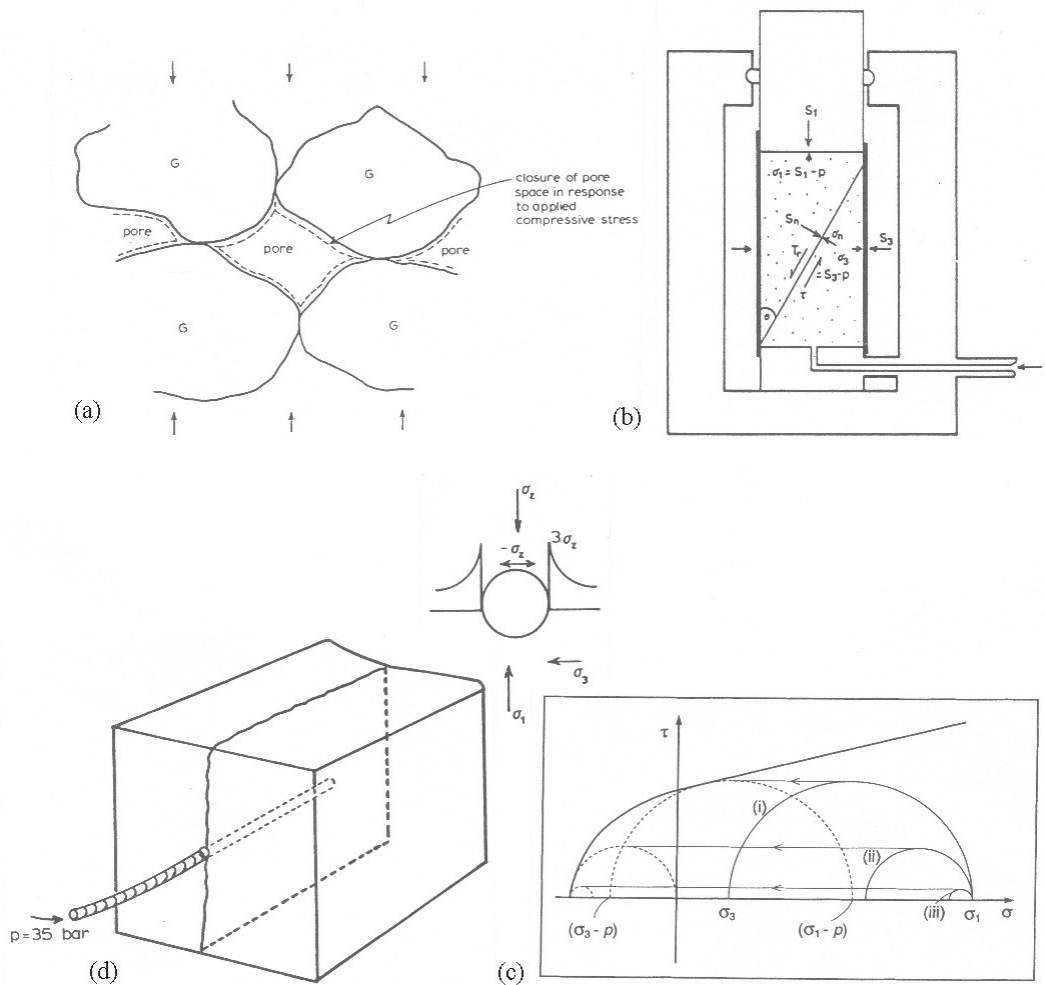


Figure 4-1. a) Figure showing how the flattening of the grains (G) at their points of contact during compression can materially change the volume of the pore spaces. b) Total and effective stresses in a triaxial test in which it is assumed that $\sigma = S - p$. c) Mohr circles for the applied stress (solid) and effective (dashed) stress states. The effect of a fluid pressure is to move the circle to the left. d) Diagrammatic representation of a cube of rock in which a single hydraulic fracture has developed in response to a fluid pressure. The stress distribution around the hole due to the body weight of the block is shown in the accompanying diagram. This gave rise to a differential stress with the least principal stress acting horizontally, so determining the orientation of the hydraulic fracture. a) b) and d) from /Fyfe et al, 1978/.

The net effect of such a fluid pressure will be to reduce the influence of the external, applied stress, so that the material behaves as though it is subjected to an 'effective stress', which can be significantly smaller than the applied stress. In this model in order to determine the magnitude of the 'effective stress' it is necessary to know the bulk compressibility of the rock and of the fluid. However, it is possible to carry out an experiment where the pore fluid pressure is not derived from or dependant upon the externally applied stress, but is controlled and maintained from an external reservoir, as indicated in Figure 4-1b. If a porous and permeable rock specimen is covered in an impervious jacket and a pore-fluid pressure p is maintained externally, then if the

specimen is subjected to external stresses, σ_1 and σ_3 , it is argued /Hubbert and Rubey, 1959/ that the law of effective stress, Equation 4-1a, holds and that the effective principal stresses are:

$$\sigma_{1e} = \sigma_1 - p \quad 4-1b$$

$$\sigma_{3e} = \sigma_3 - p \quad 4-1c$$

If the two states of stress are drawn as Mohr circles, Figure 4-1c, then the effect of the increase in fluid pressure becomes clear. The Mohr's stress circle is driven to the left by an amount equal to the fluid pressure. If as a result, it hits the failure envelope then the failure that occurs is called fluid induced or hydraulic fracturing.

Hydraulic fracturing consists in initiating, then propagating a fracture with water pressure as the source of energy. The more general term of Fluid induced failure is used in geology as there are a variety of fluids in addition to water that occur in the Earth's crust. The terms are used in this text interchangeably.

/Fyfe et al, 1978/ argue that this mechanism is perhaps the most important single mechanism of deformation operating in the upper crust. Hydraulically induced fractures range in scale from the microscopic to the regional scale. For example at the microscopic scale it is of prime importance in the development of cataclasis. On an intermediate scale it results in fractures such as joints. Hydraulic fractures are responsible for many veins that may range in size from the microscopic to that of the 'Mother Lode' in California. It can also account for the development of concordant and discordant sheet like intrusions.

An experiment where failure is induced in a block of rock by the application of a fluid pressure in a pre-existing hole is shown in Figure 4-1d. It can be seen that the rock failed along a vertical fracture. The orientation of the fracture was determined by the orientation of the hole and the fact that the body weight of the block resulted in a small vertical stress. Thus the rock failed by forming a fracture parallel to the maximum principal compressive stress, when the water pressure exceeded the confining pressure, σ_3 , plus the tensile strength, T, of the rock. This condition for the formation of hydraulic fracturing can be written:

$$\sigma_3 = p + T \quad 4-2a$$

This expression is a satisfactory criterion of failure when, as here, the fluid pressure 'p' is External to the system. From a geological point of view this model of external fluid pressure is often appropriate. Fluids which are external to a single bed or sequence of beds may accumulate in the crust and then, providing the correct rock and fluid pressure exist, hydraulic fractures may develop in the adjacent beds. However, when the fluid pressure exists only within some specific bed or unit it is necessary to consider the mechanism of hydraulic fracturing more carefully.

In the example shown in Figure 4-1d and in the discussion leading to the development of Equation 4-2a, it is clear that the mode of failure induced by the high fluid pressure is Mode I i.e. extensional failure. In order to understand in more detail the process of fluid induced fracture better it is useful to consider briefly the theory of extensional failure. It can be shown that the theoretical Tensile strength of an ideal crystalline solid is immense. In fact the tensile strength, T_B , necessary to disrupt the atomic bonds is given by $T_B = E/10$, where E is Young's modulus. Consequently, the ideal tensile strength of many rocks should be close to 10^5 bars (1.4×10^6 lb./in.²). There is therefore an observed discrepancy between the ideal and actual tensile strength of a material which

frequently approaches three orders of magnitude. /Griffith, 1924/ suggested that this vast discrepancy could be attributed to the intense local stress concentrations that develop in the vicinity of the microscopic flaws. In his theoretical analysis, he considered a homogeneous and isotropic solid containing randomly oriented elliptical flaws, which were subjected to a ‘macroscopic’ i.e. far-field stress. He showed that there was a stress concentration which formed at the tips of the flaws and that the magnitude of this stress magnification depended upon the orientation of the flaw (it is largest when the flaw has its long axis perpendicular to the axis of minimum principal compression, σ_3) and its shape. The more eccentric the ellipse the greater the magnification.

Griffith suggested that the ‘hairline’ cracks within a rock could be likened to elliptical cracks with eccentricities (ratio of long to short axes) of many hundreds or even thousands. He argued that in this way the application of a relatively small remote macroscopic stress could, by this process of stress magnification at crack tips produce local stresses sufficient to overcome the strength of the atomic bonds. Thus the most suitably oriented and most eccentric flaws will propagate first. This propagation increases the eccentricity and resultant stress magnification causes further propagation leading to a catastrophic growth of the fracture and macroscopic failure.

Stress magnification around circular and elliptical flaws has been quantified by /Kirsch, 1898/ and /Inglis, 1913/ respectively. Inglis recognised that an elliptical hole in an elastic plate concentrates stress in proportion to the ration c/b of the semi axes of the ellipse, Figure 4-2a. This can be written:

$$-\sigma_t = -\sigma_h[1 + 2c/b] \quad 4-2b$$

where

$-\sigma_t$ is the local tip stress,

$-\sigma_h$ is the applied far-field tensile stress and

c and b the semi long and short axes of the ellipse respectively.

For a circular hole, $c/b = 1$ and it follows from Equation 4-2b that $\sigma_t = 3\sigma_h$ i.e. there is a threefold stress magnification, Figure 4-2a. Several details concerning stress magnification are important. First stress at the edge of an elliptical hole can become much larger than the average stress to which the material is subjected. Second the stress magnification depends on the shape of the hole not its size. Third, for an elliptical hole the stress magnification increases in inverse proportion to the radius of curvature, r_c , at the narrow end of the ellipse:

$$r_c \sim b/c. \quad 4-2c$$

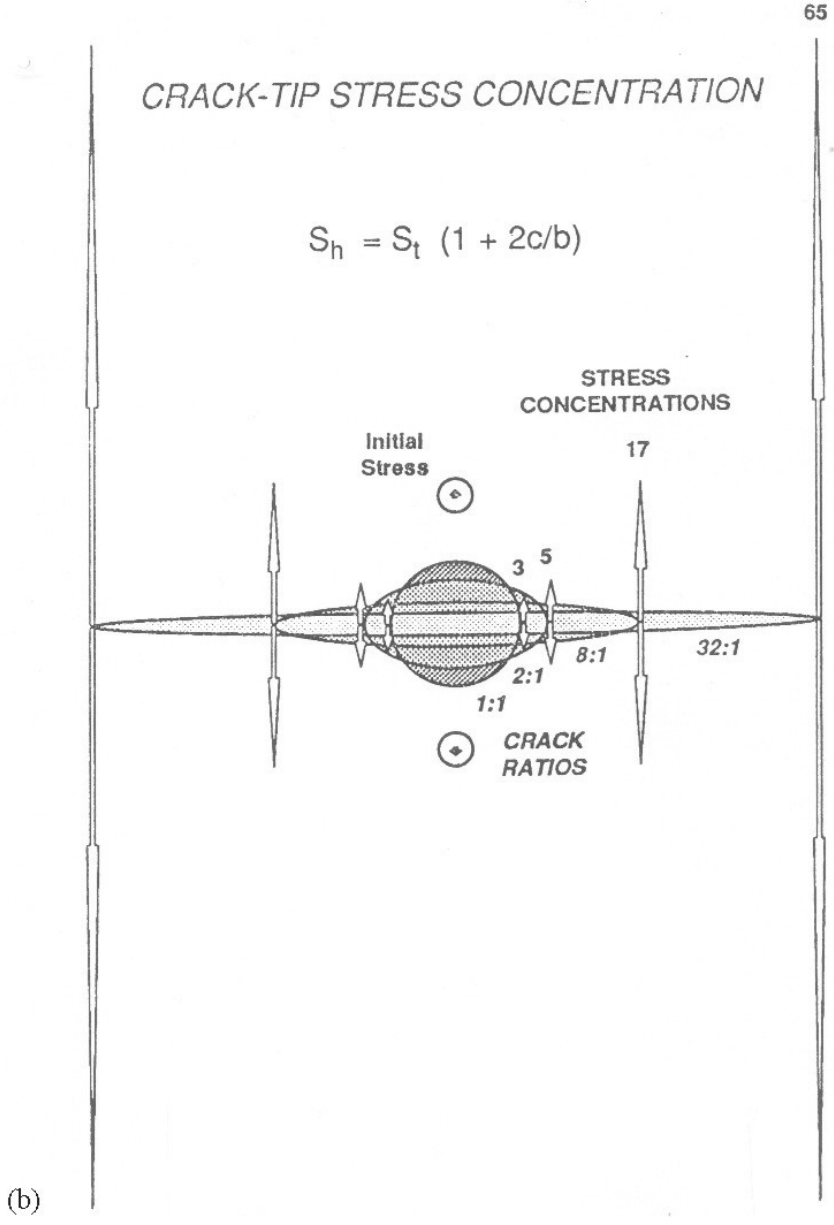
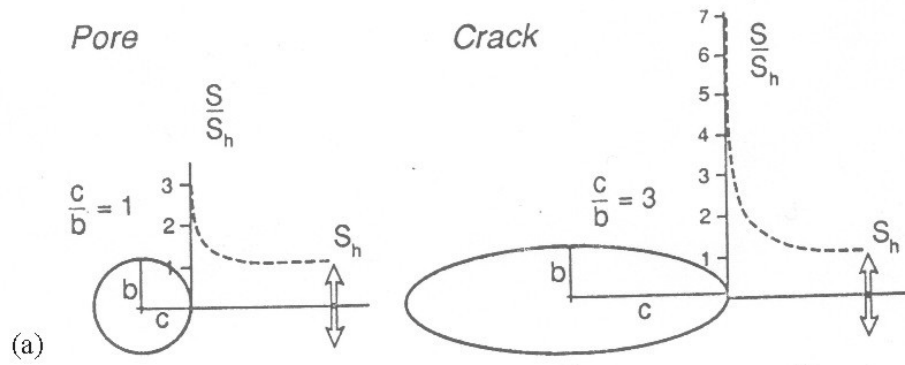


Figure 4-2. a) Stress concentration around a circular pore and an elliptical crack. b) Variation in stress concentration as a function of crack aspect ratio. From /Engelder, 1992/.

Many flaws in rocks are not round pores but rather penny shaped cracks which have the shape of ellipses in cross section. The stress concentration at the tips of these elliptical cracks becomes extreme as the axial ratio increases. This point is illustrated in Figure 4-2b where a far field compression is magnified 65 times at the tip of an elliptical crack with an axial ratio of 32:1.

/Secor, 1968/ used Griffiths Criteria of extensional failure to explain the mechanism of hydraulic fracturing. In this study he modified the conceptual model proposed by Griffith in which a homogeneous, isotropic rock contained a randomly distributed series of flaws of various sizes and eccentricities. In the Secor model these flaws are assumed to be sufficiently spaced one from the other so that the micro-stress fields associated with one flaw did not interfere with that of the nearest adjacent flaw. However, it was also assumed that the flaws were interconnected by series of channels through which fluids could flow, so that all flaws initially contained fluid at some specific initial pressure, p_i , Figure 4-3a.

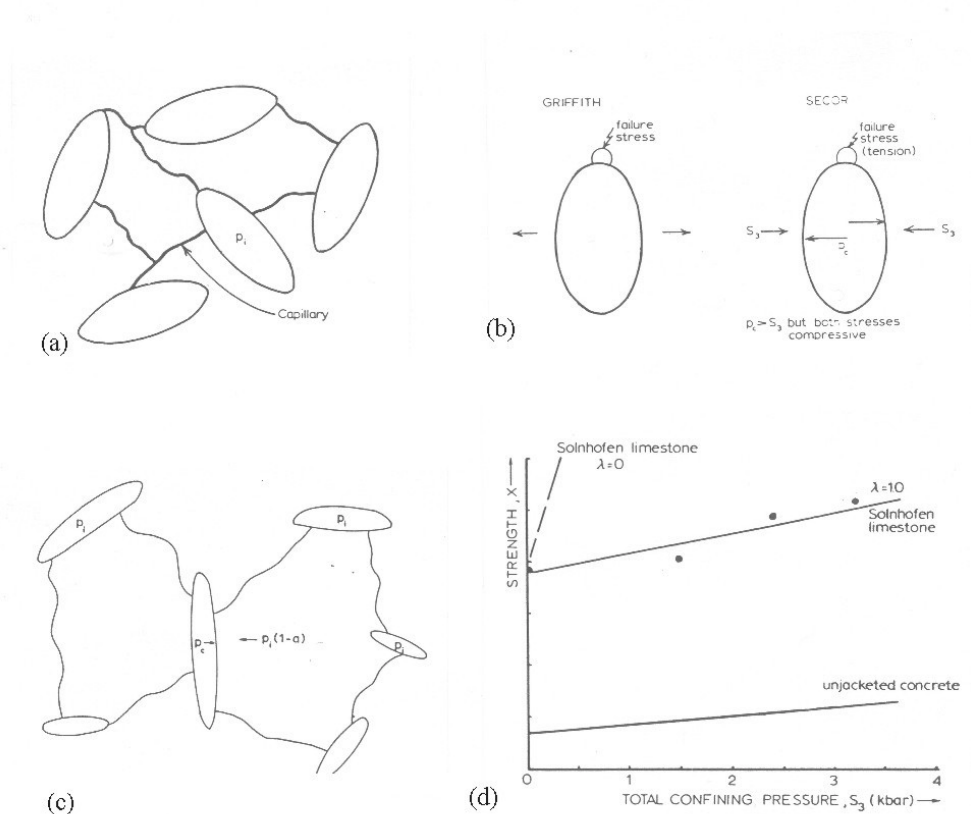


Figure 4-3. a) Hypothetical model indicating randomly oriented flaws interconnected by a network of capillary channels. b) Comparison of the Griffith model is concerned with real tensile stresses while the Secor model deals with effective tensile stresses. c) A hypothetical model indicated in a) but here it is assumed that the effective stress is given by $\sigma = S - p(1-a)$. It can be seen that if $p_i > p_c > p_i(1-a)$ the flaw can propagate. d) Data indicate small increase of strength at high confining pressures even when $S_3 = p$, for concrete (data from /McHenry, 1948/) and Solnhofen limestone (data from /Rutter, 1970/). From /Fyfe et al, 1978/.

It was then argued that when the pore fluid pressure in the most suitably oriented, large, eccentric, flaw exceeded the least principal stress by an amount equal to the tensile strength of the rock, the conditions comparable with that for the Griffith-type tensile failure obtain, Figure 4-3b. An important point to note is that in this model all the macroscopic (i.e. far-field) stresses are compressive. Only the effective stress (σ_3-p) and the microscopic stresses near the tip of the flaw are tensile.

Secor continues the argument by suggesting that when $\sigma_3-p = T$ the ‘critical’ flaw propagates. However, when propagation takes place, the flaw experiences an infinitesimal and virtually instantaneous increase in volume. This rapid volume increase is automatically accompanied by a decrease in the fluid pressure from p_i to p_c in the hitherto propagating flaw so that further propagation momentarily ceases. The fluid pressure in the adjacent flaws is unaffected by this propagation in the ‘critical’ flaw and therefore there exists a hydraulic potential between the critical and adjacent flaws given by (p_i-p_c) . It is then argued that fluids will migrate through the postulated interconnecting passageways into the critical flaw until the fluid pressure p_c approaches p_i and further propagation takes place. Secor suggests that this whole sequence is repeated many times until the critical flaw develops slowly into a macroscopic ‘tension’ or ‘extension’ fracture.

Unfortunately the analysis presented by Secor contravenes the ‘Simple Law of Effective stress’ i.e.

$$\sigma_e = \sigma - p \quad 4-3$$

where σ_e is the effective stress and σ the lithostatic stress. The ‘Simple Law of Effective stress’ given in this equation depends upon the assumption that the influence of the pore fluid pressure p is felt equally, everywhere in the body of rock. One can represent the mechanical situation required by both the Secor Model and the Simple Law of Effective Stress, as indicated by Figure 4-3c. It can be seen from the diagram that because both models require that the fluid pressure p_c and the general fluid pressure p_i , in the remainder of the rock, act over the whole length l of the flaw, propagation of the flaw is only possible if $p_c > p_i$.

This situation can be obtained only when the fluid pressure is supplied externally (e.g. Figure 4-1d). In such a situation a hydraulic gradient would exist so that fluid may migrate out of the fracture into the rock. Many examples of fractures in the field show that there has been a mass outward migration of fluids resulting in a staining of the rock adjacent to the fracture. However, evidence also exists in the form of spalled fragments of country rock incorporated in the vein material within a fracture, that fluids can also move into fractures from the country rock.

This problem can be overcome, for it can be inferred that the Secor model is not incompatible with hydraulic fracturing provided that the rock mass does not obey the Simple Law of effective stress given by equation 4-1a, but does obey the more ‘General Law’ expressed by equation 4-4.

$$\sigma_e = \sigma - p(1-a) \quad 4-4$$

where a is a dimensional constant and can be considered as a factor which reduces the efficiency of p . Thus the configuration of stresses represented in Figure 4-3c satisfies where both the Secor model and the General Law of effective stress provided that $p_c > p_i(1-a)$, even though $p_i > p_c$.

Confirmation that rock types which obey the Simple Law of effective stress behave in a markedly different manner to those which obey the General Law has inadvertently been obtained when experiments conducted at high confining pressures and also high pore pressures, go wrong. Thus, in such a test on Solenhofen limestone (a rock which obeys the General Law of effective stress), if failure of the seal occurs, there follows a catastrophic and abrupt loss of confining pressure σ_3 . The high pore-fluid pressure results in tensile fracture of the rock on one or more planes parallel or sub-parallel to the long axis of the specimen. Carrara marble however, obeys the Simple Law of effective stress and if in a test of the type described above there is an accident and an abrupt loss of confining pressure, the specimen of marble fails, not by one or more fractures but by 'disaggregation', i.e. the specimen is turned into calcite sand.

/Fyfe et al, 1978/ point out that many rocks, especially those with large grains and relatively high porosity, obey the simple law of effective stress exactly. Some rocks, and some soils and other materials appear not to.

For example, in tests on concrete in which the pore fluid pressure was maintained equal to the total confining pressure, the relationship between the total principal stresses σ_1 and σ_3 at failure and similar results obtained from tests on Solenhofen limestone, are shown in Figure 4-3d. In both examples it is evident that the law of effective stress as defined by Equations 4-1, is not exactly obeyed. It can be seen from this figure that the strength X at a total confining pressure of 3kbars is equivalent to the strength the rock exhibits if subjected to a real confining pressure of 100bars.

Similar observations caused workers in soil mechanics to propose that the Law of Effective Stress should be expressed in an identical form to Equation 4-4. It was argued that 'a' is a material constant which is zero for some rocks but which may attain a value of 3–5% in many rock types and in some soils.

Based on intuitive arguments, /Skempton, 1961/ suggested that

$$A = K_b/K_m \quad 4-5$$

where K_b and K_m are the bulk modulus of the whole rock or soil, and the constituent mineral respectively. This suggestion was later substantiated by /Nur and Byerlee, 1971/ using a more rigorous approach.

/Engelder's, 1992/ approach to understanding the effect of pore pressure on stress and ultimately on brittle failure focuses more on fracture mechanics than that of Fyfe, Price and Thompson described above.

In his discussion of the effect of Pore Pressure on Stress he notes, quoting /Terzaghi, 1943/ and /Hubbert and Rubey, 1959/, that the introduction of pore fluid under pressure has a profound affect on the physical properties of porous solids. Most physical properties of porous rock obey a law of effective stress that depends on the difference between pore pressure, p, and applied stress, σ :

$$\sigma_e = \sigma - p \quad 4-1a$$

The magnitude of the Tensile effective stress ($\sigma_{3e} = \sigma_3 - p < 0$) in the earth is maintained within certain bounds by the rock strength. In this case the limiting strength parameter is the fracture toughness rather than the shear strength of intact rocks or frictional strength along existing fractures which are the limiting strength parameters for shear failure and reshear. Failure under $\sigma_3 < 0$ is by tensile crack propagation rather than shear crack

propagation or frictional slip. Two general situations lead to the development of tensile conditions:

- First, $\sigma_{3e} < 0$ may develop if p approaches lithostatic stress by one of several mechanisms /Hubbert and Rubey, 1959/.
- Second, $\sigma_{3e} < 0$ may also develop if p remains at hydrostatic levels but $\sigma_{3e} = \sigma_{h \min}$ (the minimum horizontal stress) is reduced by thermal cooling and lateral contraction accompanying uplift and erosion /Haxby et al, 1976; Narr and Currie, 1982/. $\sigma_{3e} < 0$ is most commonly achieved in the upper crust in the presence of a significant fluid pressure, p , while σ_3 is compressive. The differential stress, $(\sigma_1 - \sigma_3)$, does not factor directly into limiting σ_{3e} , nor does tensile crack propagation act to limit or reduce it. However, the differential stress must be relatively low as p increases or the rock will fail in shear before tensile conditions develop.

4.2.2 Poroelastic Behaviour

The influence of pore pressure on total stress is best described in the context of poroelastic behaviour. Total stress is defined by rearranging Equation 4-1a:

$$\sigma = \sigma_e + p \quad 4-6$$

Such a rearrangement indicates that the term total stress and applied stress have the same meaning. Applied stress is used in the laboratory to indicate the stress a piston transfers to a test cylinder of rock. That piston not only has to push on the sample but it also has to resist the outward force exerted by any pore fluid. A change in p within the rock cylinder is counterbalanced by a change in load on the piston to maintain the original shape of the sample. Total stress is often used if one wants to make it clear that stress across some boundary is a combination of rock matrix stress plus pore pressure.

Equation 4-6 suggests that pore pressure is totally transferred to an arbitrary boundary from the internal portion of an aggregate. Such is indeed the case for sand but not so for rock consisting of grains with elastic grain-grain contacts and pore space between the grains. Imagine a rock of grains, elastic grain-grain contacts, and pore space connected so that the rock has a relatively high permeability. The rock is placed in a container with rigid walls but open at the top (i.e. the uniaxial-strain model applies) (Figure 4-4).

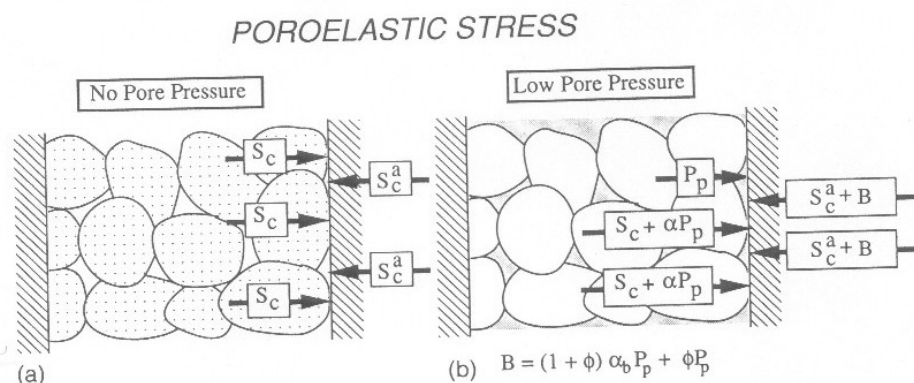


Figure 4-4. The effect of changing pore pressure p on the total stress exerted by a rock against the rigid walls of a container. a) Dry rock. b) Rock with pore fluid at pressure = p . From /Engelder, 1992/.

Assume that contacts between grains and the rigid wall are totally impermeable. Initially the rock is dry so that the grains press against the rigid walls of the container with an average stress, S_c^a . The actual stress under the grain contacts, S_c is larger:

$$S_c = [1/(1-\Phi)] S_c^a \quad 4-7a$$

where Φ is the porosity of the rock, which represents the percentage of open pore space against the wall of the container. The container is then filled with a pore fluid at a relatively low pressure, p . Assume that pore fluid cannot penetrate the grain-container wall contact. The addition of pore fluid will not cause a uniform increase in stress along the wall of the container. Where pore fluid is in direct contact with the wall, the pressure on the wall will increase by p . Where grains are in contact with the wall the normal stress on the wall will increase by a fractional portion of p . The average total stress, S_h , on the wall of the container will increase by less than p according to:

$$\Delta S_h = \Phi p + (1-\Phi)\alpha_b p \quad 4-7b$$

This fractional increase in normal stress arises because the grains are connected by cement so that the elastic contacts take up part of the force exerted by pore fluid inside pores. This partial transfer of pore pressure to the container wall is known as the 'poroelastic effect' /Biot, 1941/.

In basins subject to a high fluid pressure, p , the total vertical stress, σ_v , is still calculated by the standard equation;

$$\sigma_v = z.\rho.g \quad 4-8$$

where z is the depth, ρ the density of the overburden and g the acceleration due to gravity. The poroelastic effect does not apply to the vertical stress largely because the surface of the Earth does not act as a fixed boundary and strain is allowed to absorb any increase in pore fluid pressure. To look at the effect of p on the horizontal stress one defines a tectonically relaxed basin as one in which σ_h is proportional to σ_v through the uniaxial elastic strain model /e.g. Engelder, 1992, Equation 1.17/:

$$\sigma_h = [v/(1-v)]\sigma_v = [v/(1-v)] z.\rho.g \quad 4-9$$

Solving Biot's elasticity equations for uniaxial strain yields

$$\sigma_h = [v/(1-v)]\sigma_v + [(1-2v)/(1-v)]\alpha_b p \quad 4-10$$

4.3 The stress-pore pressure relationship at fracture initiation

We will now briefly examine the situation associated with the initial propagation of fracture within an intact body of rock. Here we want to understand the stress conditions that favour fracture propagation within fracture-free "young" rocks. Except for fracture propagating above the water table where total stress may be tensile /e.g. Schmitt, 1979/, propagation takes place when fluid pressure (p_i) in the initial flaw or pre-existing crack is larger than the total stress (σ_3) acting to close that flaw or initial crack. Based on LEFM (Linear Elastic Fracture Mechanics) /Engelder, 1992/ shows that the amount by which p_i needs to exceed σ_3 in order to propagate the fracture depends on fracture toughness, K_{Ic} , crack length $2c$, and shape Y (Y is different for different shapes /see Sih, 1973/, e.g. for a penny shaped crack $Y = 2/\sqrt{\pi}$).

$$p_i = [K_{Ic} / Y \sqrt{c}] + S_h$$

4-11

where p_i , which produces a net tension on the initial crack, must counterbalance the remote compressive stress, S_h , as well as the fracture toughness. In deriving Equation 4-8 it is assumed that the wall of the crack is impermeable. Experiments on crack propagation have shown that cracks will propagate when the stress intensity factor $K < K_{Ic}$ at the crack tip. This phenomenon is a process called sub-critical crack growth and is permitted by a chemical reaction at the crack tip, known as stress corrosion, which acts to weaken the atomic bonds in the vicinity of the crack tip. Under the influence of stress corrosion, crack propagation may take place at velocities less than 1mm/sec. In contrast, when cracks propagate under tip stresses equal to K_{Ic} , the cracks travel unstably at speeds that may approach the shear wave velocity of the host rock.

It should be noted that while the rules for fracture initiation apply even if the pore fluid pressure p is hydrostatic, fluid pressures within the crust are frequently abnormally high. There are a number of mechanisms for the development of abnormally high fluid pressure in the schizosphere. Two basic classes of mechanisms are dynamic mechanisms, which lead to steady-state high pressures through continual recharge, and transient mechanisms, which cause a momentary production of fluids or pressure, followed by a pressure drop accompanying leakage. Note that all rocks have an intrinsic permeability, which will eventually allow abnormal pressures to bleed to hydrostatic unless they are renewed. Dynamic mechanisms include artesian flow from topographic highs /Toth, 1980/. Quasi-dynamic mechanisms include the release of gas during the maturation of hydrocarbons /Tissot and Welte, 1978; Hunt, 1989/. Transient mechanisms include pore collapse during compaction under overburden load /Magara, 1978; Bethke et al, 1988/; tectonic compaction /Berry, 1973/, clay dehydration /Powers, 1967/; and aquathermal pressuring /Barker, 1972/. Rapid uplift and decompaction can lead to abnormally low pressures /Russell, 1972/.

However, there are several reasons why, even with a high crack-driving pressure, it is not intuitively obvious that a net tensile stress can be generated within an initial flaw. For example:

1. if uniaxial-strain behaviour is assumed, a normal stress acting to close the flaw increases as a function of the pore pressure p ;
2. excess fluid pressure can readily drain from the initial flaw into other pore space; and so
3. pores of the rock behind the flaw are also subject to the same pressure.

One explanation for joint initiation is found in the poroelastic behaviour of rock, which is responsible for the generation of a net tensile stress against the face of a flaw. Poroelastic behaviour is illustrated using a model of the force-balance along the flaw-rock interface where the initial condition is that the average normal stress across the rock-flaw interface exceeds the fluid pressure within the flaw and, therefore the flaw is closed Figure 4-5. Consider the effect of increasing pore pressure by an amount, Δp , so that fluid pressure in the flaw, $p_f = p + \Delta p$. p_f is balanced by $p + \Delta p$ where pore space is against the interface. But by the poroelastic effect (Equation 4-7b), the pore pressure increase does not cause the average normal stress on the rock side of the interface to increase at the same rate as p_f . Hence, as p continues to increase, p_f will eventually exceed the average normal stress exerted by grains on the interface. Once this condition is reached a net tensile force will act to compress the rock and push the fracture-rock interfaces apart. At this point $p_f = p_i = p$. Joint initiation occurs only after the crack

(i.e. initial flow) walls are pulled apart or subject to a net tensile stress as a consequence of the poroelastic effect. For the case of initial propagation of a vertical fracture, Equations 4-10 and 4-11 are combined to account for fracture toughness, poroelastic behaviour, and stresses arising from fixed vertical boundaries:

$$P_i = \left\{ \frac{K_{Ic}}{Y\sqrt{c}} \right\} + \frac{\nu}{1-\nu} S_v + \frac{(1-2\nu)}{(1-\nu)} \alpha_b P_p \quad 4-12$$

This equation indicates that the fluid pressure needed for fracture initiation, p_i , can vary significantly depending on the size of the pre-existing crack. Again, for the initial propagation of a fracture $p_i = p$.

In a more recent discussion of fluid induced fracturing, /Mandl, 1999/, carefully separates two modes of fluid induced failure terming them Internal and External hydraulic fracturing. He points out that an analysis of these problems requires an understanding of the stress-strain laws for elastic porous rocks.

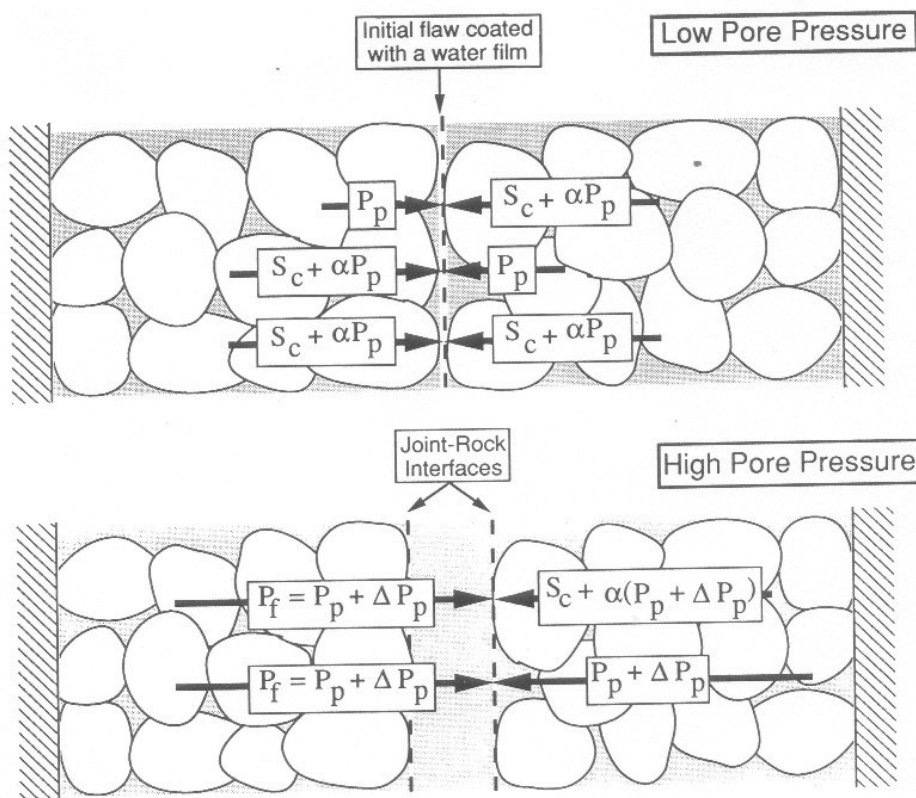


Figure 4-5. Poroelastic model for a rock with an initial flaw and constrained by rigid boundaries on all sides. The model consists of grains, elastic grain-grain contacts, and interconnected pore space. Vectors are shown to represent the balance of forces along the initial flaw interface and the joint-rock interface. From /Engelder and Lacazette, 1990/.

Mandl agrees with previous workers in arguing that at some depth in the Earth's crust all total stresses are compressive, and the formation of extension fractures requires fluid pressures which overcome the tensile strength of the rock and push aside the rock walls against the action of the total rock pressure. He notes that this fluid induced or hydraulic fractures may start from micro fractures or flaws inside a bed or from irregularities at bed boundaries, when the pore pressure inside the bed is uniformly raised to a sufficient level, or the bed is ruptured by the 'wedging' action of a highly-pressured fluid injected from outside. The first type of extension fractures he calls internal hydraulic fractures, the second type hydraulic intrusion fractures. The two fracture types are schematically shown in Figure 4-6 for horizontal layers.

Internal hydraulic fracturing (Figure 4-6A) requires that a rise in pore pressure $\Delta p > 0$ reduces the smallest effective stress to the value of the tensile strength T of the material. During the process of overpressuring, the rock layer may be allowed to extend or it may remain laterally confined. We consider two extreme boundary conditions:

1. where interlayer shear resistance is negligibly small, and the layer is completely free to expand in elastic response to a uniform pressure rise Δp , and
2. where the layer is confined and not allowed to extend in lateral directions. In both cases, the principal stresses remain vertical and horizontal during the rise in pore pressure, with $\sigma_1 = \sigma_v$ and $\sigma_3 = \sigma_h$. But σ_h behaves differently in the two cases.

When the layer is free to extend in horizontal directions the total normal stresses σ_v and σ_h remain unchanged. Hence, all normal effective stresses are reduced by the pore pressure Δp , and the Mohr circle in Figure 4-7A is shifted towards the tension domain without change in diameter. Note that, in order to satisfy the second condition for tensile fracturing in the figure, σ_3 must be smaller than $3T$, at the onset of fracturing.

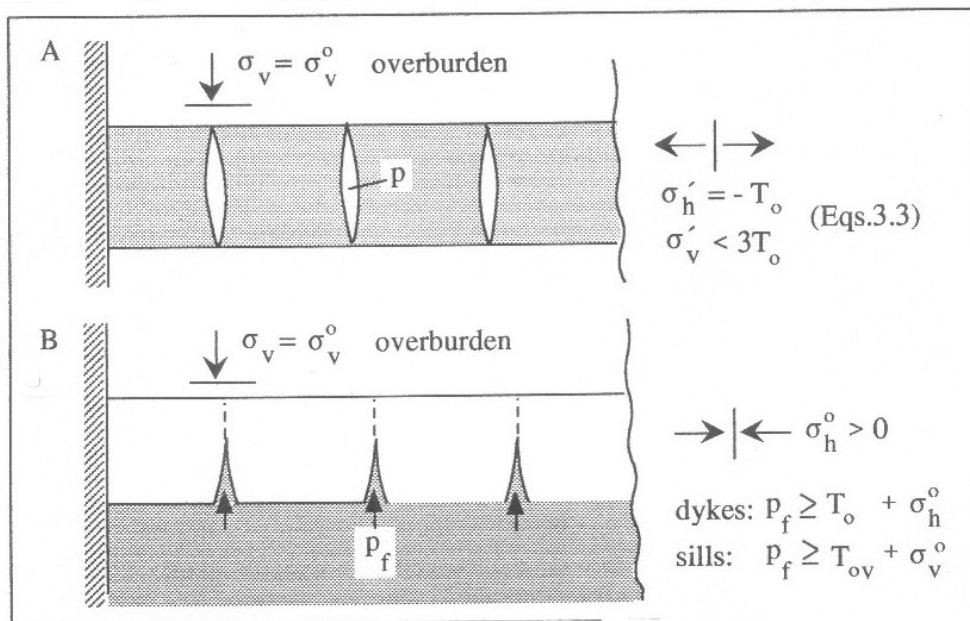


Figure 4-6. Hydraulic extension fractures: A) internal fractures, B) intrusion fractures. From Mandl, 1999/.

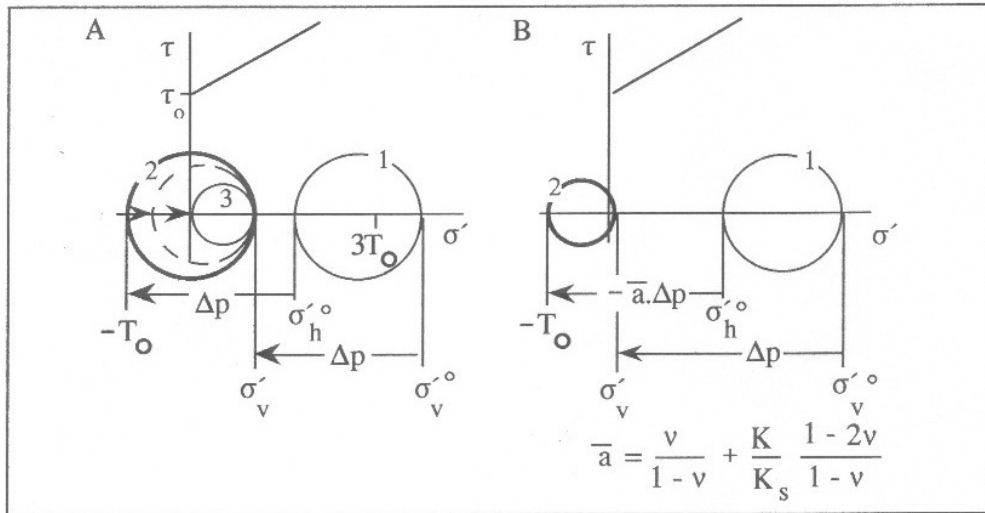


Figure 4-7. Mohr diagrams of stress changes in horizontal layer due to rise in pore pressure: A) unrestrained layer, B) laterally confined layer. From /Mandl, 1999/.

Since the differential stress ($\sigma_1 - \sigma_3 = \sigma_v - \sigma_h$) remains constant during the rise in pore pressure, and $\sigma_h = T$ the tensile strength at the onset of fracturing, the condition $\sigma_v - \sigma_h < 4T$ must be satisfied. Relating the horizontal stress σ_h of the tectonically undisturbed layer to σ_v , by the empirical parameter $K_0 = \sigma_h / \sigma_v < 1$, the condition becomes;

$$\sigma_v < 4T / (1 - K_0) \quad 4-12a$$

where σ_v and T are in MPa. This imposes a restriction on the depth down to which the hydrofractures can be generated. If the overburden has an average density of 2500 kg/m^3 and the pore fluid is water under normal hydrostatic conditions, increases by 15 MPa per km depth. The limit distance from the free surface is then:

$$z_{\text{lim}} = 4T / 15(1 - K_0) \quad 4-13$$

where z_{lim} is in kilometres and T in MPa. Choosing reasonable values for T and K_0 , the limit depth becomes a few kilometres.

Next, we consider the case where the layer is laterally completely confined, but can still deform in vertical direction against the constant overburden load σ_v . Assuming material isotropy in all horizontal directions, all horizontal stresses will change by the same amount $\Delta\sigma_h^*$ when the pore pressure is increased by Δp . Inserting $\Delta e_1 = \Delta e_2 = 0$ in the poroelastic relations /Mandl, 1999, Equation 5.25/ for the horizontal x_1 and x_2 axes gives the relationship between changes in vertical and horizontal general effective stresses:

$$\Delta\sigma_h^* = [v/(1-v)]\Delta\sigma_v^* = -a \cdot [v/(1-v)]\Delta p \quad 4-14$$

or, in terms of the horizontal effective stress, Equation 4-4 ($\sigma_h' = \sigma_h^* - p(1-a)$)

$$\Delta\sigma_h' = -a^* \cdot \Delta p \quad 4-15$$

with $a^* = 1 - a \cdot (1 - 2v)/(1 - v)$, and $a = 1 - K/K_s$.

Thus, the horizontal effective normal stress decreases much less than the vertical effective stress. Therefore, the stress circle in Figure 4-7B shrinks, while it is shifted towards the tension regime by the increase in the pore pressure.

4.4 The expression of hydraulic fractures in rocks and sediments

The forgoing discussions assume that the mode of fluid induced failure is Mode I i.e. extensional failure. However, as is discussed in the following section it can be argued that high fluid pressures can also give rise to shear failure. In fact the expression of fluid induced failure in rocks can be extremely varied ranging from the fluidisation of an unconsolidated clastic sediments through randomly oriented extensional fractures that, if close enough together can generate a breccia texture, to aligned extensional fractures and finally conjugate shear fractures. This discussion is a brief summary of a paper by /Cosgrove, 1995/.

The stress conditions necessary for the formation of shear and tensile failures are shown in Figure 4-8. In this figure the Navier-Coulomb criteria of shear failure and the Griffith criteria of tensile failure are expressed graphically, and the stress states are represented by Mohr circles.

In order for tensile failure to occur the Mohr circle must touch the brittle failure envelope at the point $\tau = 0$, $\sigma_3 = T$ where T is the tensile strength of the rock. It follows from the geometry of the failure envelope (Figure 4-8) that this can only occur if the diameter of the Mohr circle (the differential stress $\sigma_1 - \sigma_3$ is small, i.e. $< 4T$. Mohr circles representing four stress states that satisfy these conditions are shown in Figure 4-9, and in the following section the orientations of the fractures that form in response to these stresses are discussed.

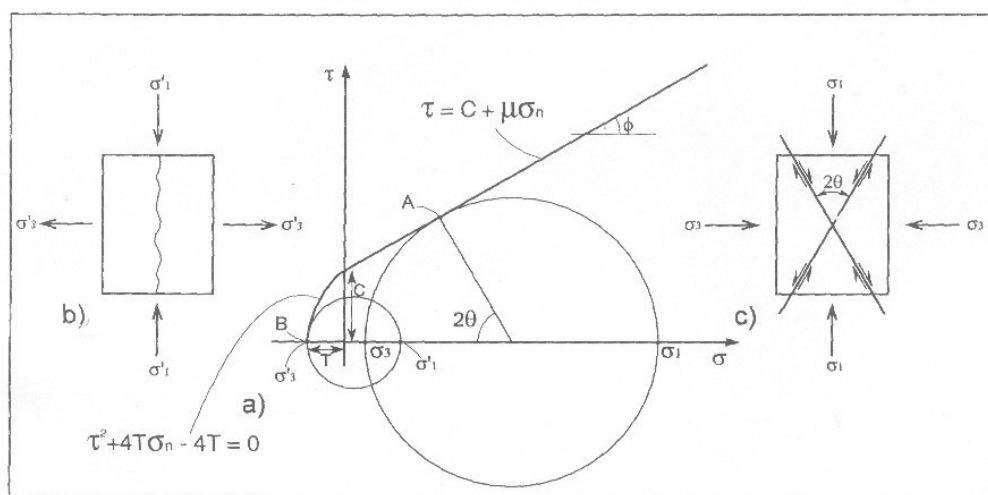


Figure 4-8. The graphical expression of the two brittle failure criteria (shear and extension) and Mohr circles representing stress states capable of causing tensile (a) and shear (b) failures.

4.4.1 The orientation of fluid induced tensile fractures

Consider the orientation of fractures that form in response to the range of differential stress states represented by the Mohr circles shown in Figure 4-9, all of which satisfy the conditions for tensile failure. The differential stresses vary from just $<4T$ (circle i Figure 4-9) to zero ('circle' iv, Figure 4-9). Note that when the differential stress is zero, the stress state is hydrostatic and the Mohr circle collapses to a point.

Tensile fractures form parallel to the maximum principal compressive stress, σ_1 , i.e. they open in the direction of the minimum principal stress, σ_3 (Figure 4-8a). Thus, in the stress state represented by Mohr circle i in Figure 4-9, which has a relatively large differential stress, there is a definite direction of easy opening for the tensile fractures, i.e. parallel to σ_3 . The fractures would therefore exhibit a marked alignment normal to this direction (Figure 4-9b i). However, for the stress states represented by the Mohr circles ii–iv, the differential stress becomes progressively smaller until, for the hydrostatic stress represented by Mohr 'circle' iv, the differential stress is zero. In a hydrostatic stress field the normal stress across all planes is the same and there is therefore no direction of relatively easy opening for the tensile fractures. Thus, the fractures will show no preferred orientation and, if they are sufficiently closely spaced and well developed, will produce a brecciation of the rock (Figure 4-9b, iv). It is to be expected, therefore, that as the differential stress becomes progressively lower (stress states i–iv Figure 4-9), so the tendency for the resulting tensile fractures to form a regular array normal to σ_3 decreases. Tensile fracture systems ranging from well aligned fractures to randomly oriented fracture arrays are to be expected in rocks, and field observations (Figure 4-10a and b), support this idea.

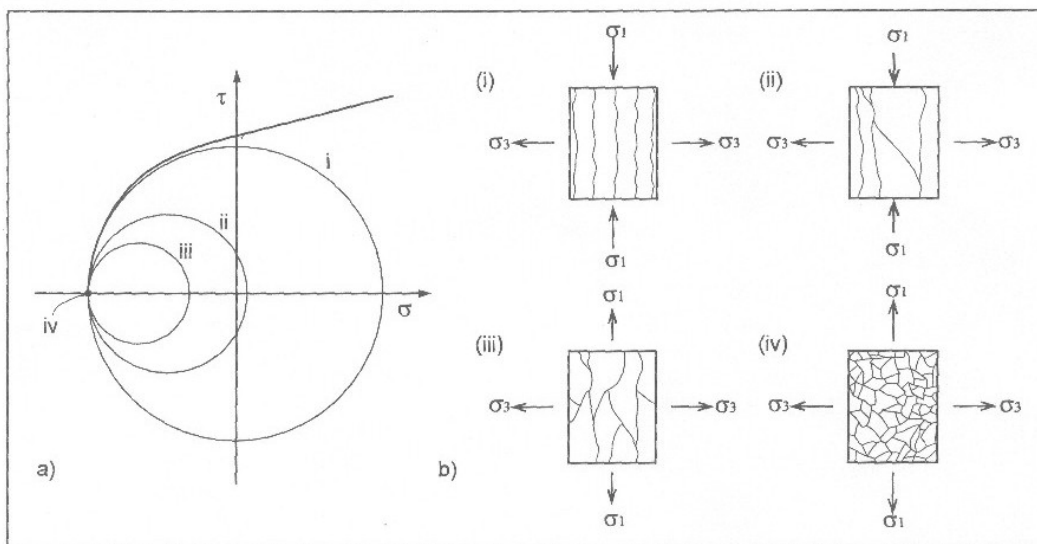
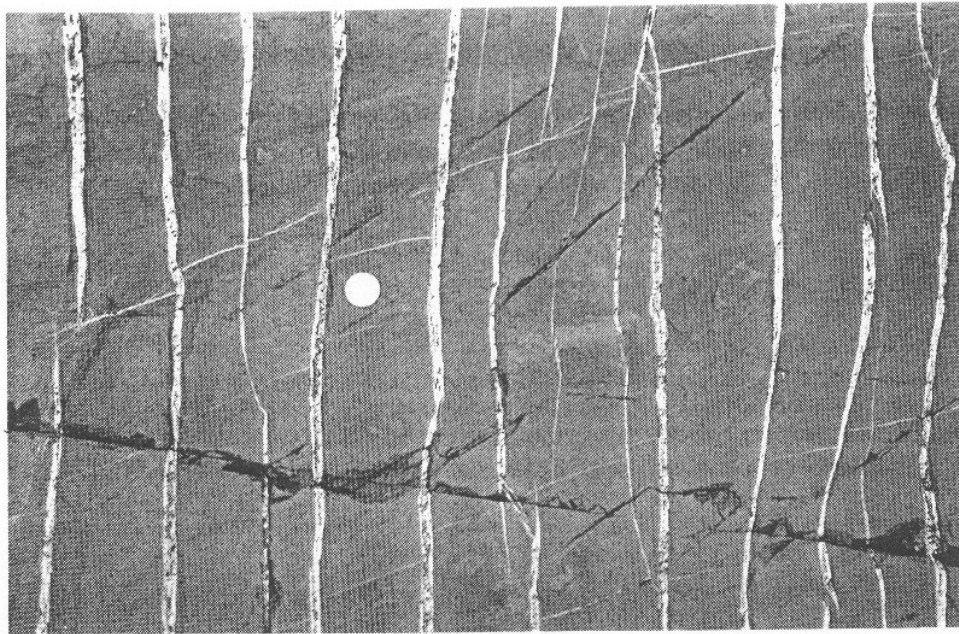


Figure 4-9. a) Mohr circles (i–iv) representing a range of stress states which will lead to tensile failure. The Mohr 'circle' iv that represents hydrostatic stress is a point. b) (i–iv) Patterns of tensile fractures generated, respectively, by the four stress states shown in (a). From /Cosgrove, 1995/.



(a)

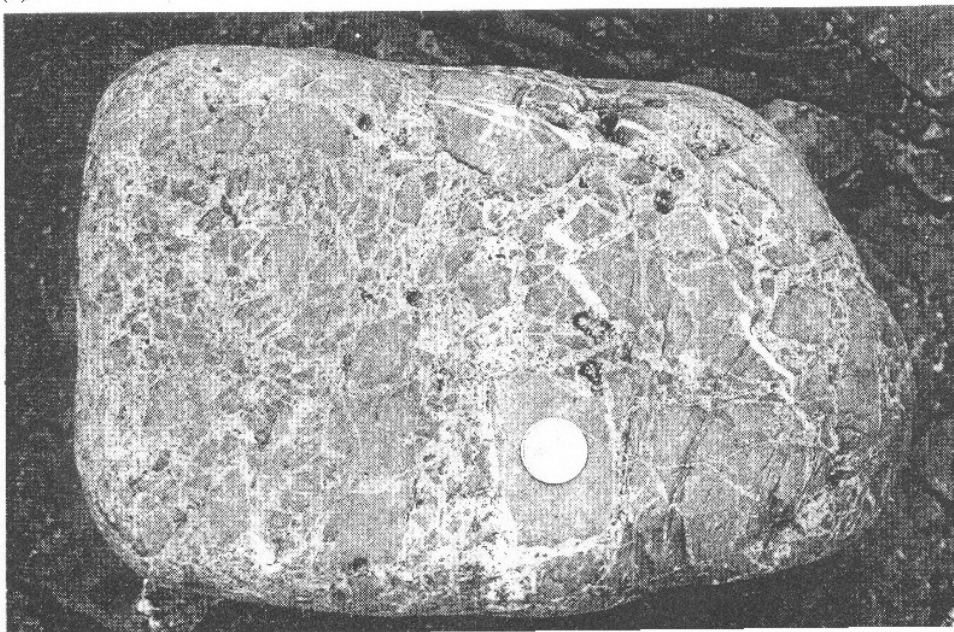


Figure 4-10. a) A regular array of tensile fractures exposed on a bedding plane in Carboniferous sandstone from Millook, North Cornwall. The alignment of the veins indicates that a significant differential stress existed during fracturing. b) Devonian sandstone at Combe Martin, North Devon, cut by randomly oriented extension fractures. This indicates a hydrostatic state of stress during fracturing. The diameter of the coin is 3cm. From /Cosgrove, 1995/.

4.4.2 The type of fluid induced fractures

As well as the orientation of the fluid induced fractures being controlled by the differential stress, the type of fracture also depends upon this parameter. For example, if the fluid pressures in rocks with the stress states represented by the solid line Mohr circles in Figure 4-11 were sufficiently large to cause failure, rock 1 would fail by shear failure and rocks 2–4 by tensile failure, as indicated by the dashed Mohr circles. As mentioned earlier, as the differential stress is reduced, so the tendency for the tensile fractures to form normal to σ_3 decreases until in the limit when $\sigma_1 = \sigma_3$, the fractures are randomly oriented (Figure 4-9b, iv).

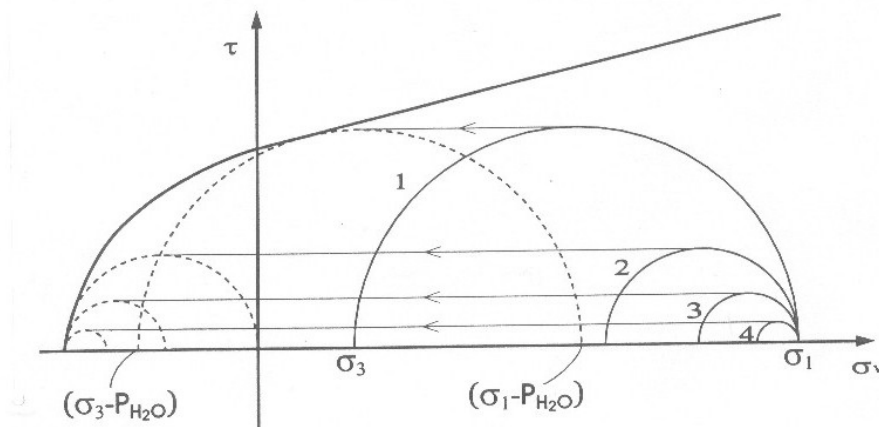


Figure 4-11. Mohr circle representation of four stress states (solid circles 1–4), which will not cause failure. The effect of fluid pressure is to move the stress state to the left by an amount P_{H_2O} . If the new circle (dashed) touches the failure envelope hydraulic fracturing occurs. Whether this failure is by shear or tension depends on the differential stress. From /Cosgrove, 1995/.

It is a common misconception that the result of hydraulic fracturing in rock is the formation of randomly oriented tensile fractures and the generation of breccia textures (Figure 4-10b). The above discussion shows that, depending on the differential stress, the expression of hydraulic fracturing can range from randomly oriented tensile fractures through aligned tensile fractures to shear fractures.

4.4.3 Fluidisation

Now consider the effect of hydraulic fracturing on uncemented sediments with no intrinsic cohesion, such as uncemented sandstone lens in a shale. A material such as this has no strength and therefore cannot support a differential stress. Thus, the stress state within it will be close to hydrostatic. If the fluid pressure is such that hydraulic ‘fracturing’ can occur then the grains of the sediment will simply move apart slightly and the sediment will fluidise. Thus, an additional diagram should be added to Figure 4-9b showing the effect of hydraulic fracturing under conditions of hydrostatic stress in a material with zero cohesion such as an uncemented sediment (Figure 4-12).

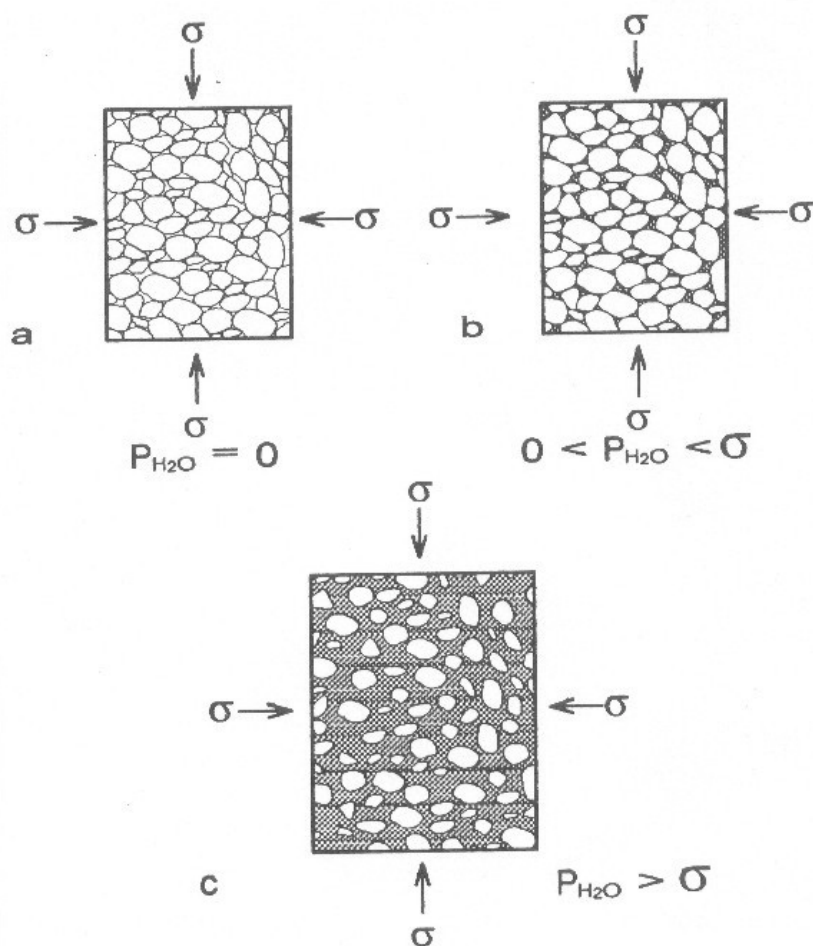


Figure 4-12. Diagrammatic representation of fluidisation. The build up of fluid pressure in the pores of an uncemented granular sediment (a) reduces the normal stress acting across the grain contacts, thus facilitating flow (b). The normal stress may be reduced to zero and the grains may move apart (c). From /Cosgrove, 1995/.

Evidence for two different modes of tensile failure occurring at the same depth and at the same time in different 'rocks' is provided by sandstone dykes frequently found cross cutting shales. Because of the electrostatic charges between clay particles making up a shale there is an intrinsic cohesion in the sediments from the moment they are deposited. This cohesion will increase with compaction and cementation. However, sand lenses interbedded with the shale will remain cohesionless until the processes of cementation are initiated. Thus, during the early stage of burial the shales will possess cohesion and the sandstones will not. If, during this stage, the fluid pressures become high enough to cause hydraulic fracturing in both sediments, the shales, because of their intrinsic cohesion, will be able to sustain a differential stress. If the differential stress is $<4T$ of the shale, tensile failure will occur and the resulting fractures will be vertical. At the same time the effect of the high fluid pressure on the sand lenses, which have no cohesion, will be to cause fluidisation. Fluidised sand will then be injected into the vertical fractures in the shales wherever these fractures intersect the sand bodies.

4.5 Conclusions

A study of the literature on fluid induced fracturing leads to the recognition of three systems which are the two end members and an intermediate form of a continuous spectrum of materials ranging from unconsolidated and incohesive sediments, through cemented but porous rocks to crystalline rocks with no intrinsic porosity and whose only porosity relates to that imparted by the fracture network that the rock contains.

The effect of high fluid pressure on the three systems is very different:

The uncemented sediment will respond to a high fluid pressure by fluidisation and this provides a medium that can be injected into pre-existing fractures to form sedimentary dykes. Alternatively the fluid may generate its own fractures, which it subsequently fills.

The porous sedimentary rock responds to the build up of pore pressure by hydraulic fracturing. The appropriate analysis for understanding its behaviour in response to high fluid pressure is that based on the theory of poro-elasticity. This theory, known as the theory of internal hydraulic fracturing, is able to predict the type and orientation of the fractures that will form.

The non-porous, crystalline rock containing fluid filled, isolated or linked fractures, can also respond to an increase in fluid pressure by hydraulic fracturing i.e. the propagation of an existing fracture or the generation of a new fracture. The theory best suited to analyse such a system is based on fracture mechanics and is known as the theory of external hydraulic fracturing.

It is clear that high fluid pressures are extremely conducive to the formation of sedimentary intrusions (dykes, sills). They can provide the dyke material by fluidisation and can either open existing fractures or generate new ones into which the dyke material can flow.

5 The sedimentary dykes in the Småland granite

5.1 Introduction

The Precambrian granite basement of the Äspö region along the Baltic coast of southern Sweden contains numerous sandstone dykes. These dykes are sub-vertical, have a fairly consistent trend (N35°E) and range in thickness from a few tens of centimetres to a few millimetres. The dykes are filled with clastic sediments and sometimes contain angular clast of the granitic country rock.

A study of these dykes has been undertaken in order to determine whether their emplacement was the result of passive gravitational infill or of forceful injection as a result of high fluid pressures. This latter process relates directly to the problem of fluid induced fracturing of crystalline rock masses with effectively zero intrinsic permeability such as the rock that hosts the Äspö laboratory.

The aim of the field work and of the report as a whole is to establish the role of high fluid pressure on the emplacement of the dykes and thus to obtain a better understanding of how the fractured basement rocks would respond to any future episode of high fluid pressures such as might occur during the next glacial advance.

There are important textural differences between passively and actively intruded sedimentary dykes and the present study has therefore focussed on these features of the dykes.

Six localities located at Händelöp, Tindered, Granhulteå, Emån, Götemar-Kråkemåla quarries and a road cutting north of Västervik were studied and these are discussed in turn in the following section. Particular attention is paid to features of the dykes that are relevant to their age and mode of emplacement and the section concludes with a discussion of the implications of the field observations regarding these two questions.

5.2 Händelöp

A roadside exposure at Händelöp, (Figure 1-1 and Figure 5-1) contains sub-vertical fractures. Some are barren but others are filled with either calcite (Figure 5-1b), fluorite or sandstone (Figure 5-1a). The orientation of the dyke is strike N 60°E dip 80°N and of the calcite vein is strike N 50°E dip 85°S. The fractures containing the sandstone dykes are irregular in both profile and plan and the thickness of the dykes rather constant. The barren fractures have different orientations to the dykes and calcite filled veins. They are sub-vertical and strike N 35°W, N 50°W and N 80°W, i.e. sub parallel to the major basement lineaments which determine the shape of the islands inlets and lakes of the region and which can be seen so clearly on aerial photographs and maps.

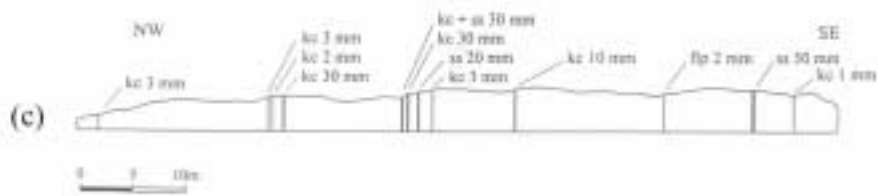
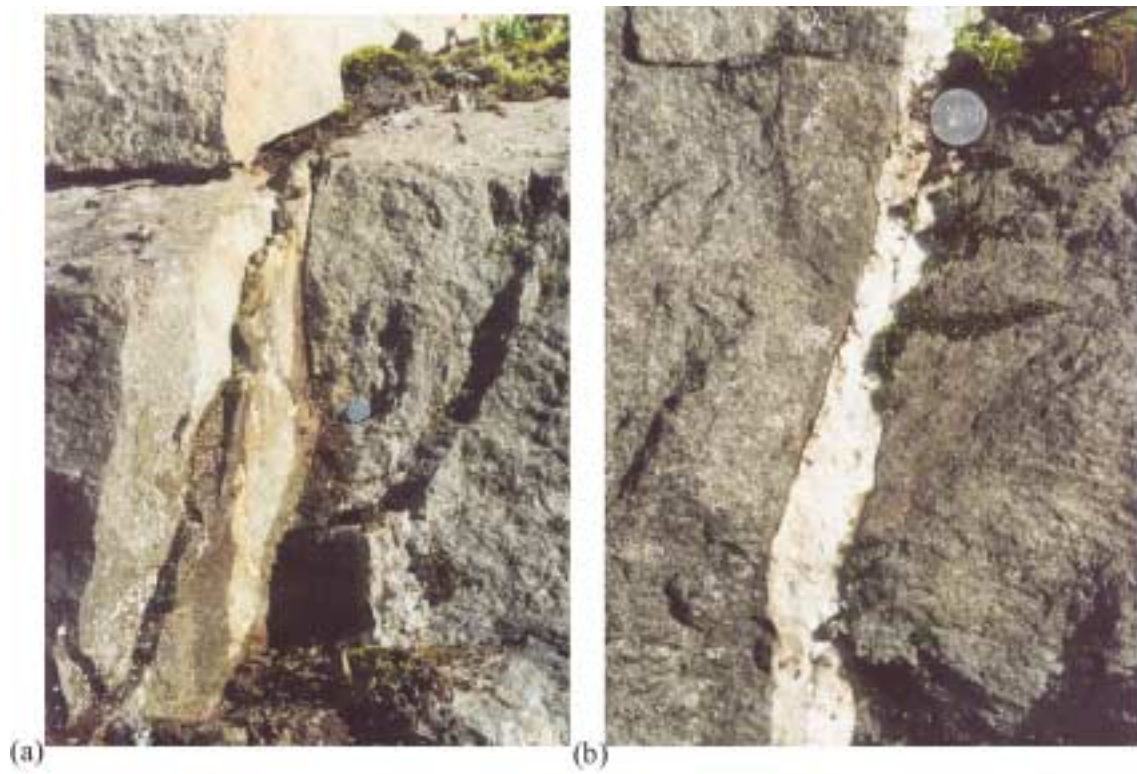


Figure 5-1. a) Vertical sandstone dyke and b) vertical calcite vein in a road cutting the basement rocks of Händelöp. c) Shows the location and cross section with the distribution and thicknesses of the calcite veins (kc), the dykes (ss) and the veins. (c. From /Milnes and Gee, 1992/).

The implication of these observations is that the fractures are probably of different ages the barren fractures being the youngest. /Sundblad and Alm, 2000/ notes that some fractures contain both sandstone dykes and calcite and on the basis of field observations conclude that the calcite veins post-date the dykes. Work by /Nordenskjöld, 1944/ in the Simpervarp area near Äspö shows that the orientation of the sandstone dykes and barren fractures at Händelöp are compatible with observations elsewhere within the Precambrian basement, Figure 5-2e and f, and a study of the fracturing of the Ordovician limestones (Milnes and Gee) which cover most of the island of Öland which runs parallel to the coast from Äspö southwards, shows that there are two important post-Ordovician fracture sets that have affected the area, Figure 5-2a–d. The earliest trends NW-SE and the later NE-SW.

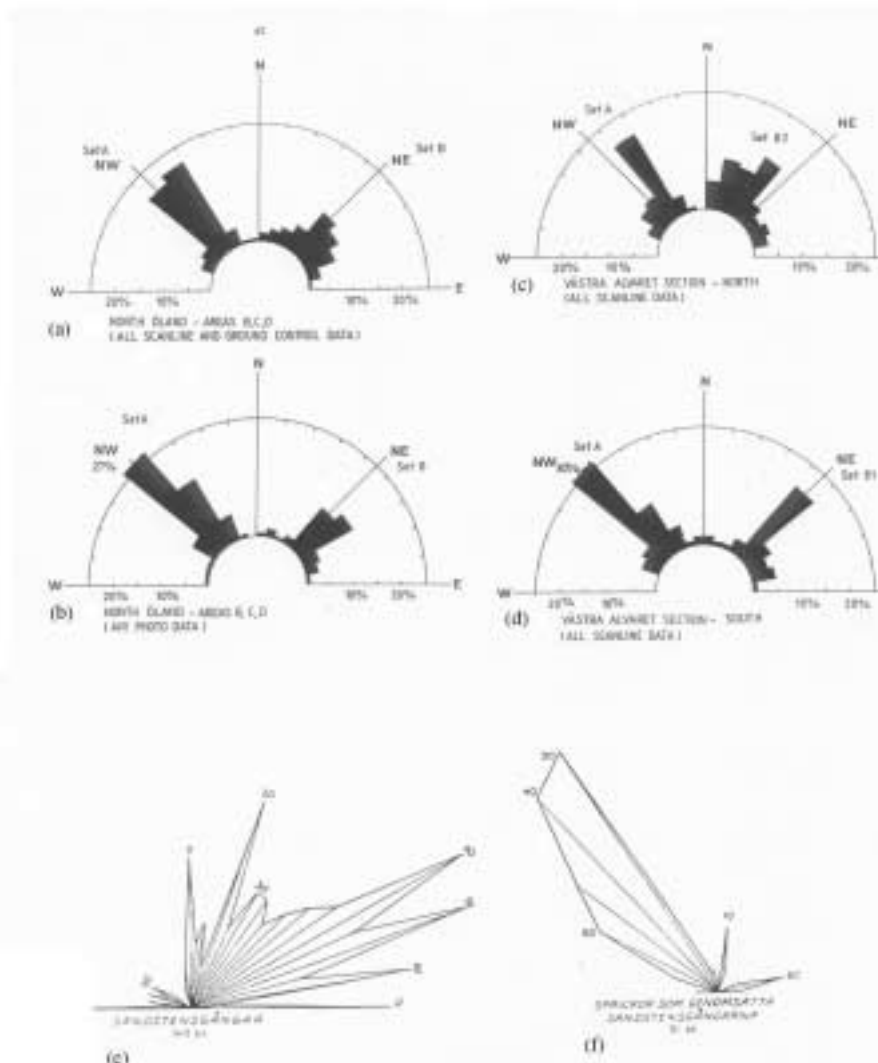


Figure 5-2. a)–d) Orientation data of the fractures in the Ordovician limestones exposed along the western coast of Northern Öland. a)–c) Represent scan-line data from three subareas and d) air photo analysis of area a). The fracture data shown in e) and f) are from the Precambrian basement rocks from the Äspö area (Simpervarp) on the Swedish mainland. e) Shows the orientation of the sandstone dykes and f) the barren fractures which post date them. [a)–d) from /Milnes and Gee, 1992/ and e) and f) from /Nordenskjöld, 1944/].

Evidence for the relative age of the sandstone dykes and the barren fractures is presented in the section on the Göttemar and Kråkemåla quarries where sub-vertical sandstone dykes trending N 78°E are cut by sub-vertical barren fractures trending N 30°W. These observations are compatible with the conclusions of /Nordenskjöld, 1944/ and /Sundblad and Alm, 2000/ Figure 5-2e and f and show that the barren fractures in the Precambrian basement are parallel to the earliest formed fractures to develop in the Ordovician sandstone. This implies that the fractures are either of post-Ordovician age or that pre-Ordovician fractures in the basement with this orientation subsequently propagated upwards into the overlying Postcambrian rocks as a result of various tectonic events.

5.3 Tindered

The road cuts around Tindered (Figure 1-1) reveal a series of sub-vertical sandstone dykes cutting the Precambrian basement. They have approximately the same trend (N30E) and there is evidence that although they were emplaced along pre-existing fractures the process of injection also generated new fractures.

This can be seen when a dyke following a particular fracture deviated sideways to link with an adjacent parallel fracture. An example of this is shown in Figure 5-3b, which is a field notebook sketch of two sub-parallel, offset dykes trending approximately N30°E linked across the intervening relay zone by a short, rather irregular dyke striking approximately N30°W. It is suggested by the present authors that this link was generated by fluid induced fracturing during the active injection of the fluidised sandstone into the main N30°E trending fracture set. This trend of fractures has been reported by Sollien, 1999, see Figure 5-3c.

The dyke array illustrated in Figure 5-2a and b also shows how the formation of links between adjacent dykes can produce isolated blocks of country rock (granite) within the dyke. The mixture of mature (i.e. well-rounded) sand grains and angular clasts of the granitic country rock, which is seen in many of the sandstone dykes when viewed in thin section, is taken by the authors to indicate the active, i.e. forceful injection of the dyke material into the fractured granitic rock mass of the basement. This is discussed in more detail in the section on the Kråkemåla and Göttemar quarries later in this section.

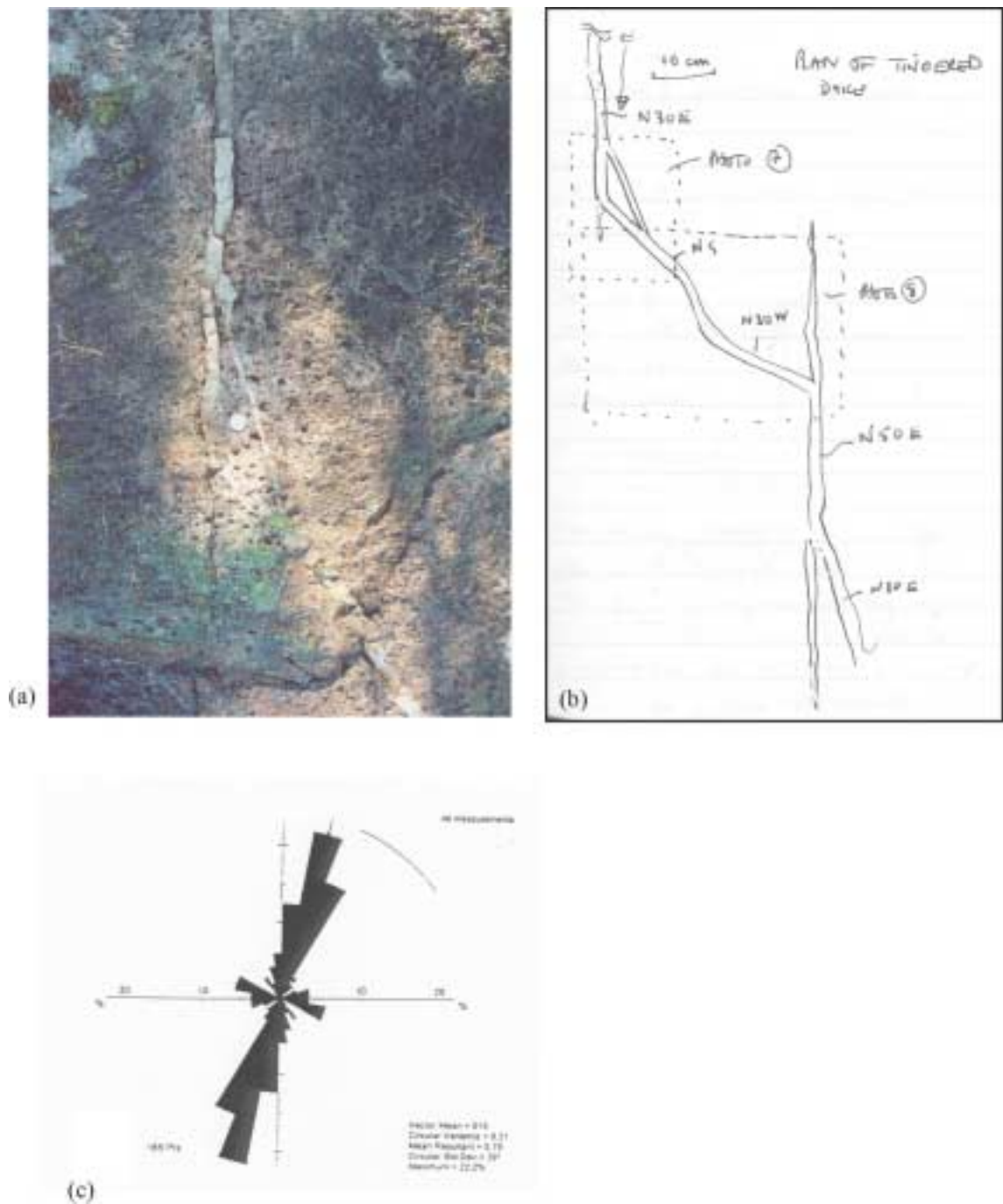


Figure 5-3. a) A portion of a sandstone dyke array at Tindered. b) Filed notebook sketch of the sandstone array showing the position of a), (Photo No. 7). c) Fracture and dyke orientation data from Tindered, /from Sollien, 1999/.

5.4 Granhultea

The railway cutting at Granhultea contains the thickest sandstone dyke observed during this study. Figure 5-4a and b. The dyke is 10cm wide, sub-vertical, trends N15°E and is remarkable in that it is the only example found in which the foliation in the dyke material is not parallel to the dyke walls. Foliation parallel to the dyke walls is indicative of an active i.e. forceful mode of emplacement initiated as a result of high fluid pressures.



Figure 5-4. a) 10cm wide vertical sandstone dyke cutting the Precambrian basement along the railway cutting at Granhultea. b) Shows a detail of a) and c) a polished cross section. The internal structure of curved, sub-horizontal layering concave upward is characteristic of a dyke that has been passively infilled.

Instead, the foliation within the dyke is at right angles to the dyke walls. The polished cross section illustrated in Figure 5-4c shows that the internal structure consists of curved, sub-horizontal layering concave upward. Layering with this orientation and geometry is characteristic of a dyke that has been infilled passively i.e. by gravity infill from above rather than by injection under high fluid pressure.

Typical examples of sedimentary dykes generated by passive infill are shown in Figure 5-5. These examples are from Urra in SE Spain and show sedimentary material filling fractures in a brecciated volcanic rock. Despite the irregular orientation of the fractures the foliation within the fracture infill remains consistently sub-horizontal indicating gravitational fill from above.

Another example of a sedimentary dyke cutting the volcanic rocks of Urra is shown in Figure 5-6. This dyke is interesting as it shows textures typical of both passive and active infilling. The dyke is approximately 1m wide and inspection of its internal fabric (Figure 5-5b) reveals that the right hand half of the dyke shows a fabric parallel to the wall, a feature characteristic of active injection and that the left-hand side shows a fabric normal to the dyke wall, a feature characteristic of passive infilling. The juxtaposition of these two fabrics indicates that more than one episode of dyke formation occurred. The dyke fabrics from the Urra region illustrated in Figure 5-5 and Figure 5-6 and discussed briefly above are worthy of further study in order to better understand the interplay between passive and active dyke formation and the processes that lead to the formation of breccias, which are apparently matrix supported by a sediment with a relatively uniform sub-horizontal layering. However this is outside the remit of the present study and the important points to note from these examples is that the layering orientation within sedimentary dykes is one of the best diagnostic features for differentiating between passively and actively emplaced dykes.

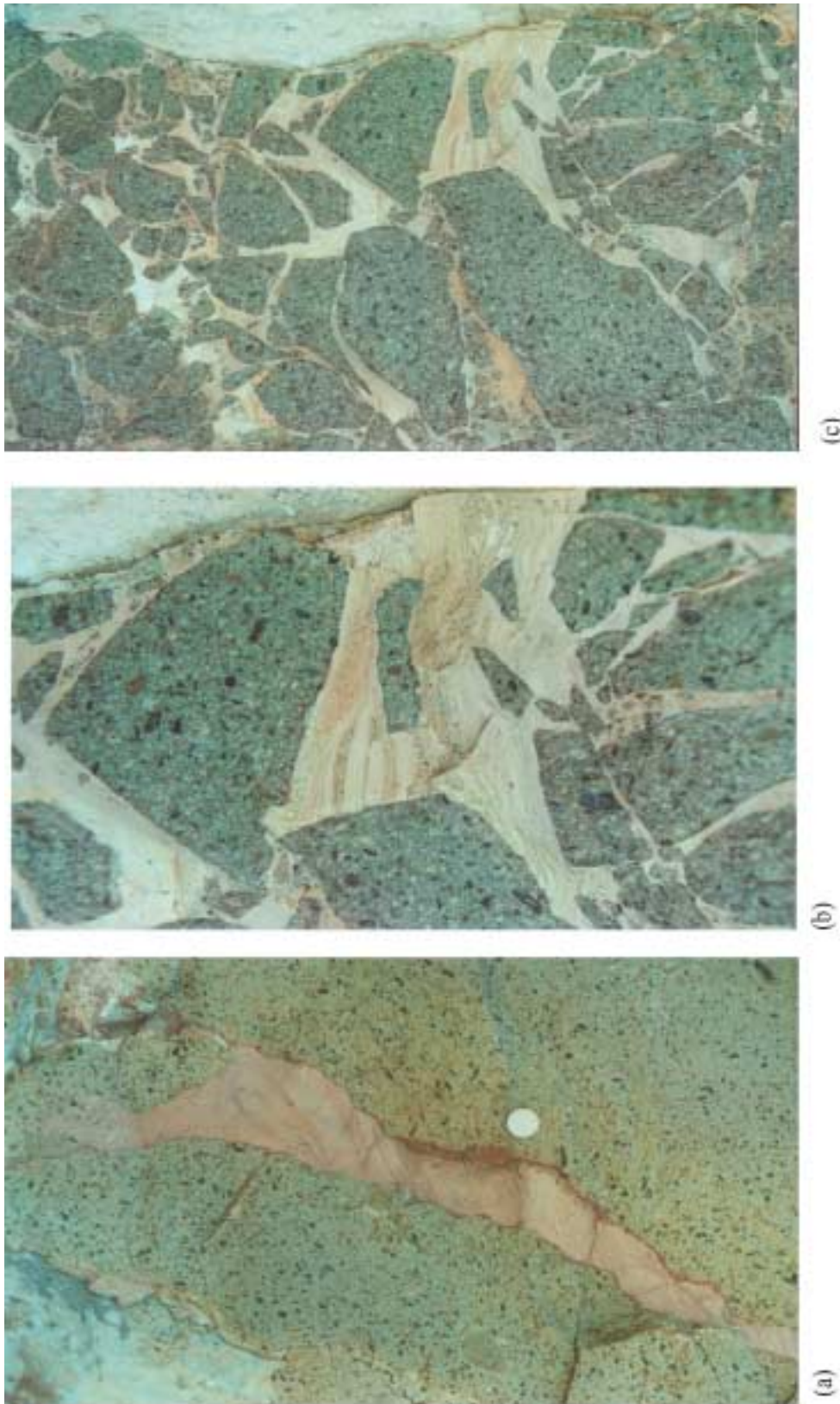


Figure 5-5. a) A sub-vertical sedimentary dyke with a sub-horizontal fabric, cutting volcanic rocks. Urra, SE Spain. b) and c) Brecciated volcanic rock infilled with sediments. The fabric in the sediments is dominantly sub-horizontal.

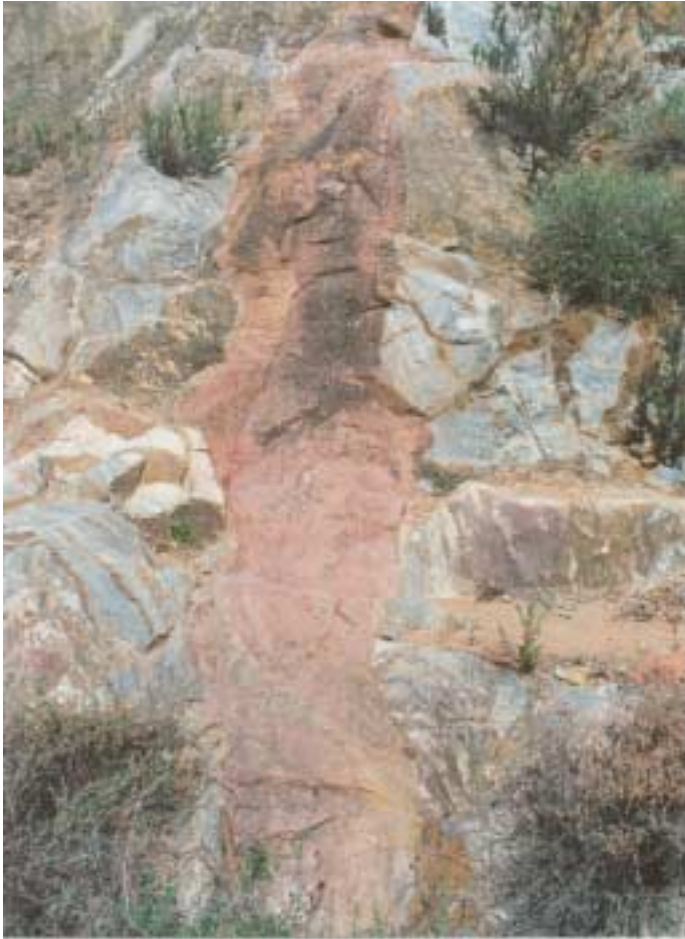


Figure 5-6. a) A 1.5m sedimentary dyke cutting volcanic rocks. Urra, SE Spain. b) Detail of a) showing evidence of multiple intrusions. The right-hand half of the dyke shows a fabric parallel to the wall, a feature characteristic of active injection. The left-hand side shows a fabric normal to the dyke wall, a feature characteristic of passive infilling.

With the exception of the dyke at Granhulteå, the layering observed in the dykes of the study area was invariably parallel to the dyke wall indicating forceful rather than passive infilling. One of the aims of this study is to determine the mechanism of formation of the dykes in the Äspö area, to establish whether they were emplaced as a result of high fluid pressure and if so to determine the likely effect on the fractures in the basement of an further increase in fluid pressure. These observations combined with a detailed study of the dyke textures in thin section (see later in this section) provide convincing evidence that the dykes are the result of injection under conditions of high fluid pressure.

5.5 Emån

In the road cutting at Emån a complex sandstone dyke outcrops in such a way that its three dimensional geometry can easily be seen. As can be seen in Figure 5-7 the strike of the dyke changes abruptly. This is because it was intruded along more than one fracture. It is important to note that the thickness of the dyke is different in the two fractures. This is clearly seen in the lower of the two photographs that show the relatively thick section of the dyke occupying the fracture sub-parallel to the photograph and the thin portion the fracture approximately normal to the photograph.

It is interesting to consider the mechanical implications of the synchronous formation of dykes along sub-vertical fractures with different strikes and different thicknesses. The problem relates to fluid induced failure in fractured rock masses rather than to the initiation of a new fracture in an unfractured rock. The following brief discussion relates to fluid induced failure in fractured rocks.



Figure 5-7. Three-dimensional view of a sandstone dyke cutting the granite basement at Emån. The strike of the dyke changes because it was intruded along more than one fracture, and the thickness of the dyke is different in the two fractures. This is clearly seen in the lower of the two photographs which shows the relatively thick section of the dyke occupying the fracture sub-parallel to the photograph and the thin portion of the fracture approximately normal to the photograph.

5.5.1 Fluid induced fracturing in simple fracture network

The general condition for fluid fracturing along any plane is that the fluid pressure, P_{fluid} , must be equal to or greater than T the tensile strength of the rock normal to that plane and the normal stress acting across it, Equation 5-1.

$$P > T + \sigma \quad 5-1$$

In an isotropic rock this condition is first met along the plane normal to the least compressive principal stress, σ_3 . However, in an anisotropic rock, i.e. one in which the tensile strength varies in different directions, this is not necessarily so.

Consider a well-laminated shale with a marked planar anisotropy parallel to the bedding. The tensile strength normal to the bedding, T_n , will be considerably less than that parallel to it, T_p . In a tectonic setting where crustal extension is occurring the vertical stress will be the maximum principal compression σ_1 and σ_3 will be horizontal. It follows from Equation 5-1 that the condition for tensile failure by fluid fracturing parallel and normal to bedding are:

$$P_{\text{Fluid}} > T_p + \sigma_h \quad 5-2$$

$$P_{\text{Fluid}} > T_n + \sigma_v \quad 5-3$$

Which of these two conditions is satisfied first depends upon the relative values of the differential stress, $(\sigma_1 - \sigma_3)$ and the difference between the two tensile strengths $(T_p - T_n)$. If $(\sigma_1 - \sigma_3) > (T_p - T_n)$, then as the fluid pressure increases Equation 5-2 is satisfied first and the resulting fluid-generated extensional fractures would form normal to σ_3 , i.e. would be vertical. If the differential stress is less than the difference between the two tensile strengths then the condition represented by Equation 5-3 will be satisfied first and extensional fractures will form parallel to bedding, i.e. normal to σ_1 . If the condition $(\sigma_1 - \sigma_3) = (T_p - T_n)$ occurs then the fluid pressure required to form fractures parallel and normal to the bedding would be the same and there would be an equal likelihood that both sets of fractures would form. An example of this is illustrated in Figure 5-8, which shows vertical veins of quartz with small horizontal off shoots forming along the bedding.

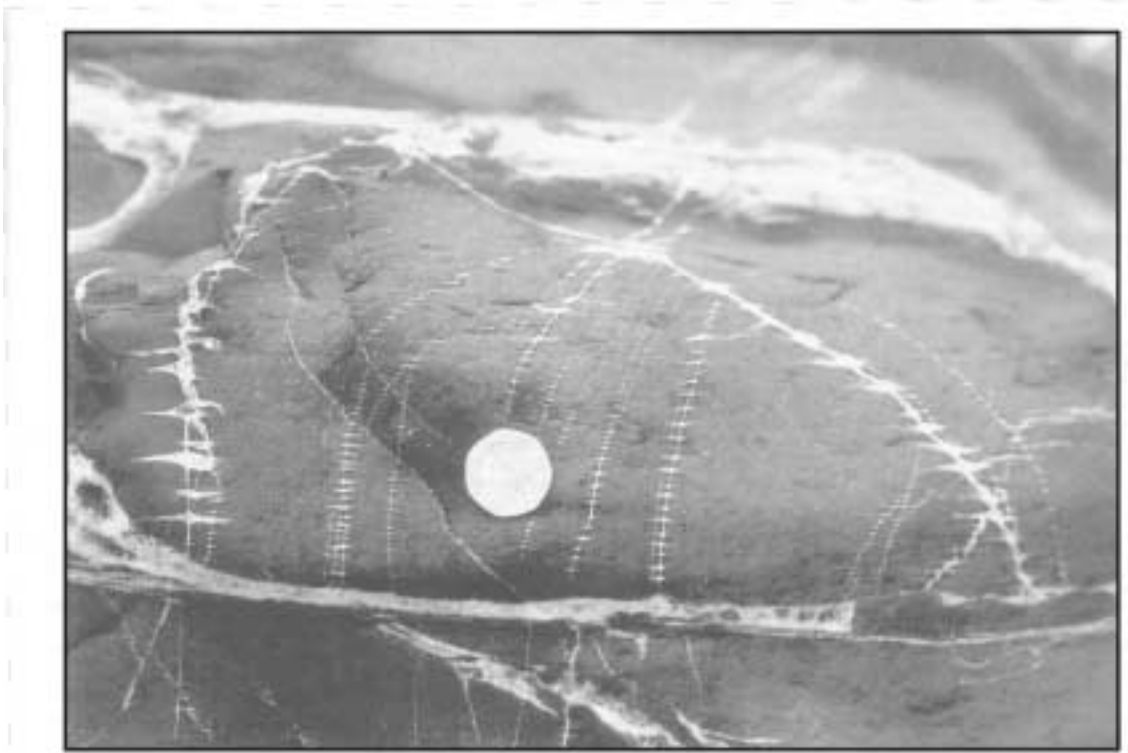


Figure 5-8. Hydraulic fractures infilled with quartz veins in a shale. The bedding is sub-horizontal and the maximum principal stress is thought to have acted vertically during the formation of the veins. The sub-horizontal and sub-vertical veins formed synchronously and indicate that at the time of their formation $(\sigma_1 - \sigma_3) = (T_p - T_n)$ /from Cosgrove, 1997/.

5.5.2 Fluid induced fracturing in complex fracture networks

As mentioned in section 3.2.5, /Delaney et al, 1986/ has considered the more general case of the effect of fluid pressure on the opening of fractures in a rock mass with a range of fracture orientations. They were interested in the exploitation of pre-existing vertical joints by ascending magmas and in their model the maximum and minimum principal stresses are horizontal and represented by S_H and S_h respectively. They derive a relationship between these regional stresses, the magma pressure P_m and the range of orientations of fractures that can be dilated by the fluid. This relationship has already been introduced in section 3.2.5 (Equation 3-1).

$$\frac{(P_m - S_H) + (P_m - S_h)}{S_H - S_h} > -\cos 2\alpha \quad 5-4$$

α is the angle between the normal to the fracture and the least principal stress, inset in the upper diagram of Figure 3-6. Delaney et al term the right hand expression the stress ratio R and point out that this equation defines four fields on a graph of stress ratio R versus the angle α , Figure 3-6 top diagram. They note that in the lowest field, $R < -1$, the magma pressure is less than the least regional compressive principal stress and is therefore insufficient to dilate a joint of any orientation. In the highest field, $R > 1$, the magma pressure is greater than the most compressive regional horizontal stress and is therefore sufficient to dilate any vertical joint. Two fields are contained within the

middle region, $-1 < R < 1$. Above the curve defined by Equation 5-4 the magma pressure is sufficient to dilate suitably oriented joints (assuming that there is negligible tensile strength across the fracture); below the line suitably oriented joints are absent but the magma pressure may be sufficient to propagate new fractures.

/Jolly and Sanderson, 1995/ use this idea to account for the variation in the geometry of dykes arguing that as the magma pressure rises from the least horizontal stress, S_h , to the maximum horizontal stress, S_H , so the resulting dykes can exploit a progressively larger range of fractures with the result that the dyke arrays *and* the individual dykes become progressively less linear, lower diagram in Figure 3-6.

It can be argued that the direction of easiest opening (i.e. the direction of the least principal compression σ_3) is defined by the direction in which the two dykes have the same thickness.

The arguments outlined above relating to the range of fracture orientations that will open in response to a fluid pressure assumes that the variously oriented dykes were emplaced during the same event and are not the result of several separate injections which may have occurred under different regional stress regimes. To demonstrate that this is so thin sections and polished sections of the junction between the two dykes shown in Figure 5-7 were made. These are shown in Figure 5-9. The texture indicates that the two sections of the dyke were intruded at the same time rather than being formed at different times and that the fluid pressure during their formation was greater rather than just equal to the least principal stress.

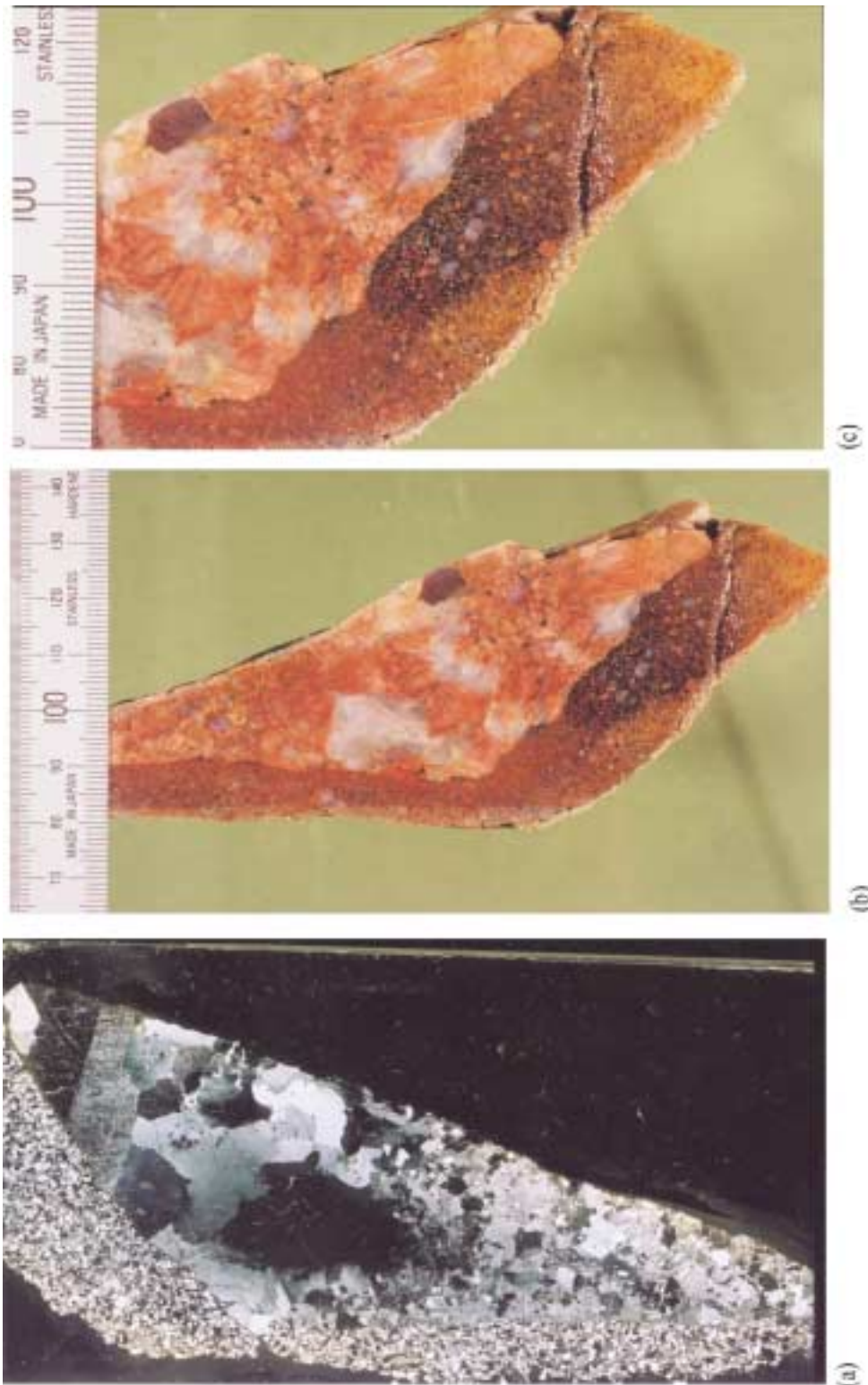


Figure 5-9. a) Thin section taken under crossed nicols and b) and c) polished cross section of the junction between the relatively thick and thin sections of the dyke shown in Figure 5-7. The texture indicates that the two sections of the dyke were intruded at the same time rather than being formed at different times. This has implications regarding the fluid pressure of the dyke material at the time of injection. See text for discussion.

5.6 The quarries at Kråkemåla and Götemar

Excellent exposures of sedimentary dykes occur at these quarries (Figure 5-10). They provide an insight into some of the problems relevant to the present study, i.e. the mechanism of injection and the age of the dykes.

One of the best-exposed sedimentary dykes at the Kråkemåla quarry is dyke number 92 (Fig. 3.10), Figure 5-11. It is sub-vertical, trends N35°E and has a thickness of approximately 6cm.

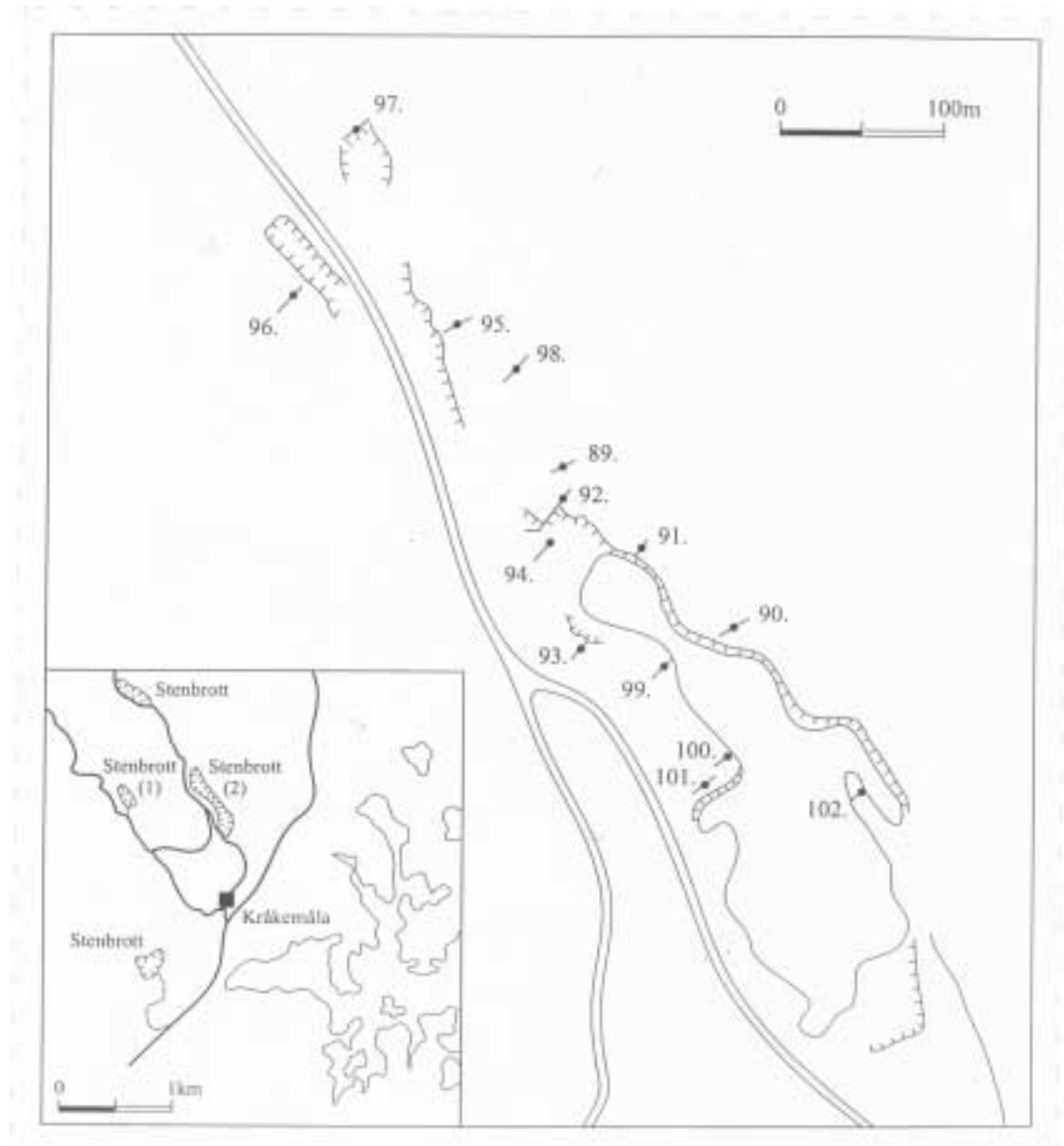


Figure 5-10. Location map of the Götemar and Kråkemåla quarries (1 and 2 respectively) showing the location and orientation of the sandstone dykes.

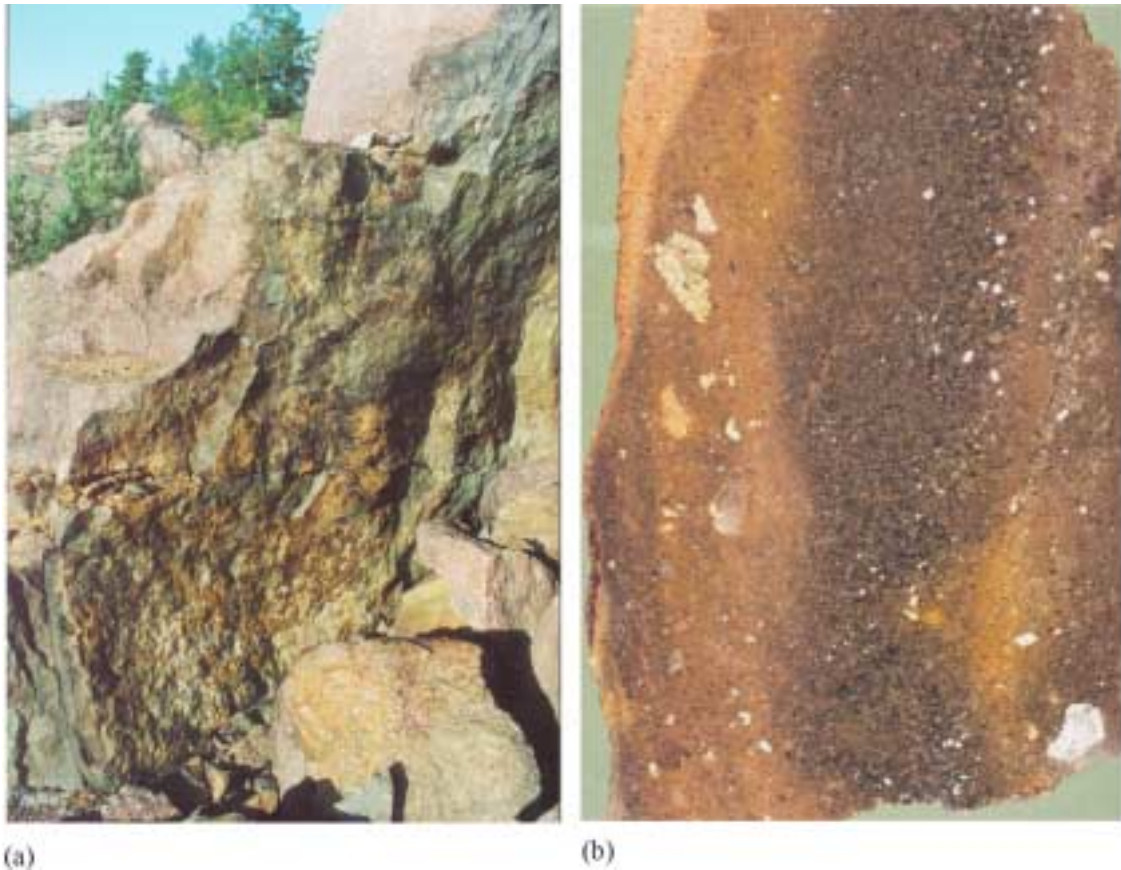


Figure 5-11. a) Sub-vertical sandstone dyke (No 92 Fig. 3.10) cutting the granite basement in the Kråkemåla Quarry. b) Polished section across the dyke showing a layering parallel to the edges of the dyke and grading (decrease in size of the sandstone grains) from the centre to the edges. These features are characteristic of active injection rather than passive infill.

Polished sections across the dyke (e.g. Figure 5-11b) show a layering parallel to the edges of the dyke and grading (decrease in size of the sandstone grains) from the centre to the edges. These features are characteristic of active injection rather than passive infill.

Other thin sections from this and other dykes in the Kråkemåla quarry (Figure 5-12) also show clast size grading parallel to the dyke walls (which are horizontal in the views shown). The particle size is largest in the middle of the dyke where the flow velocity was largest and decreases towards the dyke edges where the flow velocity was least. These textures are taken to demonstrate that there was a flow of fluidised sand being driven along the fractures by a high fluid pressure. The dyke parallel fabric is the result of the grading in clast size that occurs at right angles to the dyke wall as a result of the non-linear velocity profile. For a Newtonian viscous fluid flowing between parallel walls under a pressure gradient the velocity varies across the aperture in an approximately parabolic manner being greatest midway between the two walls and least at the walls. This accounts for the fining of the sediments from the centre of the dyke where the greater velocity can support larger clasts to the edges where the drop in flow velocity is reflected by a decrease in grain size.

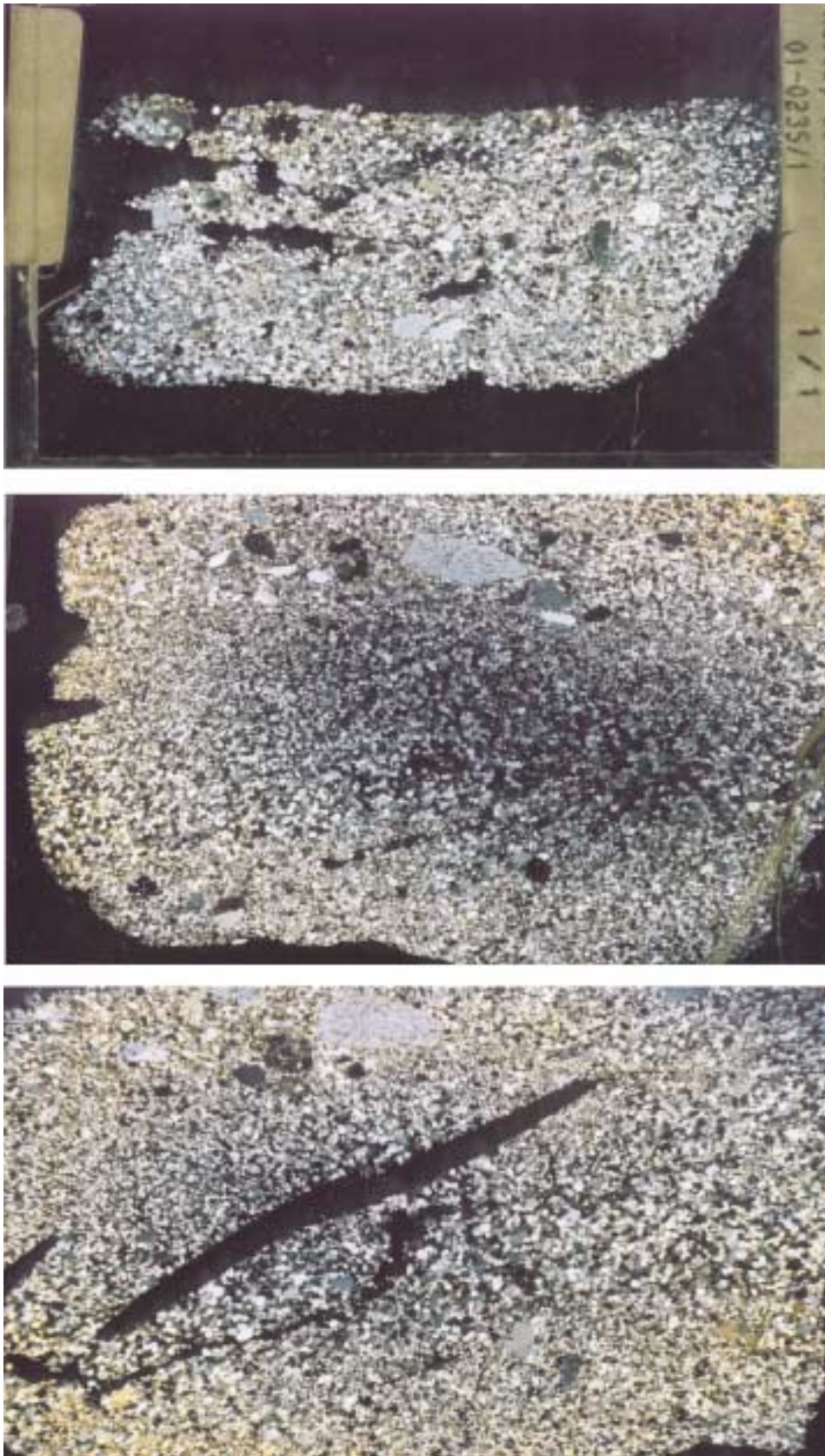


Figure 5-12. Thin sections (crossed nicols) of dykes from Kräkemåla quarry showing clast size grading parallel to the dyke walls (which are horizontal in the views shown). The particle size is largest in the middle of the dyke where the flow velocity was largest and decreases towards the dyke edges where the flow velocity was least.

The linkage of adjacent dykes provides other evidence of dyke formation under conditions of high fluid pressure. As noted earlier in the discussion relating to the dykes at Tindered, Figure 5-3, it seems likely that the dykes were injected into an existing fracture set in the granite basement which is sub-vertical and trends approximately N35°E. Figure 5-13, shows linkage between two parallel dykes occupying pre-existing sub-vertical fractures by the generation of a new fluid induced fracture oblique to the dykes.

In the discussion of the dykes at Emån (Figure 5-7) where it was demonstrated that injection had occurred into two sub-vertical fractures with different orientations during a single event, it was argued that both fractures existed prior to injection and that the fluid pressure was sufficiently high to open a range of fractures rather than just those ideally oriented i.e. those normal to the least principal stress σ_3 .

However, the synchronous injection of dyke material into two differently oriented fracture (i.e. the original fracture set and the linkage fracture which is oblique to them) shown in Figure 5-3b and Figure 5-13 is not taken as proof that the fluid pressure was sufficiently high to overcome the resistance to opening of a large range of fractures. In these examples it is suggested that the linkage is the result of local stress concentrations in the relay zone between two offset, parallel overlapping fracture tips. The concentration of stresses at these localities is discussed in section 1 of this report. The present authors argue that the locally induced high stresses at the tips of the fracture into which the sediments were being injected were of sufficient magnitude to generate new fractures and thus enable the linkage of two overlapping fractures to occur.

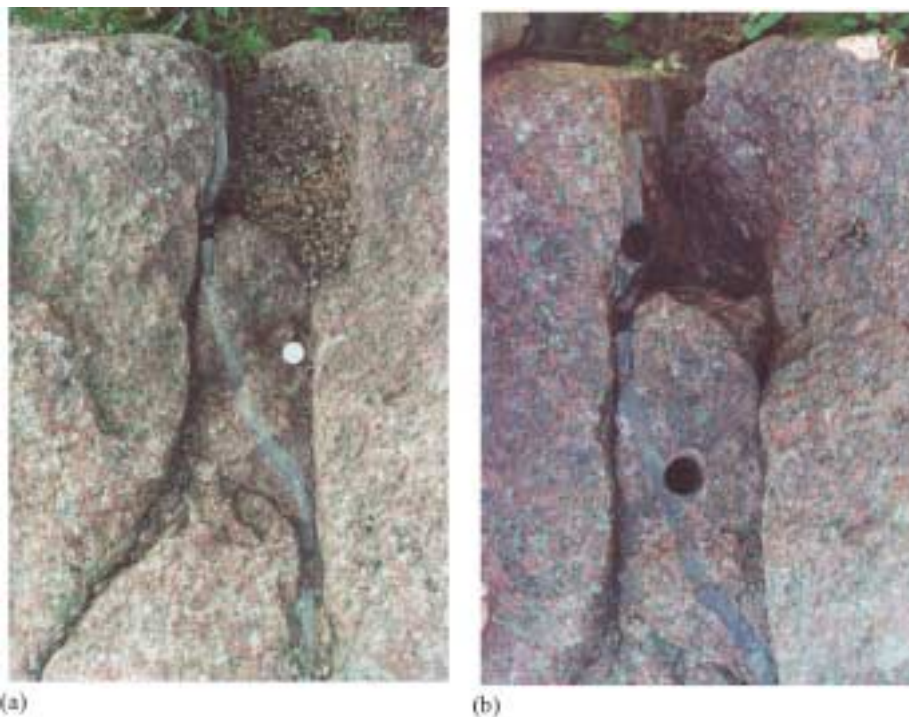


Figure 5-13. Linkage between two parallel dykes occupying pre-existing sub-vertical fractures by the generation of a new fluid induced fracture oblique to the dykes. Kråkemåla quarry. b) Shows the position of the cores taken.

An attempted linkage of two parallel dykes by the formation of a fluid induced fracture normal to the dykes is shown in Figure 5-14. This linkage does not appear to be related to fracture tips and it is therefore difficult to argue that it occurred as a result of the stress magnifications discussed in the previous paragraph. It may be that the fluidised sediment was simply exploiting a pre-existing fracture and that the fluid pressures operating during the injection of the sediments was equal to or greater than the maximum principal compressive stress σ_1 and was therefore capable of opening fractures in all directions.

To summarize, the dyke parallel layering the clast size grading and the formation of linkages between adjacent dykes all point to the process of dyke formation under conditions of high fluid pressures i.e. pressures probably considerably in excess of the least principal compression σ_3 .

The majority of the dykes are made up of well-rounded quartz grains and indicate clearly that the clasts had been reworked and eroded during transportation prior to being injected into the granite basement. The thin section shown in Figure 5-15 shows the well-rounded geometry of the quartz clasts. However, closer inspection of the clasts shows that some of them are still relatively angular and that the more angular material seems to be concentrated towards the margin of the dykes, Figure 5-16. In addition it is clear from Figure 5-16a that many of the quartz clasts now have significant quartz overgrowths on them.

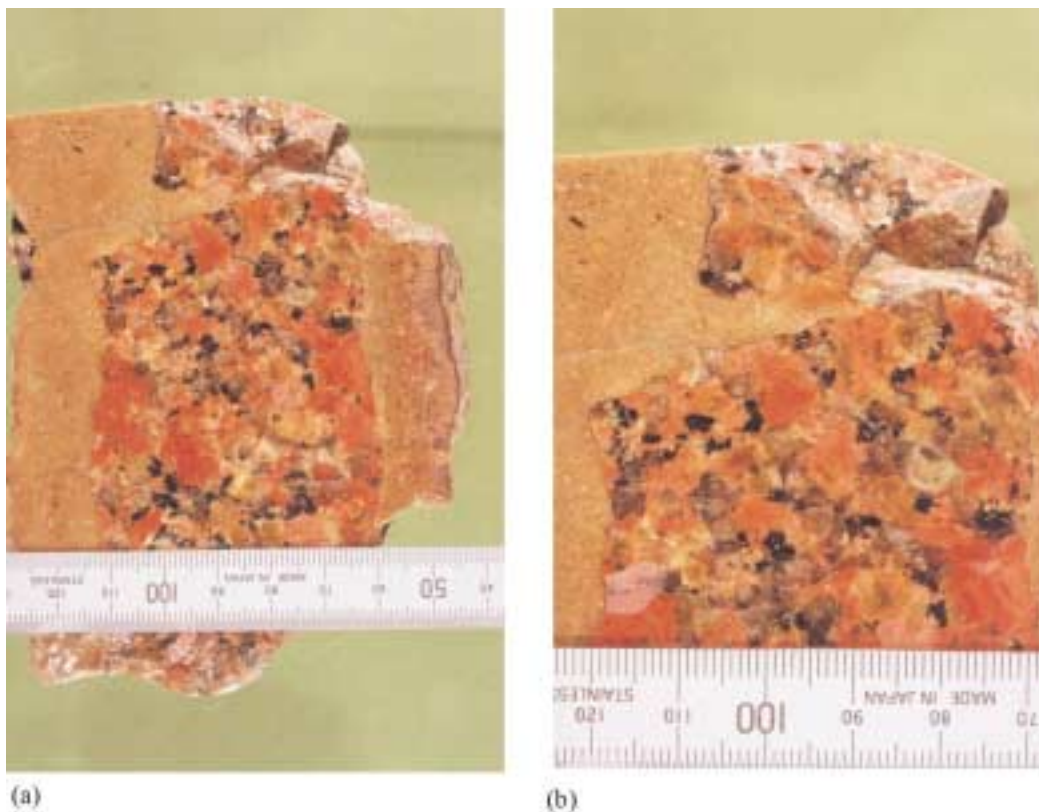
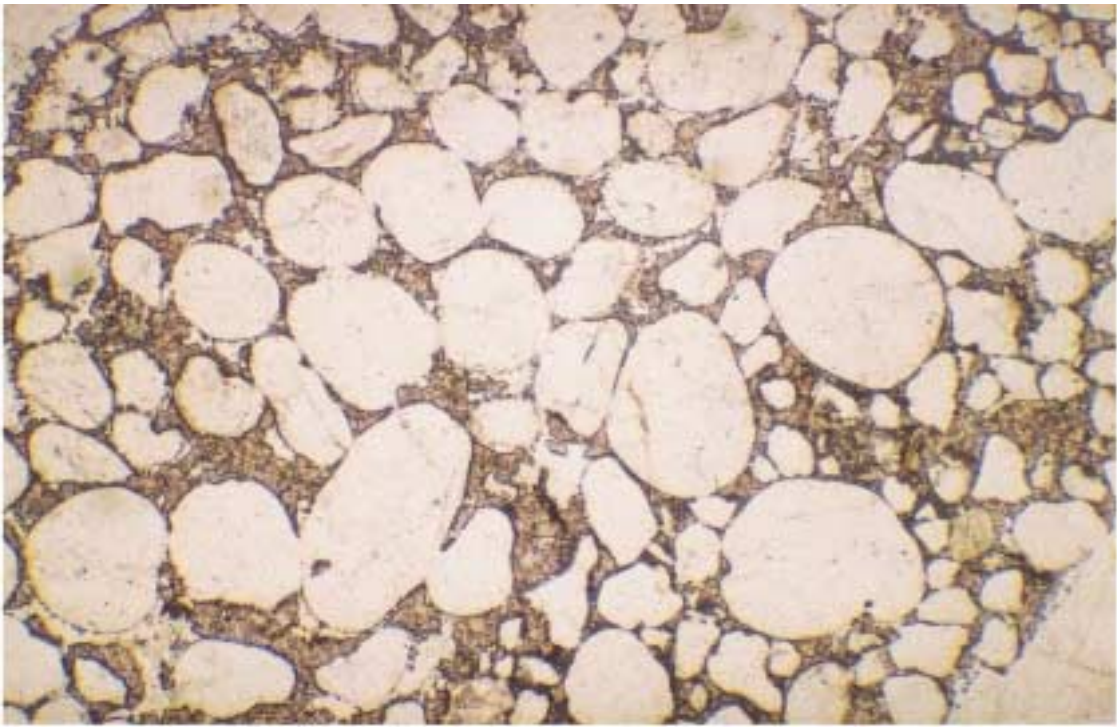
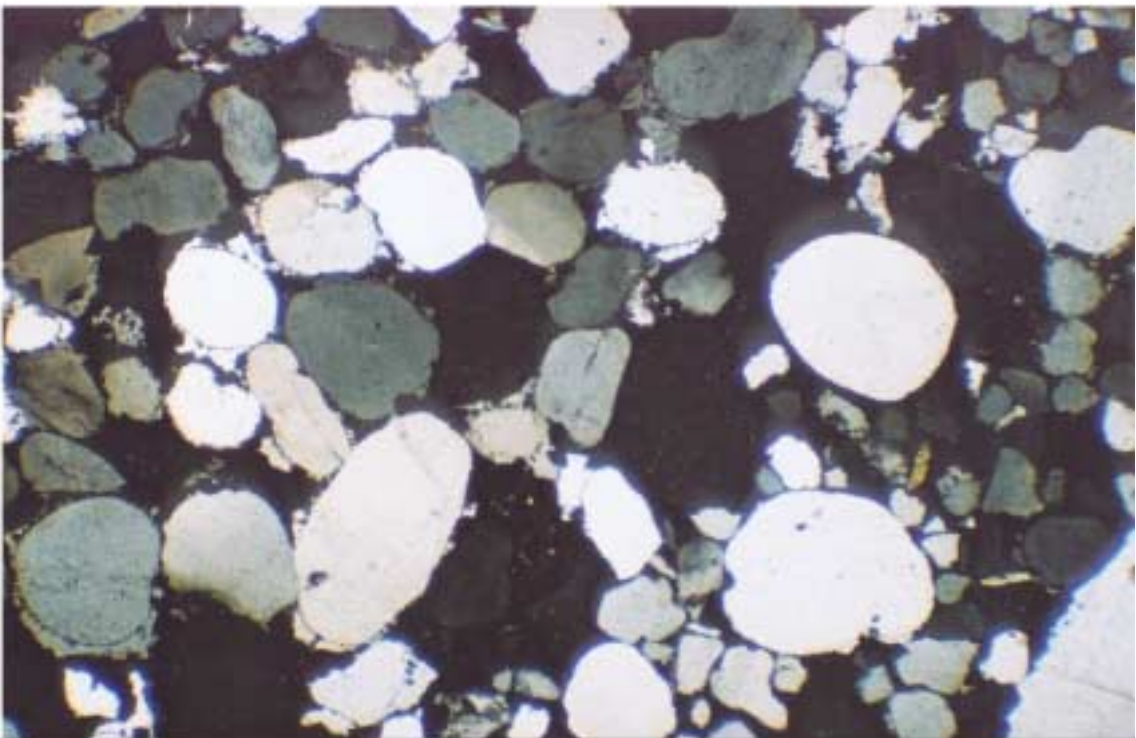


Figure 5-14. The attempted linkage of two parallel dykes by the formation of a fluid induced fracture normal to the dykes. b) Shows a detail of then lateral injection from the left-hand dyke towards the right-hand dyke. Kråkemåla quarry.



(a)



(b)

Figure 5-15. Thin sections in a) polarised light and b) under crossed nicols showing the well-rounded geometry of the quartz clasts making up the majority of the dyke.

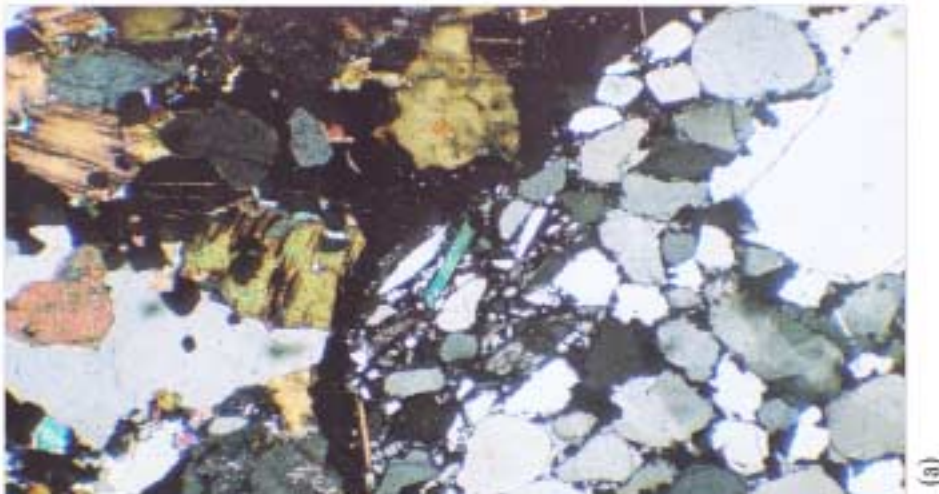
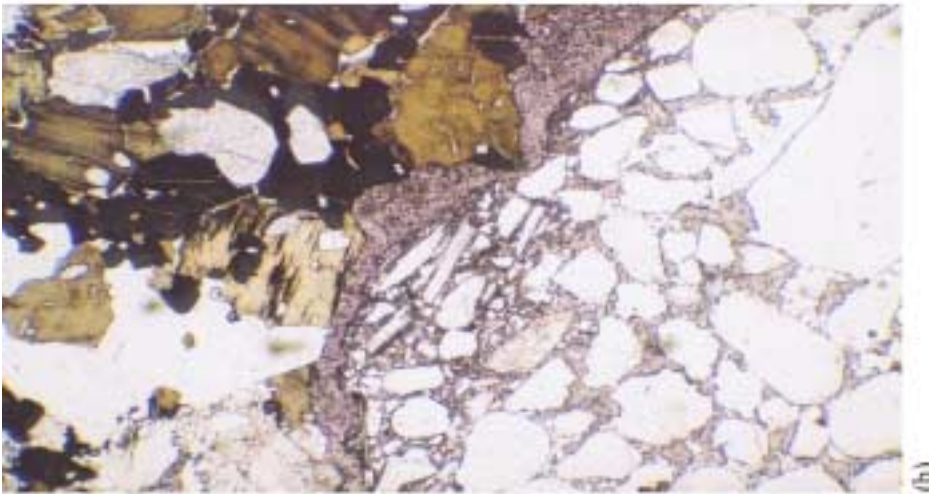
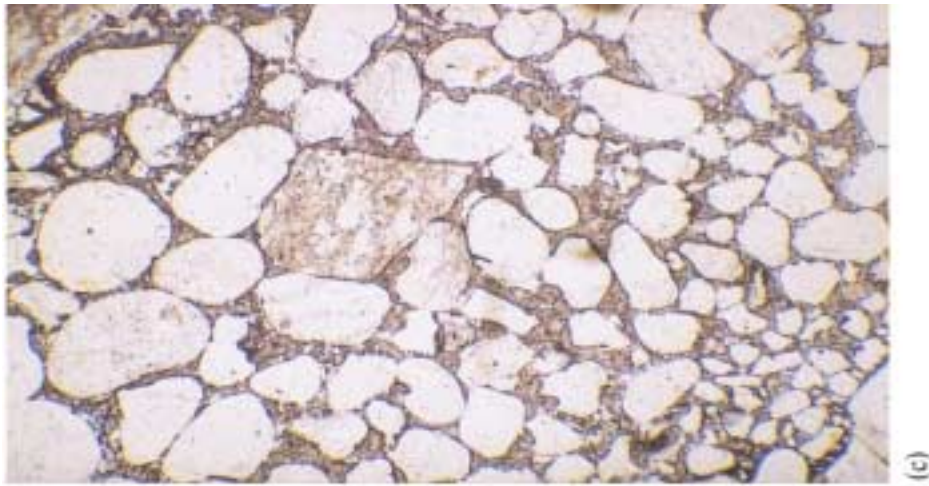


Figure 5-16. Thin sections of a) a dyke/country rock contact showing the accumulation of 'lags' of fine material and small inequant mica flakes along the edge of a dyke. Image taken under cross nicols. b) The same image under plane polarised light. c) Thin section showing clear grading from the large clasts in the centre of the dyke to smaller clasts at the edges. Image taken in plane polarised light.

In an attempt to prove that the formation of the dykes was the result of forceful rather than passive infill, a study of the dyke tips was made in order to see if dyke material was injected into the process zone of the fractures they were generating. The thin dykes were extracted from the outcrop by drilling and polished sections and thin sections of these dykes are shown in Figure 5-17, Figure 5-18 and Figure 5-19 respectively.



(a)



(b)

Figure 5-17. a) Longitudinal and b) transverse sections through 2.5cm diameter cores through the tip regions of the thin sedimentary dykes.

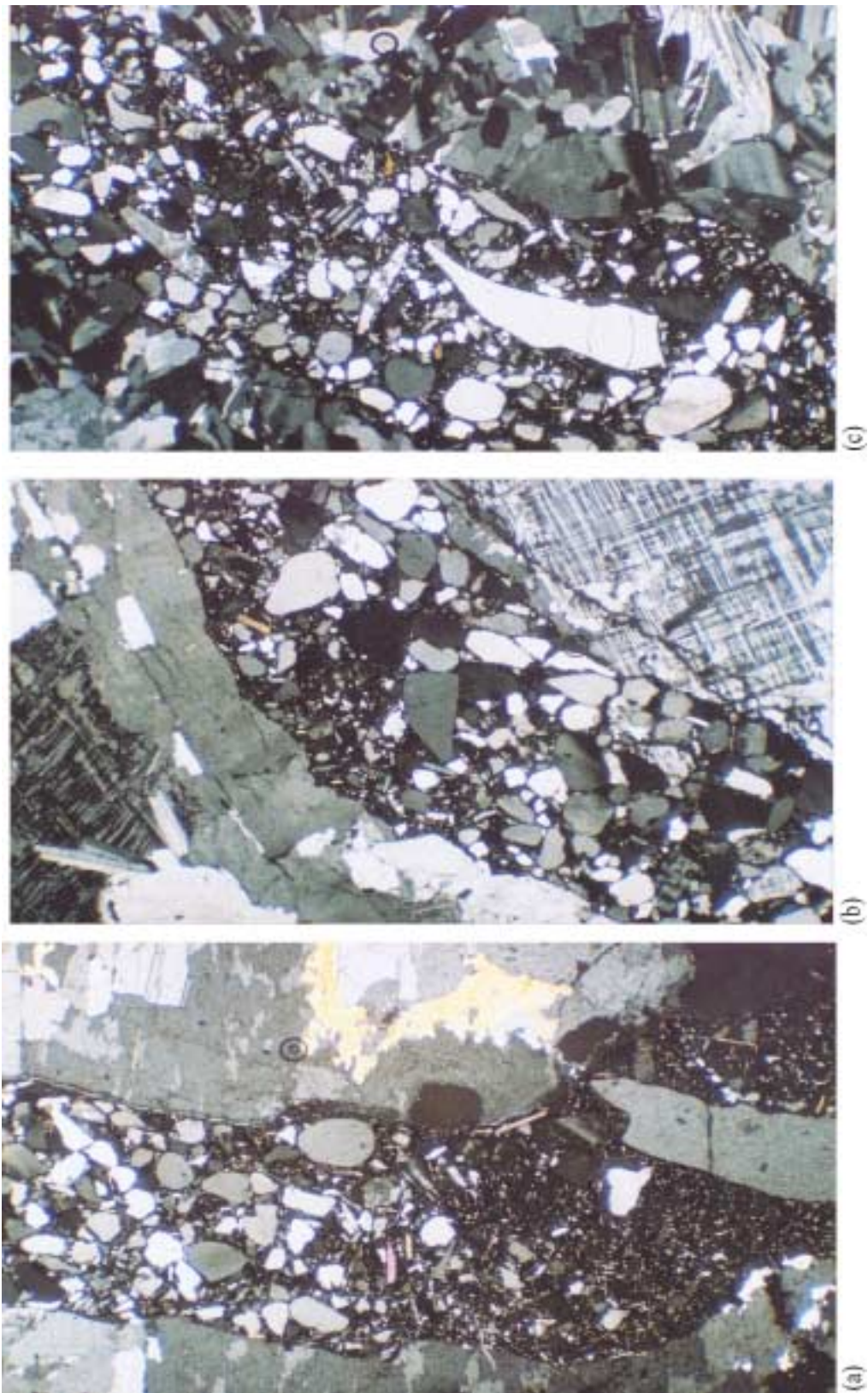


Figure 5-18. Thin sections of thin sedimentary dykes showing complex grading a) parallel to the dyke walls and b) and c) normal to the dyke walls. Note also the large variety of grain shapes ranging from well-rounded to angular and the mixture of sand grains from a primary sandstone and angular grains of feldspar presumably plucked from the granitic wall rock during the active fluid induced fracturing of the country rock.

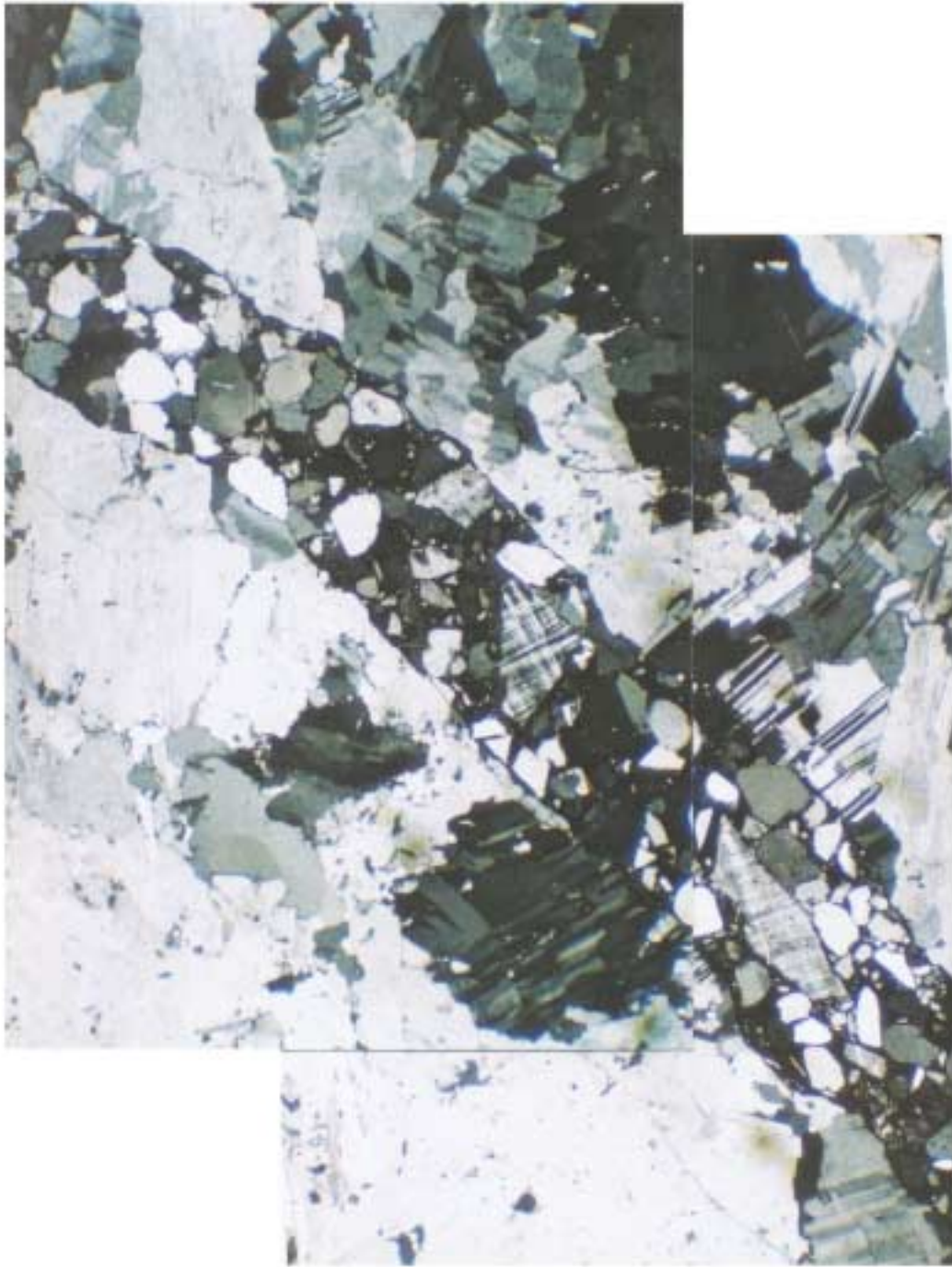


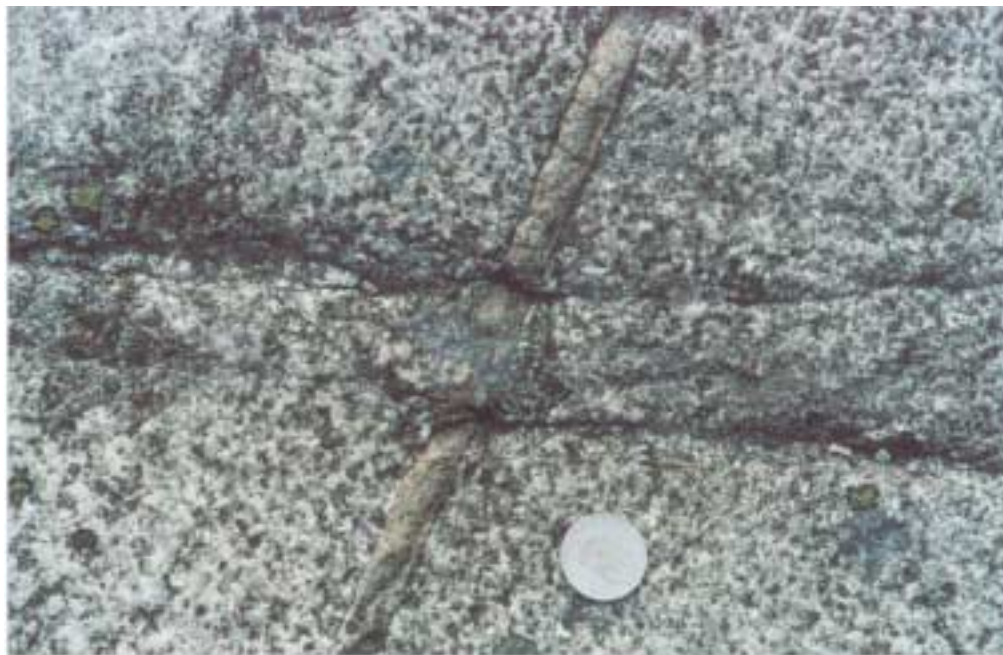
Figure 5-19. Thin (approx. 2mm wide) dyke containing approximately equal amounts of rounded sand grains and angular fragments of the granitic country rock. This is strong evidence that the dyke is the result of fluid induced fracturing of the granite rather than the passive infill of a pre-existing fracture.

These dykes are often only a few grains wide and their textures are more complex than those observed in the larger dykes. For example the dykes shown in Figure 5-18 show complex grading. In Figure 5-18a clast size grading is parallel to the dyke walls whereas in Figure 5-18b and c it is normal to the dyke walls. . Even when the grading is normal to the dyke walls (e.g. Figure 5-18b and c) the dykes are too thin compared to the size of the grains for the grading profile (fine-course-fine) across a dyke to be well displayed. In some dykes (e.g. Figure 5-19) no grading can be discerned.

An interesting feature of these thin dykes is the shape and composition of the grains. Unlike many of the thicker dykes where the shape is 'well rounded' and the composition dominantly quartz, (e.g. Figure 5-15) the thin dykes are characterized by a variety of grain shapes ranging from well-rounded to angular and a mixture of sand grains from a primary sandstone and angular grains of feldspar' (Figure 5-18 and Figure 5-19). As noted earlier, the present authors suggest that the angular clasts of the granitic country rock were plucked from the dyke walls during active fluid induced fracturing of the country rock by fluidised sediments under high pressure.

It can be seen from the preceding discussion that the field evidence obtained from the majority of dykes indicates that they were formed by the forceful injection of fluidised sediments under fluid pressures in excess of (probably considerably in excess of) the minimum principal compression σ_3 .

Field evidence also exists relating to the timing of dyke intrusion. For example one of the dykes in the Kråkemåla quarry (dyke No. 120, Fig. 3.10) shown in Figure 5-20, is crosscut by later fractures. The sub-vertical fracture containing the dyke strikes N78°E and the barren fractures that cut it strike N30°W. These observations are compatible with the fracture and dyke orientations measured elsewhere in the region (Figure 5-2e and f and Figure 5-3c) and demonstrate that the dykes pre-date the barren fractures.



(a)



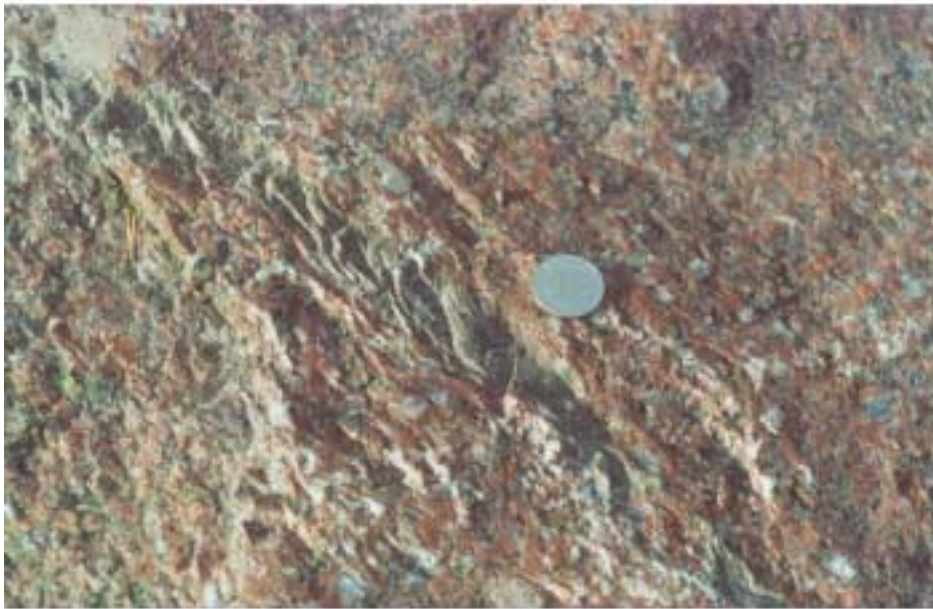
(b)

Figure 5-20. Sandstone dyke in the quarry at Kråkemåla (No. 120, Fig. 3.10) crosscut by later fractures, b) is a close up of a).

Sometimes the dykes contain fractures that are confined to the dyke and do not effect the granitic country rock. For example the two dykes shown in Figure 5-21a and b contain fractures normal and oblique to the trend of the dyke. These fractures are not present in the country rock and indicate that the tectonism that generated them post-dates dyke intrusion. This supporting the idea that the dykes are not related to the Quaternary glaciation.



(a)



(b)

Figure 5-21. a) Normal and b) oblique fractures cutting sandstone dykes in the quarry at Kråkemåla, indicating tectonism post dyke intrusion and therefore supporting the idea that the dykes are not related to the Quaternary glaciation.

Another phenomenon indicating that the dykes are of considerable antiquity is the mineralisation found in association with them. Many of the dykes have been affected by a phase of fluorite mineralisation which in places has enriched the pores of the dykes and the dyke walls with fluorite. Three views of fluorite mineralisation along the edge of a sandstone dyke in the Kråkemåla quarry are shown in Figure 5-22. The mineralisation is probably related to the break up of Pangea in the Permian and provides evidence for a Permian or older age of the dykes.

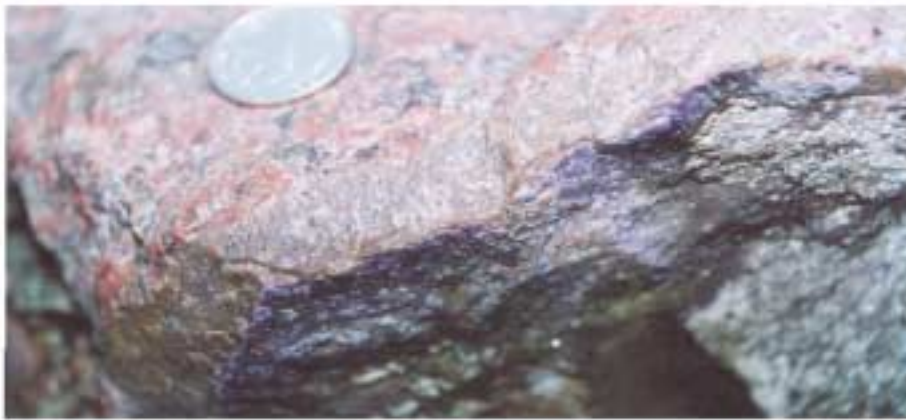
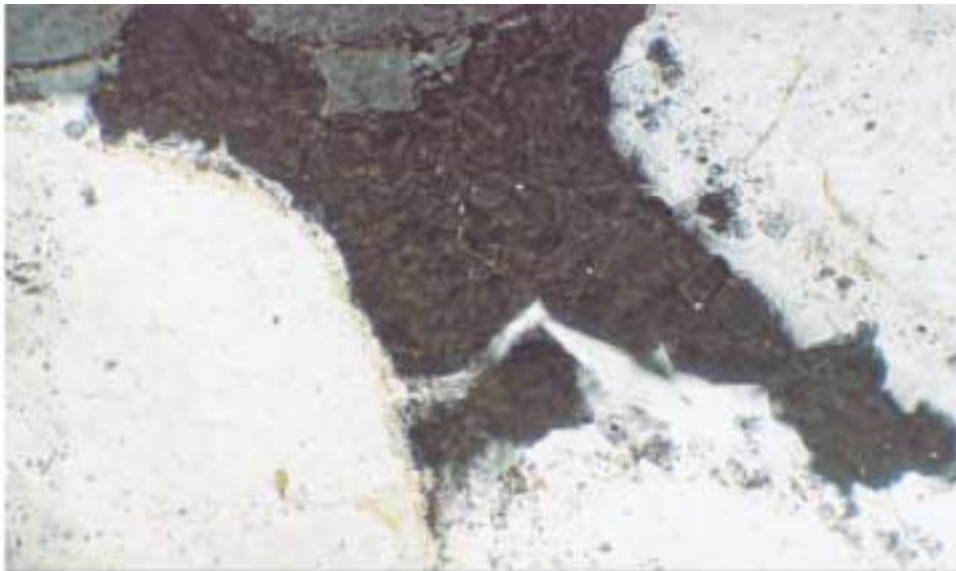
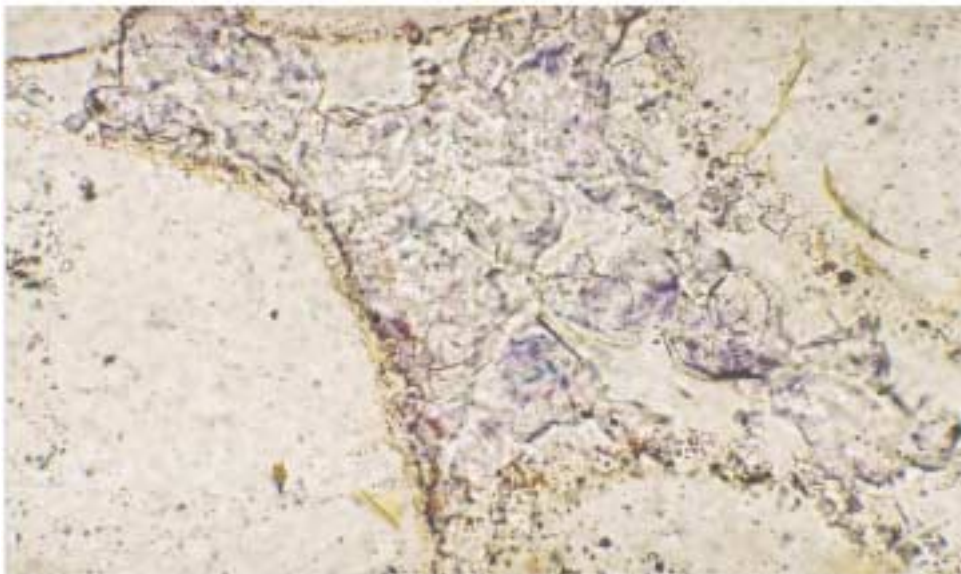


Figure 5-22. *Three views of fluorite mineralisation along the edge of a sandstone dyke in the Kråkemåla quarry. The mineralisation is probably related to the break up of Pangea in the Permian and provides evidence for the pre-Permian age of the dykes.*

A study of the dykes in thin section (Figure 5-23 and Figure 5-24) shows mineralisation of the pore spaces between the sandstone clasts. The cubic form of fluorite and its characteristic blue colour can be seen in Figure 5-23b which shows a section under plane polarised light. Its cubic habit is confirmed by the extinction shown when the section is viewed under crossed nicols, Figure 5-23a.



(a)



(b)

Figure 5-23. Thin section of a mineralised pore in a sandstone from the Kråkemåla quarry. The cubic form of fluorite and its characteristic blue colour can be seen in b) which shows the section under plane polarised light. Its cubic habit is confirmed by the extinction shown when the section is viewed under crossed nicols, a).

Three images of the same thin section are shown in Figure 5-24. The quartz grains and the infilled pores can be clearly seen in Figure 5-24a and b, which are taken in plane polarised light and under crossed nicols respectively. The presence of fluorite in the pore material is shown by the characteristic blue colour under plane-polarised light and extinction under crossed nicols. The quartz overgrowth on the right hand edge of the quartz grain to the centre left of the pictures contains beautifully preserved cubes of fluorite indicating that the formation of the overgrowth and the fluorite mineralisation was occurring synchronously.

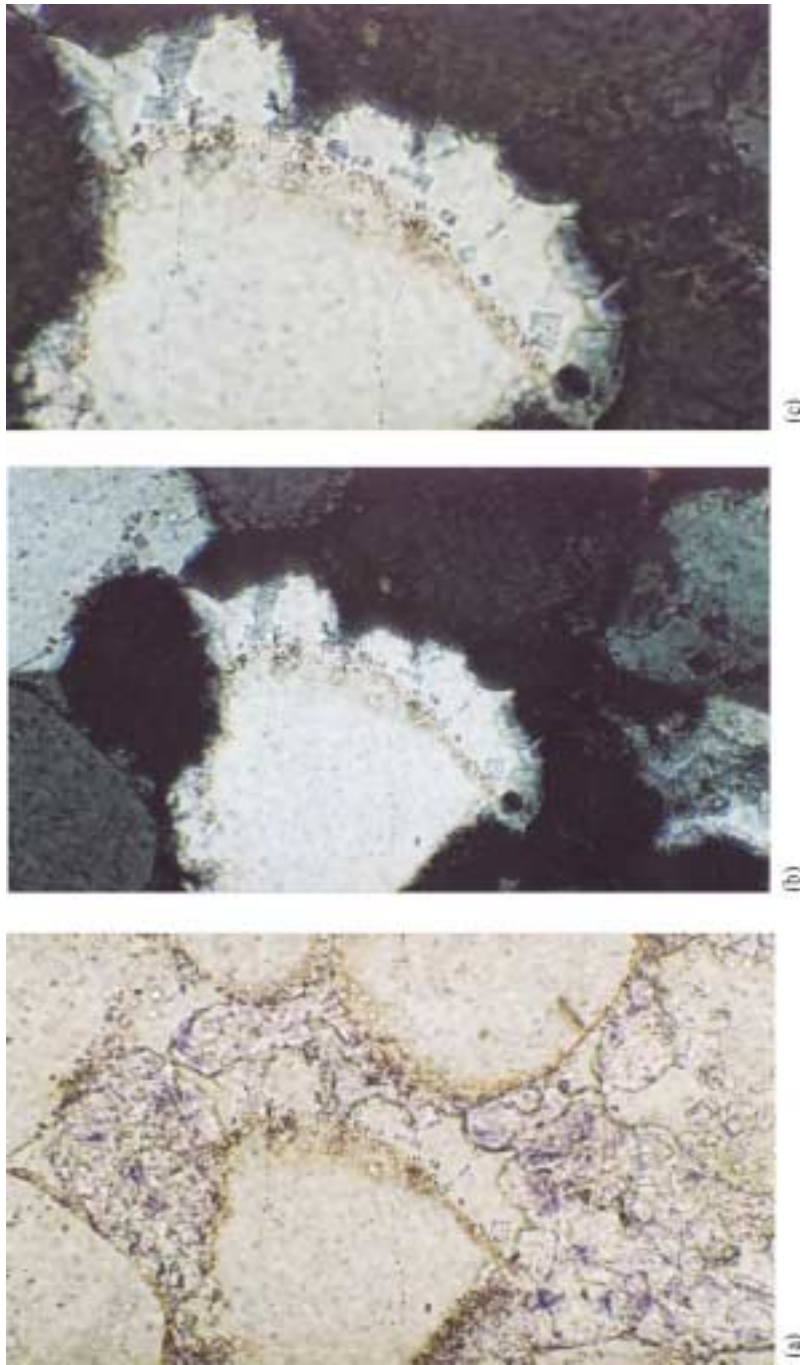


Figure 5-24. Cubes of fluorite entrapped in pores and quartz overgrowths in a sandstone dyke from the Kråkemåla quarry, a) in plane polarised light, b) under crossed nicols. c) Shows extinction of the pore infill material caused by the abundance of fluorite and in addition cubes of fluorite in a quartz overgrowth on a quartz again.

Evidence that the dykes have been subjected to a phase of mineralisation after their intrusion can also be seen in the field and in hand specimens. For example the sandstone dykes from the Kråkemåla quarry illustrated in Figure 5-25 show a sandstone matrix supporting clasts of granite. The dyke edges and the margins of the granite clasts are clearly mineralised.



Figure 5-25. Sandstone dykes from the Kråkemåla quarry showing a sandstone matrix supporting clasts of granite. The dyke edges and the margins of the granite clasts are clearly mineralised. The dykes pre-date the mineralisation which is thought to be of Permian age.

5.7 Road section north of Västervik

The majority of dykes, fractures and veins discussed in this report are sub-vertical. There are however sub-horizontal fractures and sometimes these low dipping fractures are mineralised. An example of such horizontal veining can be seen in a road cutting on the E22, 16km north of Västervik. Figure 5-26 shows three views of the fracture system at this locality. An intimate link between vertical fractures and the formation of relatively short horizontal veins is apparent. Some of the vertical fractures contain quartz veins and where these veins cut sub-horizontal fractures the veins are seen to extend along these fractures for a short distance (ranging from a few cms. to a few 10s of cms.). The process of hydraulic fracturing in a fractured rock mass has been discussed earlier in connection with the fractures at Emån under the section 5.5.1. It was noted there that in a fracture system made up predominantly of horizontal and vertical fractures where the principal compression acted vertically, that the response of the fracture network to a fluid pressure depended upon the relative magnitude of the differential stress and the difference between the bulk cohesion normal to the two fracture sets. If the differential stress is greater than the difference in cohesion then the stress determines the fracturing and the vertical fractures open and if the difference in cohesion is greater than the differential stress then the material properties of the rock determines the fracturing and the horizontal fractures open. When the two parameters are approximately the same it is possible that both sets of fractures will open as illustrated in Figure 5-26 and Figure 5-8.

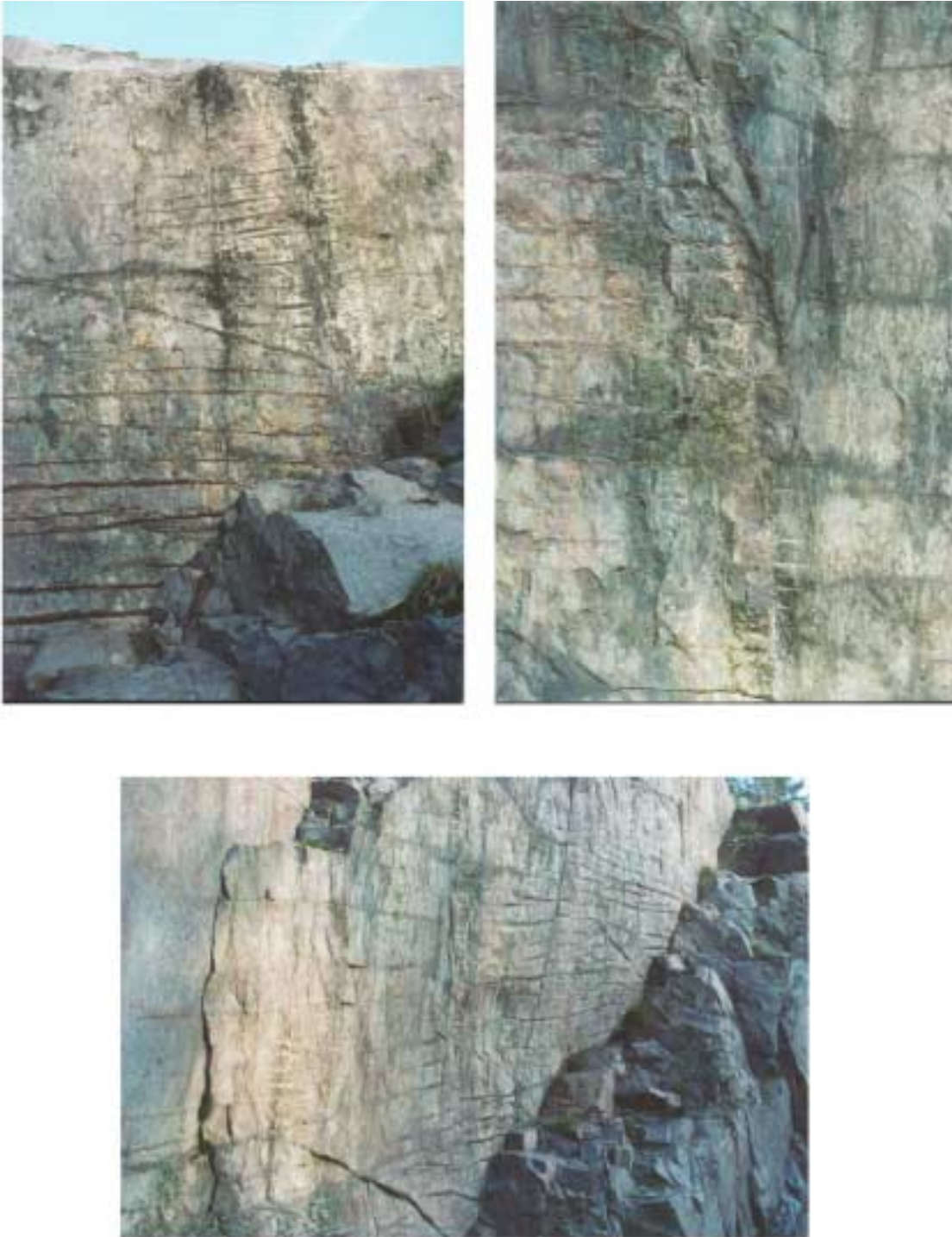


Figure 5-26. Three views of the fracture system seen in a road cutting on the E22, 16km north of Västervik. An intimate link between vertical fractures and the formation of relatively short horizontal veins is apparent. See text for discussion and Figure 5-8.

6 Discussion

6.1 General

The aim of this study of the sedimentary dykes within the Precambrian basement of SE Sweden, particularly around the site of the Äspö Hard Rock Laboratory is to determine the likely response of the rock mass to an increase in fluid pressure such as might be associated with the next glacial advance.

The study is divided into three sections namely 1) a review of the literature on sedimentary dykes 2) a review and consideration of the process of fluid assisted fracturing and 3) an account of the fieldwork carried out during this project.

The literature review on sedimentary dykes indicates a remarkable consensus on the modes of formation of these structures. Based on their fabrics (particularly layering generated in part by variations in clast size) and the composition of the infilling material, two modes of origin have been recognised. These are passively infilled dykes where the dyke material has entered an open fracture or cavity under the influence of gravity, and active i.e. forceful injection of a fluidised sediment under high pressure into a pre-existing fracture or into a fracture generated by the high-pressure fluid.

The size of sedimentary dykes, particularly those formed as a result of high-pressure fluids can vary from a few mm in width and length to dykes up to 100m wide and several kilometres long. Not surprisingly many sedimentary dykes linked to high-pressure fluids were formed in high-energy environments e.g. along active faults. Their formation is often associated with earthquakes where the release of stored strain energy is used in part to fluidise the sediments and in part to open fractures or generate new fractures along which the dykes can intrude.

In the simplest examples the orientation of the dykes can be directly related to the opening direction (perpendicular to σ_3) of the stress field operating during their emplacement. However, sometimes the strike distribution of the dykes shows a more complex pattern. It seems likely in these examples that the fractures formed in response to a stress field that pre-dated the stress field operating during dyke injection and that the dykes exploited these pre-existing fractures. The degree to which non-ideally oriented fractures can be used by the fluidised sediments is determined by the relative magnitude of the fluid pressure and the applied principal stresses, (Figure 3-6).

In the majority of examples described in the literature, sedimentary dykes are the result of upward injection of older or younger sediments into a host rock. However, one notable exception has been reported from Southeast Sweden where the dykes appear to have been intruded downward into the underlying basement. These Swedish dykes are the focus of this study.

The second section of this report relates to the theory of fluid induced fracturing and a study of the literature on this topic leads to the recognition of three systems which are the two end members and an intermediate form of a continuous spectrum of materials ranging from unconsolidated and incohesive sediments, through cemented but porous rocks to crystalline rocks with no intrinsic porosity and whose only porosity relates to that imparted by the fracture network that the rock contains.

The effect of high fluid pressure on the three systems is very different. The uncemented sediment will respond to a high fluid pressure by fluidisation and this provides a medium that can be injected into pre-existing fractures to form sedimentary dykes. Alternatively the fluid may generate its own fractures which it subsequently fills. The porous sedimentary rock responds to the build up of pore pressure by hydraulic fracturing and the appropriate analysis for understanding its behaviour is one based on the theory of poro-elasticity. This theory, known as the theory of internal hydraulic fracturing, (Figure 4-6) is able to predict the type and orientation of the fractures that will form.

The non-porous, crystalline rock containing fluid filled, isolated or linked fractures can also respond to an increase in fluid pressure by hydraulic fracturing i.e. the propagation of an existing fracture or the generation of a new fracture. The theory best suited to analyse such a system is one based on fracture mechanics and is known as the theory of external hydraulic fracturing (Figure 4-6). From the point of view of the sedimentary dykes in the study area around the Hard Rock Laboratory at Äspö, where the dykes occur in the granitic Precambrian basement, the most appropriate model for their formation is clearly that of external hydraulic fracturing.

Chapter 5 of this report is concerned with the implication of the field observations regarding the mechanism of emplacement of the sedimentary dykes. With the exception of the dyke at Granhultå (Figure 5-4), whose internal fabric clearly indicated gravitational infill from above, all the dykes examined by the present authors have fabrics and textures characteristic of forcefully injected sediments, i.e. clasts fining from the centre of the dykes to the edges and as a result layering forming parallel to the dyke walls.

The textures of the dykes and their geometries can also indicate something about the magnitude of the fluid pressures operating during dyke formation. Although it is thought that the fluidised sediments that fed the dykes exploited a pre-existing sub-vertical fracture set trending approximately N35°E, there is evidence of the fluid pressures being of sufficient magnitude to be capable of generating new fractures. This is well illustrated by the formation of 'links' between two parallel overlapping and offset dykes (e.g. Figure 5-3 and Figure 5-13). Other evidence for the occurrence of high fluid pressures during dyke emplacement is provided by the ability of the fluidised material to open fractures in more than one orientation, (Figure 5-7), implying that the fluid pressure not only equalled the minimum principal compression (σ_3) but exceeded it (see Figure 5-7 and the related discussion).

In addition, although most of the dyke material is made up of well-rounded quartz grains, (e.g. Figure 5-15), in many of the dykes these are mixed with various amounts of angular grains of granitic material, (e.g. Figure 5-18 and Figure 5-25), clearly derived by fluid induced failure of the country rock during the process of dyke emplacement.

Two lines of evidence relating to the timing of dyke emplacement indicate that the sedimentary dykes are relatively ancient features i.e. that they are not associated with the Quaternary glaciation. The first is the relationship between the basement fractures and the dykes. Figure 5-20 shows basement fractures cross cutting the dykes indicating that the dykes pre-date the tectonic event with which the fractures are associated. The second line of evidence for the age of the dykes comes from their association with fluorite mineralisation, thought to be linked to the Permian break-up of Pangea. This mineralisation occurs within the pores of the dykes and along the dyke/country wall interface, (Figure 5-23, Figure 5-22 and Figure 5-25), and, if the mineralisation is Permian, places the dykes as Permian or older.

6.2 The implication of the field observations regarding the mechanism of emplacement of the sedimentary dykes

The major difference between the ‘texture’ of a vertical sedimentary dyke filled by gravitational infill and a dyke injected by fluidised sediments under high pressure is the orientation of the resulting foliation. Gravitationally fed dykes are characterized by layering normal to the dyke wall. (Figure 5-4c, Figure 5-5 and Figure 5-6) and those generated by the injection of high-pressure fluids by layering parallel to the dyke walls, (Figure 5-11b and Figure 5-12). With the exception of the dyke at Granhultea (Figure 5-4), the present authors have found that whenever a fabric is discernible in dykes in the study area, it is always parallel to the dyke walls. Inspection of thin sections of the dykes shows that this foliation is in part the result of a systematic variation in clast size across the dyke. The larger clasts are concentrated in the central part of the dyke and the smaller grains along the dyke/wall contact. This grading profile is compatible with the velocity profile generated in a fluid flowing between two parallel plates and being driven by a pressure gradient. The velocity profile approximates closely to a parabola and the lower velocity at the dyke margins is the result of the frictional drag as the dyke material moves past the wall rock.

Although it is thought that the fluidised sediments that fed the dykes exploited a pre-existing sub-vertical fracture set trending approximately N35°E, there is field evidence of the fluid pressures being of sufficient magnitude to be capable of generating new fractures as for example during the formation of a ‘link’ between two parallel overlapping but offset dykes (Figure 5-3 and Figure 5-13).

Other evidence for the occurrence of high fluid pressures during dyke emplacement is provided by the ability of the fluidised material to open fractures in more than one orientation, (Figure 5-7), implying that the fluid pressure not only equalled the minimum principal compression (σ_3) but exceeded it (see Figure 5-7 and the related discussion). In addition, although most of the dyke material is made up of well-rounded quartz grains, (e.g. Figure 5-15), in many of the dykes these are mixed with various amounts of angular grains of granitic material, (e.g. Figure 5-18 and Figure 5-25), clearly derived by fluid induced failure of the country rock during the process of dyke emplacement.

6.3 The implication of the field observations regarding timing of dyke emplacement

Two lines of evidence indicate that the sedimentary dykes are relatively ancient features i.e. that they are not associated with the Quaternary glaciation. The first is the relationship between the basement fractures and the dykes. Figure 5-20 shows basement fractures cross cutting the dykes indicating that the dykes pre-date the tectonic event with which the fractures are associated. In addition, some of the dykes, (e.g. Figure 5-21a and b), also contain systematic fracture sets that do not affect the country rock. This also indicates that subsequent to dyke intrusion the dykes have been affected by tectonism.

The second line of evidence for the age of the dykes comes from their association with fluorite mineralisation, thought to be linked to the Permian break-up of Pangea. This mineralisation occurs within the pores of the dykes and along the dyke/country wall interface, (Figure 5-23, Figure 5-22 and Figure 5-25), and, if the mineralisation is Permian, places the dykes as Permian or older.

6.4 Cause of intrusion

The sedimentary dykes of SE Sweden are unusual in that they provide one of the few known examples of downward injection of dykes. Clastic dykes injected into crystalline basement rocks have been recorded elsewhere but this was by upward injection into an overthrust basement block. The other notable occurrence of downward injection is found in association with glaciation (see Figure 6-1). Here the weight on an advancing ice sheet drives fluidised sediments into the underlying sediments in a series of dykes and sills. The increase in overburden stress generated by the overriding ice subsequently may cause the dykes to buckle.

It is interesting to note that the most likely cause of an increase in fluid pressure of the sediments overlying the basement in Sweden and of the formation of dykes and the associated hydraulic fracturing is the advance of the next glaciation. The Äspö Hard Rock Laboratory is situated at a depth of approximately 500m. A key question relating to the effects of the next glacial advance is the depth to which the effects of fluid induced fracturing will extend. Sedimentary dykes have been observed at depths of 50m in tunnels through the granite basement.

In this regard, the increase in horizontal stress with depth in the crust (Equation 4-9), related to the overburden load tends to close the fracture at depths more than higher in the crust thus driving fluids upward and impeding downward injection. Conversely an upward intruding fluid will be encouraged to rise by this stress gradient and in addition will have a larger pressure at depths further encouraging intrusion (see Figure 6-2).

In summary, in the ascending fluid example the fluid pressure gradient and the gradient in horizontal stress both act to drive upward intrusion. In contrast the two gradients operate to impede downward movement of a fluid.

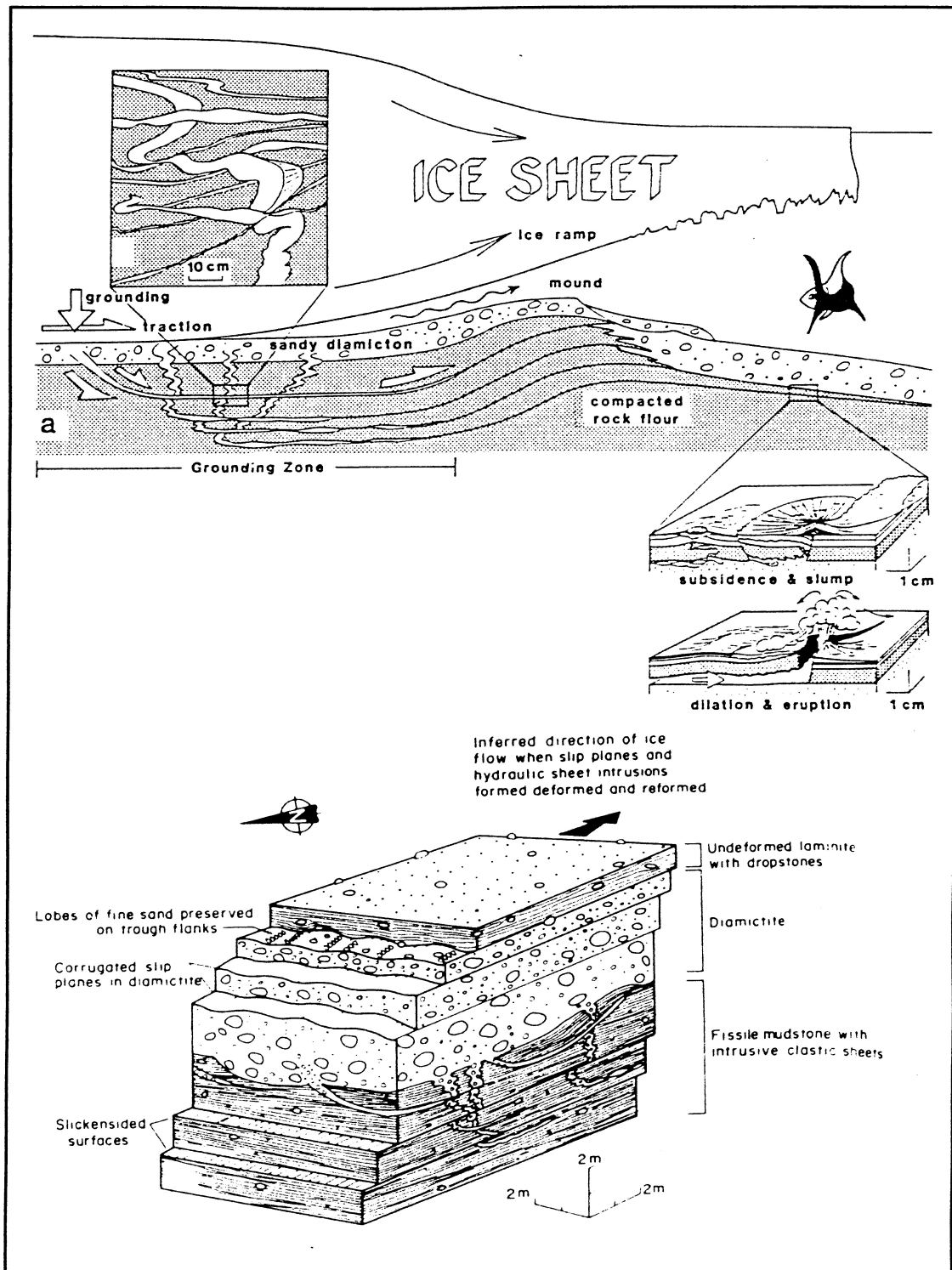


Figure 6-1. a) The formation of sedimentary dykes associated with an ice sheet. The illustration relates to the meeting of an ice sheet with a tidal sea but the build up of fluid pressures associated with the advance of an ice sheet over land could also generate high fluid pressures and the downward injection of fluidised sediments into the underlying basement. b) Block diagram of rocks and structures thought to have been formed by glacial overpressures. It shows clastic intrusions extending from an arenaceous diamictite source rock into underlying fissile muds. a) from /Talbot and von Brun, 1989/ and b) from /von Brun and Talbot, 1986/.

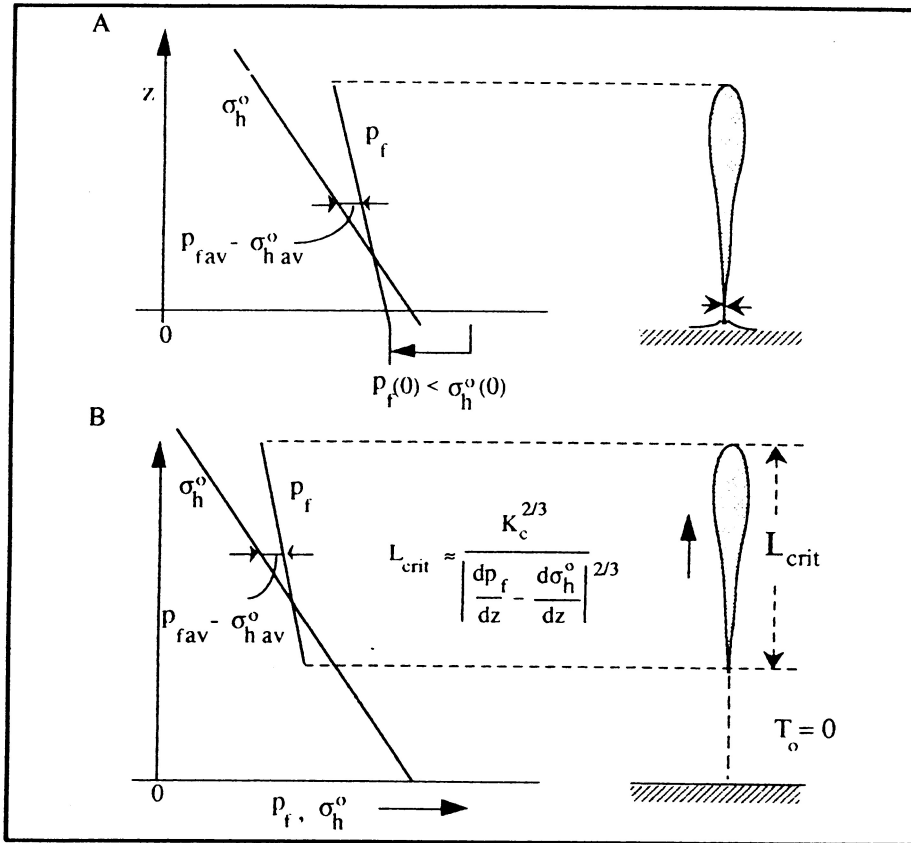


Figure 6-2. Rising hydraulic fracture (with a greatly exaggerated cross-sectional teardrop shape). A) Hydraulic fracture closed at the base by a drop in injection pressure. B) Rising stable fracture of critical length. From /Mandl, 1999/.

7 Conclusion

- On the basis of the textural and other evidence it is concluded that the majority of the dykes investigated in the Oskarshamn-Västervik area are injected into the basement forcefully c.f. passively.
- The dykes have been injected downwards into the basement an unusual situation according to the records described in the literature.
- Injection has occurred into a rigid, intrinsically non-porous, fractured rock mass and it is argued therefore that the external fluid pressure model of /Mandl, 1999/ is the most appropriate for describing this process.
- It is noted that the dykes have a fairly consistency of strike. This may indicate either that there was only one important sub-vertical fracture set at the time of injection or that there were other sets but that the fluid pressure only rose high enough to exploit the most appropriately oriented fractures (those normal to the least principal; stress σ_3) in a rock mass containing fractures in a variety of orientations. Independent evidence in the form of (i) the formation of new fractures in the basement by the fluidised sediment, (Figure 5-13) and (ii) the synchronous injection of dykes along fractures different orientations, (Figure 5-7 and Figure 5-9), indicates that the fluid pressure was probably greater than the minimum principal stress.
- Field evidence shows that the dykes are cross cut by fractures which affect both the dykes and country rock and that they have experienced a post-dyke intrusion fluorite mineralisation. This mineralisation are investigated by /Sundblad and Alm, 2000/ who also concluded a syn and post dyke age in early Palaeozoic time.
- The analysis of the sedimentary dykes in the granite basement in the vicinity of the Äspö Hard Rock Laboratory described in this report has indicated that the appropriate model for the generation of the dykes is that of external fluid fracturing and that the fluid pressure during dyke emplacement was probably considerably in excess of that required to open ideally oriented basement fractures. The stress boundary conditions operating during dyke injection are likely to have been those of a vertical maximum principal compression and an increasing horizontal stress with depth and injection occurred into a rigid rock mass containing a set of isolated (or interconnected) fractures which the dykes exploited.

These well defined boundary conditions could be used to numerically model the effect of an increased overburden generated by an overriding ice sheet moving over water saturated (glacial) sediments on the propagation of the fractures in the basement.

- It is proposed that such a numerical analysis be carried out to determine the relationship between the thickness of the overburden (ice sheet) and depth of penetration of hydraulic fractures and dyke injection for the boundary conditions and structuration (i.e. fracture density, length and organization) of the basement at Äspö.

References

- Allen J R L, 1982.** Developments in Sedimentology, vol. II, Elsevier, Amsterdam. 554-6.
- Alterman I B, 1973.** Rotation and dewatering during slaty cleavage formation: some new evidence and interpretation. *Geology* 1, 33–36.
- Bailey E B, Weir J, 1932.** Submarine faulting in Kimmeridgian Times: East Sutherland. *Trans. Royal Soc. Edinb.* Ivii, 429.
- Barker C, 1972.** Aquathermal pressuring – Role of temperature in development of abnormal-pressure zones: *American Association of Petroleum Geologists Bulletin*, 56, 2068-71.
- Bergman L, 1982.** Clastic dykes in the Arland Islands, SW Finland and their origin. *Geological Survey of Finland Bull.*, 317, 733.
- Berry F A F, 1973.** High fluid potentials in California Coast Ranges and their tectonic significance. *American Association of Petroleum Geologists Bulletin*, 57, 1219-49.
- Bethke C M, Harrison W J, Upson C, Altaner S P, 1988.** Supercomputer analysis of sedimentary basins. *Science*, 239, 261-67.
- Beutner E C, Jancin M D, Simon R W, 1977.** Dewatering origin of cleavage in light of deformed calcite veins and clastic dikes in Martinsburg slate, Delaware Water Gap, New Jersey. *Geology* 5, 118–122.
- Biot M A, 1941.** General theory of three dimensional consolidation. *Journal of Applied Physics*, 12, 155-64.
- Birman J H, 1952.** Pleistocene clastic dikes in weathered granite gneiss, Rhode Island. *Am. Jour. Sci.* 250, 721-84.
- Borradaile G J, 1977.** On cleavage and strain: results of a study in West Germany using tectonically deformed sand dykes. *Jour. Geol. Soc. Lon.* 133, 146–164.
- Boulter C A, 1974.** Tectonic deformation of soft sediment clastic dykes from Precambrian rocks of Tasmania, Australia, with particular reference to their relations with cleavage. *Geol. Soc. Am. Bull.* 85, 1413-20.
- Boulter C A, 1983.** Post-lithification deformation of sandstone dikes: implications for tectonic dewatering. *Am. Jour. Sci.* 283, 876-95.
- Brandon A, 1972.** Clastic dykes in the Namurian shales of County Leitrim, Republic of Ireland. *Geol. Mag.*, 109, 361-67.
- Brock W G, Engelder T, 1977.** Deformation associated with the movement of the Muddy Mountain overthrust in the Buffington window south eastern Nevada. *Geol. Soc. Am. Bull.* 88, 1667-77.
- Carson W P, 1968.** Development of flow cleavage in the Martinsburg shales, Port Jervis South area (Northern New Jersey). *Tectonophysics* 5, 531-41.

- Clark B R, 1970.** Origin of slaty cleavage in the Coeur d'Alene district: Idaho. Geol. Soc. Am. Bull. 81, 3061-72.
- Cosgrove J W, 1995.** The expression of hydraulic fracturing in rocks and sediments. In Ameen M. S. (ed.), 1995, *Fractography: fracture topography as a tool in fracture mechanics and stress analysis*. Geological Society of London, Special Publication No. 92, 187-96.
- Cosgrove J W, 1997.** The influence of mechanical anisotropy on the behaviour of the lower crust. *Tectonophysics*, 280, 1–14.
- Cosgrove J W, Hillier R D, 2000.** Forced fold development within Tertiary sediments of the Alba field, UKCS: evidence of differential compaction and post-depositional sandstone remobilization. In Cosgrove, J. W. & Ameen, M. S. (eds). *Forced folds and fractures*. Geological Society, London, Special Publications, 169, 61–71.
- Cosgrove J W, 2001.** Hydraulic fracturing during the formation and deformation of a basin: A factor in the dewatering of low permeability sediments. *American Association of Petroleum Geologists*, 85, 737-48.
- Crosby W O, 1897.** Sandstone dikes accompanying the great fault of Pass, Colorado. *Essex Inst. Bull.* 27, 113-47.
- Cross W, 1894.** Intrusive sandstone dykes in granite. *Geol. Soc. Am. Bull.* 5, 225-30.
- Darwin C, 1840.** Geological observations in the volcanic islands and parts of South America visited during the voyage of H.M.S. 'Beagle'. London.
- Delaney P T, Pollard D D, Zioney J I, McKee E H, 1986.** Field relationships between dikes and joints, emplacement processes and paleostress analysis. *Journal of Geophysical Research*, 91, 4920–4938.
- Diller J S, 1889.** Sandstone dikes. *Geol. Soc. Am. Bull.* 1, 411-42.
- Dionne J-C, Shilts W W, 1974.** A Pleistocene clastic dike. Upper Chaudiere Valley, Quebec. *Canadian Journal of Earth Sciences*. 11. 1594–1605.
- Dzulynski S, Walton E K, 1965.** Sedimentary features of flysch and greywackes. In *'Developments in Sedimentology.'* Elsevier, New York.
- Engelder T, Lacazette A, 1990.** Natural Hydraulic Fractures. In Barton, N. and Stephanson, O, eds, *Rock Joints*, Rotterdam, A. A. Balkema, 35–44.
- Engelder T, 1992.** *Stress regimes in the lithosphere*. Princeton University Press, Princeton, New Jersey, 457pp.
- Fackler W C, 1941.** Clastic crevice fillings in the Keweenaw lavas. *Jour. Geol.* 49, 550–556.
- Fyfe W S, Price N J, Thompson A B, 1978.** *Fluids in the Earth's Crust*. Elsevier Scientific publishing Co, 382pp.
- Goldthwait J W, Kruger F C, 1938.** Weathered rock in and under the drift, New Hampshire. *Geol. Soc. Am. Bull.* 49, 1183-98.
- Gregg W J, 1979.** The redistribution of pre-cleavage clastic dykes by folding at New Paltz, New York. *Jour. Geol.* 87, 99-104.

- Griffith A A, 1924.** Theory of rupture. *Proceedings of the First International Congress of Applied Mechanics*, Delft, 55–63.
- Groshong R H, 1976.** Strain and pressure solution in the Martinsburg slate, Delaware Water Gap, New Jersey. *Am. Jour. Sci.* 276. 1131-46.
- Harms J C, 1965.** Sandstone dikes, Southern Front Range, Colorado. *Geol. Soc. Am. Bull.* 76, 981–1001.
- Haxby W F, Turcotte D L, Bird J M, 1976.** Thermal and mechanical evolution of the Michigan basin. *Tectonophysics*, 36, 57–75.
- Hayashi T, 1966.** Clastic dikes in Japan. *Trans. Jour. Japan Geol. Geography* 37, 1–20.
- Hubbert M K, Rubey W W, 1959.** Role of fluid pressure in mechanics of overthrust faulting. *Geol. Soc. Am. Bul*,70, 115-67.
- Hunt J M, 1989.** Generation and Migration of Petroleum from abnormally pressured fluid compartments. *American Association of Petroleum Geologists Bulletin*, 74, 1–12.
- Inglis C E, 1913.** Stresses in a plate due to the presence of cracks and sharp corners. *Transactions of the Institute of Naval Architecture*, 55, 219.
- Jenkins O P, 1925.** Clastic dikes of Eastern Washington and their geological significance. *Am. Jour. Sci.* 10, 234-46.
- Jolly R J H, Sanderson D J, 1995.** The variation in form and distribution of dykes in the Mull swarm. *Journal of Structural Geology*, 17, 1543-57.
- Jolly R J H, Cosgrove J W, Dewhurst D N, 1998.** Thickness and spatial distributions of clastic dykes, northwest Sacramento Valley, California. *Journal Structural Geol.* 20, No. 12 1663–1672.
- Kirsch G, 1898.** Die Theorie der Elastizitat and die Bedurfnisse der Festigkeitslehre. *Zeitschrift des Vereines Deutscher Ingenieure*, 42, 797.
- Kresten P, Chyssler J, 1976.** The Götemar massif in south-eastern Sweden: A reconnaissance survey. *Geologiska Föreningens i Stockholm Förhandlingar* 98, 155–161.
- Kruger F C, 1938.** A clastic dike of glacial origin. *Am. Jour. Sci.* 35, 305-7.
- Lidmar-Bergström K, 1996.** Long term morphotectonic evolution in Sweden. *Geomorphology* 16, 33–59.
- Lindstrom M, 1967.** ‘Funnel grabens’ and Early Palaeozoic tectonism in South Sweden. *Geol. Soc. Am. Bull.* 78, 1137-54.
- Lupher R L, 1944.** Clastic dike of the Columbia Basin region, Washington and Idaho. *Geol. Soc. Am. Bull.* 55, 1431–1462.
- Magara K, 1978.** *Compaction and fluid migration*. New York, Elsevier.
- Mandl G, 1999.** *Faulting in Brittle Rocks: An introduction to the mechanics of tectonic faulting*. Berlin (Springer). 434pp.

- Martill D M, Hudson J D, 1989.** Injection clastic dykes in the Lower Oxford clay (Jurassic) of central England: relationship to compaction and concretion formation. *Sedimentology* 36, 1127–1133.
- Matsson A, 1962.** Morphologische Studien in Sudscheden und auf Bornholm über die Nicht glaziale Formenwelt der Felsenskulptur. Lund Studies in Geography. Ser. A. Physical Geography. No. 20.
- Maxwell J C, 1962.** Origin of slaty and fracture cleavage in the Delaware Water Gap area, New Jersey and Pennsylvania. In: Engel A. E, James, H. L. and Leonard, B. F.: *Petrologic Studies – a volume in honour of A. F. Buddington*. Geol. Soc. Am. Bull. 281–311.
- McHenry D, 1948.** The effect of uplift pressure on the shearing strength of concrete. 3eme Congr. Des Grands Barrages, Stockholm, 1(R48): 1.
- Milnes A G, Gee D G, 1992.** Bedrock stability in southeastern Sweden. Evidence from fracturing in the Ordovician limestones of northern Oland. SKB Technical report 92-23.
- Moench R S, 1966.** Relation of S2 schistosity to metamorphosed clastic dykes, Rangeley-Phillips area, Maine. Geol. Soc. Am. Bull. 77, 1449-62.
- Murchison R I, 1827.** Supplementary remarks on the oolitic Series in the Counties of Sutherland and Ross, and in the Hebrides. Trans. Geol. Soc. 2, 353.
- Narr W, Currie J B, 1982.** Origin of fracture porosity – Example from Altamont field, Utah. American Association of Petroleum Geologists Bulletin, 66, 1231-47.
- Nordenskjöld C E, 1944.** Morfologiska studier inom övergångsområdet mellan Kalmarslätten och Tjust. Medd. Lunds Univ. Geog. Inst. Avh. VIII.
- Nur A, Byerlee J D, 1971.** An exact effective stress law for elastic deformation of rocks with fluids. *Journal of Geophysical Research*, 76, 6414-19.
- Peach B N, et al, 1907.** The geological structure of the North-West Highlands of Scotland. Mem. Geol. Surv. Scotland.
- Peterson G L, 1966.** Structural interpretation of sandstone dikes, North-West Sacramento Valley, California. Geol. Soc. Am. Bull. 77, 833–842.
- Peterson G L, 1968.** Flow structures in sandstone dikes. *Sedimentary Geology*, 2, 177–190.
- Powell C M, 1969.** Intrusive sandstone dykes in the Siamo Slate near Negaunee, Michigan. Geol. Soc. Am. Bull. 80, 2585-94.
- Powell C M, 1972.** Tectonic dewatering and strain in the Michigan Slate, Michigan. Geol. Soc. Am. Bull. 83, 2149-58.
- Powell C M, 1973.** Clastic dykes in the Bull Formation of Cambrian age, Taconic Allochthon, Vermont. Geol. Soc. Am. Bull. 84, 3045-50.
- Powell C M, 1974.** Tectonically dewatered slates in the Ludlovian of the Lake District, England. Geol. Jour. 8, 95–110.

- Powers M C, 1967.** Fluid-release mechanisms in compacting marine mudrocks and their importance in oil exploration. *American Association of Petroleum Geologists Bulletin*, 51, 1240-54.
- Reimnitz E, Marshall N F, 1965.** Effects of the Alaska earthquake and tsunami on the recent deltaic sediments. *Jour. Geophys. Research* 70, 2363–2376.
- Roy C J, 1946.** Clastic dykes of the Pikes Peak region. *Geol. Soc. Am. Bull.* 57, 1226.
- Russell W L, 1972.** Pressure-depth relations in the Appalachian region. *American Association of Petroleum Geologists Bulletin*, 56, 528-36.
- Rutter E H, 1970.** An experimental study of the factors affecting the rheological properties of rock in simulated geological environments. Ph.D. thesis, Imperial College, London.
- Samuelson L, 1975.** Palaeozoic fissure filling and tectonism of the Göteborg area, southwestern Sweden. *Sveriges Geol. Undersökning* 69, 3–43.
- Schmitt T, 1979.** In situ stress profile through the Alps and foreland. *Allgemeine Vermessungs-Nachrichten*, 86, 367-70.
- Schrock R R, 1948.** Sequence in layered rocks. McGraw-Hill Book Co. New York.
- Secor D T, 1968.** Mechanics of natural extension fracturing at depths in the Earth's crust. *Geological Survey of Canada Paper*, 68, 52.
- Sibson R H, 1974.** Frictional constraints on Thrusts, Wrench and Normal faults. *Nature* 249, 542–544.
- Sibson R H, Moore J, Rankin A H, 1975.** Seismic pumping – a hydrothermal fluid transport mechanism. *Jour. Geol. Soc. Lon.* 131, 653–659.
- Sih G C, 1973.** *Handbook of stress intensity factors*. Institute of fracture and Solid Mechanics, Bethlehem, Pennsylvania, Lehigh University Press.
- Skempton A W, 1961.** Effective stress in soils, concrete and rock. In: *Pore Pressure and Suction in Soils*. Int. Soc. Soil Mech. Found. Eng. Proc. Conf. London, 1960, Butterworths, London, 156pp.
- Smith K G, 1952.** Structure plan of clastic dikes. *Am. Geophys. Union Trans.* 33, 889–892.
- Smith K G, Rast N, 1958.** Sedimentary dykes in the Dalradian of Scotland. *Geol. Mag.* 95, 234-40.
- Spencer A M, 1971.** Late-Precambrian glaciation in Scotland. *Mem. Geol. Soc. Lon.* No. 6.
- Sollien D, 1999.** Control of fluorite-galena-bearing fractures and clastic sandstone dykes in Tindared area, southeastern Sweden. Project work, Norwegian University of Science and Technology, Trondheim, 26pp.
- Sundblad K, Alm E, 2000.** Flusspatforande spricksystem i den prekambiska berggrunden i Ostersjoregionen. Institutionen för geologi och geokemi Stockholms universitet. S-106 91 Stockholm, Sverige.

- Talbot C J, von Brun V, 1989.** Melanges, intrusive and extrusive sediments, and hydraulic arcs. *Geology*, 17, 446–448.
- Terzaghi K, 1943.** *Theoretical soil mechanics*. New York, John Wiley.
- Tissot B P, Welte D H, 1978.** Petroleum formation and occurrence. Springer, Berlin.
- Toth J, 1980.** Cross-formational gravity-flow of ground water: A mechanism of the transport and accumulation of petroleum (The generalized hydraulic theory of petroleum migration). *American Association of Petroleum Geologists Bulletin*, 64, 121-67.
- Truswell J F, 1972.** Sandstone sheets and related intrusions from Coffee Bay, Transkei, South Africa. *Jour. Sed. Petrology* 42, 578-83.
- Tsuneiki Y, Nakamura K, 1970.** Faulting associated with the Matsushiro swarm earthquakes. *Bull. Earthquake research Institute Tokyo Univ.* 48, 29–51.
- Van Biljon W J, Smitter Y H, 1956.** A note on the occurrence of two sandstone dykes in a Karroo dolerite dyke near Devon, southeastern Transvaal. *Trans. Of the Geol. Soc. South Africa* 59, 135–139.
- Vitanage P W, 1954.** Sandstone dykes in the South Platte area. *Jour. Geol.* 62, 493–500.
- von Brun V, Talbot C J, 1986.** Formation and deformation of subglacial intrusive clastic sheets in the Dwyka Formation of Northern Natal, South Africa. *Jour. Sed. Petrology* 56, No. 1, 35–44.
- Walton M S, O’Sullivan R B, 1950.** The intrusive mechanics of a clastic dyke. *Am. Jour. Sci.* 248, 1–21.
- Waterson C D, 1950.** Note on the sandstone injections of Eathie Haven, Cromarty. *Geol. Mag.* 87, (No. 2) 133-39.
- Williams M Y, 1927.** Sandstone dykes in southeastern Alberta. *Trans. Royal Soc. Canada* 3rd ser. 21 (section IV), 153.
- Williams D M, 1976.** Clastic dykes from the Precambrian Porsangerfjord group, North Norway. *Geol. Mag.* 113, 169-76.
- Winslow M A, 1977.** Clastic dyke swarm emplacement and early phases of deformation: structural studies in the foreland fold and thrust belt of Southern Chile. *Geol. Soc. Am. Abstracts with programs* 9 1232.
- Winslow M A, 1983.** Clastic dike swarms and the structural evolution of the foreland fold and thrust belt of the southern Andes. *Geol. Soc. Am. Bull.* 94, 1073–1080.